ARCHIVE COPY
DO NOT LOAN

ANALYTICAL STUDY OF ICING SIMULATION FOR TURBINE ENGINES IN ALTITUDE TEST CELLS

C. E. Willbanks and R. J. Schulz
ARO, Inc.

November 1973

ENGINE TEST FACILITY
ARNOLD ENGINEERING DEVELOPMENT CENTER
AIR FORCE SYSTEMS COMMAND
ARNOLD AIR FORCE STATION, TENNESSEE

NOTICES

When U. S. Government drawings specifications, or other data are used for any purpose other than a definitely related Government procurement operation, the Government thereby incurs no responsibility nor any obligation whatsoever, and the fact that the Government may have formulated, furnished, or in any way supplied the said drawings, specifications, or other data, is not to be regarded by implication or otherwise, or in any manner licensing the holder or any other person or corporation, or conveying any rights or permission to manufacture, use, or sell any patented invention that may in any way be related thereto.

Qualified users may obtain copies of this report from the Defense Documentation Center.

References to named commercial products in this report are not to be considered in any sense as an endorsement of the product by the United States Air Force or the Government.

ERRATA

AEDC-TR-73-144, November 1973
(UNCLASSIFIED REPORT)

ANALYTICAL STUDY OF ICING
SIMULATION FOR TURBINE ENGINES
IN ALTITUDE TEST CELLS

C. E. Willbanks and R. J. Schulz, ARO, Inc.

Arnold Engineering Development Center
Air Force Systems Command
Arnold Air Force Station, Tennessee 37389

Figure 20 of this report has been corrected and is printed on the reverse of this sheet.

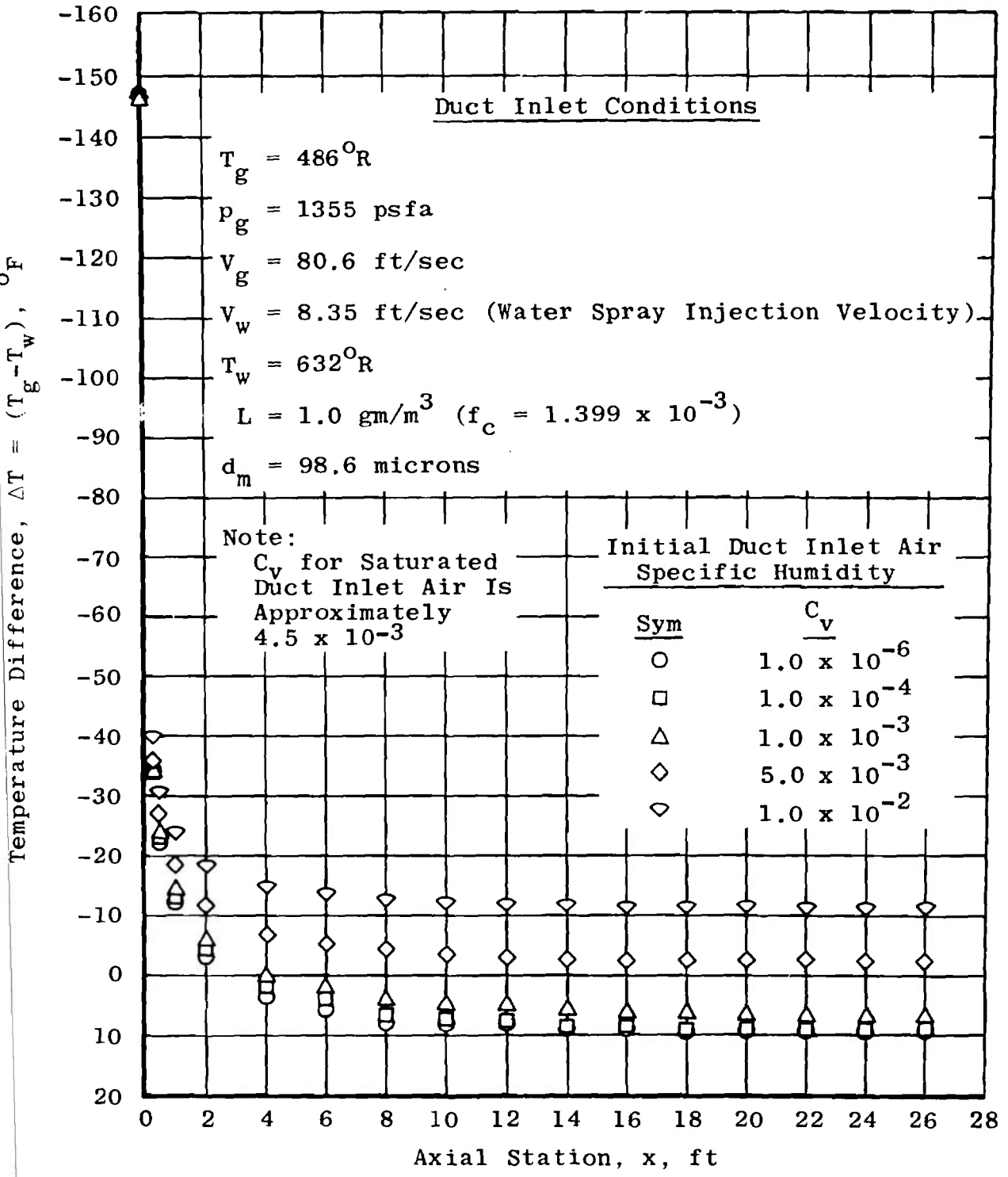

Fig. 20 Temperature Difference between Gas and Water Droplets versus Axial Location: The Effect of Duct Inlet Air Specific Humidity

ANALYTICAL STUDY OF ICING SIMULATION FOR TURBINE ENGINES IN ALTITUDE TEST CELLS

C. E. Willbanks and R. J. Schulz
ARO, Inc.

FOREWORD

The work reported herein was conducted at the Arnold Engineering Development Center (AEDC), Air Force Systems Command (AFSC), under Program Element 65802F.

The results of the research presented were obtained by ARO, Inc. (a subsidiary of Sverdrup & Parcel and Associates, Inc.), contract operator of the AEDC, AFSC, Arnold Air Force Station, Tennessee. The investigation was conducted in the Engine Test Facility (ETF) under ARO Project RW5225 from June 1971 to June 1972, and the manuscript was submitted for publication on May 9, 1973.

Acknowledgment is made to G. W. Lewis of Central Computer Operations for his assistance with the computer calculations.

This technical report has been reviewed and is approved.

EULES L. HIVELY
Research and Development
Division
Directorate of Technology

ROBERT O. DIETZ
Director of Technology

ABSTRACT

An analytical study of icing simulation for turbine engines in altitude test cells was made. A mathematical model of a typical direct-connect type of icing test cell was developed, and the governing equations were programmed for computer solution in FORTRAN computer language. A parametric study was performed to determine the effects of the test cell inlet and water spray conditions on the thermodynamic and kinetic state of the flow in the test section or at the engine compressor face. The importance of correctly simulating droplet size distribution, mean effective droplet diameter, liquid water content, and humidity was investigated. The results of the investigation lend further support to the fact that ground test facilities provide the best available capability for conducting turbine engine icing tests. The ability to define and control the simulated environment gives an altitude test cell distinct advantages not enjoyed by flight testing in natural icing environments or flight testing in artificial environments created by tanker aircraft.

CONTENTS

APPENDIXES

NOMENCLATURE

A	Cross-sectional area
A_{dT}	Droplet capture area
A_p	Projected frontal area
A_t	Throat area of venturi

a	Speed of sound
b	$w_c C_c/\bar{h}$
C	Specific heat
C_D	Drag coefficient
$C_{d,f}$	Flow or discharge coefficient
C_p	Specific heat at constant pressure
C_v	Mass fraction of water vapor
D	Cylinder diameter
d	Droplet diameter
$\bar{d}$	Mass mean droplet diameter
d_m	Mass median droplet diameter
E	Energy
E_c	Capture efficiency
f_c	Condensed phase loading factor, usually the liquid water loading factor in units mass of liquid per unit mass of dry air
h	Enthalpy
h_{fg}	Enthalpy of phase change, liquid to vapor
$\bar{h}$	Surface heat transfer coefficient
K	Inertia parameter
k_x	Mass transfer coefficient
L	Liquid water content, gm/m^3 or stere
ℓ	Liquid water content, lbm/ft^3
M	Mach number
M_d	Droplet mass
$\bar{M}$	Molecular weight

N	Number density
Pr	Prandtl number
p	Static pressure
p_t	Total pressure
p_v	Vapor pressure
Q	Heating rate parameter
q''	Heat flux per unit area
Re	Reynolds number
R_u	Universal gas constant
r	Boundary layer recovery factor
Sc	Schmidt number
T	Static temperature
T_{sf}	Temperature at which supercooled droplet freezes
T_t	Total temperature
U, V	Velocity
W	Mass flow rate
w_e	Rate of impingement of subcooled liquid onto liquid film
w_v	Rate of evaporation
x_v	Mole fraction of water vapor
x	Length, axial
Γ	Parameter related to capture efficiency
γ	Ratio of specific heats
μ	Viscosity

ρ	Density
ω	Specific humidity

SUBSCRIPTS

a	Air
c	Condensed phase, usually liquid but sometimes solid
c_f	Compressor face conditions
d	Droplet
e	Boundary layer edge conditions
g	Gas mixture; water vapor plus noncondensable gases
I	Inlet
IMP	Impinging
i	Index, usually referring to a particular size drop or injection station
max	Maximum value
nc	Noncondensable
o	Entrance region conditions of duct
s	Saturation conditions or droplet surface conditions
T	Tangential trajectory
t	Total
v	Vapor phase
w	Liquid water phase or surface condition
∞	Free-stream conditions

SECTION I
INTRODUCTION

1.1 THE ICING PROBLEM

Ice accretion on aircraft usually causes a degradation of the aircraft performance and operational safety. The degree of degradation is related to the amount of ice adhering to the aircraft and propulsion system components. Because of this, aircraft are routinely equipped with either a system for intermittently removing the accumulated ice (a de-icing system) or a system for continuously maintaining the exposed surfaces of the aircraft free from ice (an anti-icing system). These systems must be tested under conditions which closely simulate or if possible duplicate the natural atmospheric icing conditions. This requires that natural icing conditions be well known and that methods be developed for simulating these conditions for testing purposes. It follows that, to ensure good simulation, the primary variables which define icing conditions must be established and controlled in the test facility during the testing process.

A propulsion engine test facility (Fig. 1, Appendix I) provides a unique capability for simulating aircraft engine environments since the aerodynamic and thermodynamic conditions at the compressor face are accurately controllable. In this facility, the engine is coupled directly to the air supply ducting, and the attempt is made to simulate the flow conditions that would exist at the compressor face in flight. This type of facility has been utilized for conducting icing tests of turbine engines. A recent survey of the state-of-the-art of icing simulation for propulsion engine testing was reported by Kissling (Ref. 1). An important conclusion of Kissling's is that the ground test facility offers the best solution for determing anti-icing system performance because all variables which define an icing condition can be very accurately controlled.

The purpose of this study was to analyze the simulation of icing conditions in propulsion engine test cells as currently practiced. Only the direct-connect type of test cell was considered. While this limits the applicability of the results of the analysis primarily to the testing of pod-mounted engines, the basic approach is applicable to fuselage-mounted engines as well. In the case of engines having inlet ducts, as is usually the case with fuselage-mounted engines, it is, of course, necessary to consider the effect of the inlet ducting on the flow conditions at the compressor face.

1.2 TOPICS CONSIDERED IN THE REPORT

Section II of this report includes discussions of natural icing conditions and the military specifications for conducting icing tests for turbine engines. In Section III, some of the problems associated with simulating icing conditions in an altitude test cell are discussed. An analysis of flow in a direct-connect type of test cell is presented in Section IV, and an application of the analysis follows in Section V. In Section VI, a number of factors affecting icing simulation are discussed.

SECTION II
DISCUSSION OF NATURAL ICING CONDITIONS

2.1 METEOROLOGICAL DATA

The principal factors which determine an icing condition are cloud temperature, liquid water content, and water droplet size distribution, including the "mean effective" droplet diameter for the given droplet size distribution. In addition, the extent and severity of the cloud formation causing the icing condition are important factors, i.e., cloud size and shape. The NACA investigated atmospheric icing phenomena and reported the data from these studies during the period of years between 1940 and 1960. References 2 through 5 are typical reports from this era of icing investigation. Flights were made with specially instrumented aircraft through weather conditions that led to aircraft icing. The data from these flights were cloud liquid water content, cloud temperature as a function of the pressure altitude, and the relation between cloud formation or configuration and modes of ice accretion. The modes of ice accumulation were defined by the rates of ice buildup on the aircraft, that is, if the rates were small or large, and if the accumulation was continuous or intermittent in time. Also, the shape and the texture of the ice accumulation were studied.

Essentially, it was found that the severity of icing can be correlated with the type of icing cloud formation. Moreover, intermittent icing can be associated with one type of cloud formation, and continuous icing can be associated with another type cloud formation. For clarity, the method of summarizing data which was presented in Ref. 4 is quoted in this report as follows: In Ref. 4, it is stated that "the data on liquid-water content, mean-effective droplet diameter, ambient air temperature, and pressure altitude of icing conditions are divided into two categories: for stratiform and cumuliform clouds. Stratiform clouds are layer-type clouds in which the horizontal extent is greater than the vertical thickness. This cloud type includes stratus, strato-cumulus, alto-stratus, and nimbo-stratus. Cumuliform clouds are clouds with vertical extent comparable to the horizontal extent. This cloud type includes cumulus, cumulus congestus, cumulo-nimbus, and alto-cumulus-castellatus. This division of icing situations was necessary because the icing conditions in the two cloud types are very different, owing to the difference in the manner in which they are formed." The continuous mode of icing is associated with the stratiform clouds, and the intermittent icing mode is associated with the cumuliform cloud type. On the average, the liquid water content (grams of water per cubic meter of cloud) was found to be greater in the cumuliform cloud than in the stratiform cloud formations. Thus, moderate to heavy but short duration icing was encountered on the average in cumuliform clouds and light to moderate but long duration icing was incurred on the average in the stratiform cloud types. A concise summary of the meteorological data for icing conditions which occurs on the average for the cumuliform and the stratiform clouds is provided in Ref. 6 and is reproduced and presented in Figs. 2 through 5. Figures 2 and 4 present the correlation between mean effective droplet diameter and liquid water content for stratiform and cumuliform clouds, respectively. Figures 3 and 5 present the relation between ambient temperature and pressure for stratiform and cumuliform clouds,

respectively. It should be noted that the icing conditions defined at the time the data were being obtained were defined in terms of typical aircraft speed, rate of climb, and performance in that era. Icing conditions for modern aircraft may be redefined in the light of modern aircraft performance. That is, modern aircraft performance may well be sufficient reason to redefine continuous or intermittent icing and the relative severity associated with each type icing condition. It is also important to note that the FAA specifications (Ref. 6) for withstanding icing pertain specifically to icing on external aerodynamic surfaces and not to engine performance under icing conditions.

Despite the fact that there is still much of cloud physics which remains to be investigated, sufficient data have been obtained for the icing problem to enable the construction of a fairly comprehensive description of the icing environment. According to Lewis (Ref. 7), the amount of data gathered from reported icing conditions covers such a range and is sufficiently complete that further investigation of natural environments is unnecessary. If this is accepted then the data in the FAA circular can be considered as adequately describing the envelope of possible icing environments for all design and test purposes.

2.5 MILITARY SPECIFICATIONS FOR TURBOJET AND TURBOFAN ENGINE TESTING UNDER ICING CONDITIONS

From the NACA data, such as summarized by the FAA circular, standard icing conditions have been defined for the purpose of testing turbojet and turbofan engines for military applications. These conditions are specified in Ref. 8 and are presented in Table I (Appendix II). The military specifications appear to be definitive at first glance. They define the required gas temperature, the liquid water content, the flight Mach number, and the geometric altitude from which the pressure altitude can be obtained. Also specified is the "mean effective" diameter of the liquid droplets in the icing cloud. Unfortunately, there is ambiguity associated with these specifications. For example, the definition of the "mean effective" drop diameter is not precisely clear. There have been two commonly defined mean effective drop diameters. One is defined as the mass or volume mean diameter. The volume mean diameter is defined by the equation:

$$\bar{d} = \left(\sum_{j=1}^{N_t} (N_j/N_t) d_j^{\,3} \right)^{1/3}$$

where N_j equals the number of drops having a particular diameter (d_j) in a given sample and N_t is the sum total number of all drops in the sample. On the other hand, another mean effective diameter is the mass median diameter defined as the diameter (d_m) of those droplets for which one-half of the entire liquid water content in the spray cloud is contained in droplets whose diameter is less than d_m. The values taken by $\bar{d}$ and d_m from a given sample depend on the distribution of the mass of liquid water among the droplets in accordance to their diameters. Thus, the statement that the mean effective diameter should be "M" microns for icing testing is ambiguous unless the definition of the mean effective diameter is also given. It should be noted that most NACA publications

and the major engine manufacturers use the mass median diameter (d_m) as the mean effective diameter. It may be necessary to specify the droplet-size distribution for icing tests where the amount of ice accumulated is a strong function of the droplet size. This effect will be discussed in a following section of the report. In this report, the mass median diameter is used as the mean effective diameter.

Another possible source of ambiguity is in the definition of gas temperature. The gas temperature is specified as both an atmospheric air temperature and as an "inlet" temperature. The terminology is unclear, since engines are tested with and without an inlet duct. In flight, an engine which is pod-mounted is exposed directly to the free stream. Hence, the direct-connect testing of such an engine is conducted by ducting air to the compressor face, which is conditioned to simulate conditions experienced at the compressor face during flight. A turbojet engine for a fighter-type aircraft typically has the engine mounted in the interior of the aircraft (fuselage-mounted), and the free-stream airflow is ducted to the engine from some inlet air scoop. Thus, there are inlet conditions to the inlet ducting and inlet conditions to the engine compressor. Therefore, the term inlet temperature in the military specifications is not sufficiently clear. A burden is put on the test engineer to decide which inlet condition to consider. In previous icing tests, it has been assumed that the specified temperature is the free-stream total temperature. The ambiguity in the military specification can be removed if the defined conditions are specified as free-stream total conditions rather than inlet conditions. Thus T_∞ or T_{t_∞}, p_∞ or p_{t_∞}, humidity (ω_∞), liquid water content (L), M_∞, and $\bar{d}$ or d_m can completely define icing conditions. Note that in this study it is recommended that the free-stream humidity (ω_∞) be also specified. Reasons for this recommendation will be given in the following sections of this report. At present, ω_∞ is not given in the military specification. In typical previous tests, ω_∞ has been set to the saturation value corresponding to T_{t_∞} and p_{t_∞}. It is expected that, in natural icing conditions, the relative humidity is approximately 100 percent so that ω_∞ corresponds to saturation at the ambient atmospheric conditions.

Another important point to consider for defining atmospheric icing conditions is whether the drop-size distribution must be specified and required during test simulation in addition to specification of the mean-effective diameter. The reason is that the icing on engine components could be sensitive to drop-size distribution. This question is considered later in the report.

To summarize this section of the report, the military specifications for icing testing can be made sufficiently definitive by specifying free-stream static or total conditions of pressure and temperature, flight Mach number, free-stream humidity, liquid water content, and a precisely defined mean effective diameter. This latter parameter should be specified as either the mean volumetric or mass median.

SECTION III
ICING CONDITIONS IN PROPULSION ENGINE TEST CELLS

3.1 DISCUSSION

Ideally, a test cell for conducting icing tests should duplicate the flow conditions at the compressor face experienced by an engine in flight through an icing cloud. The flow conditions are characterized by temperature, humidity, pressure, velocity, liquid water content, mean effective droplet size, and droplet-size distribution. It is generally not practical and frequently impossible to duplicate all of the flow conditions encountered in atmospheric icing. Fortunately, however, it is not necessary to duplicate all of the icing conditions to get adequate simulation.

Briefly, the method used to produce ice accretion on turbojet and turbofan engine inlet components for icing testing is to inject a continuous spray of water droplets into a cold airstream directed at the engine. A typical icing test cell is shown schematically in Fig. 1. The water droplets are accelerated to near the airspeed by aerodynamic drag. Through heat and mass transfer, the droplets are expected to come to the proper supercooled condition. Air-atomizing spray nozzles are typically used to produce the spray cloud of droplets having the desired mean effective diameter.

In the previous section, it was noted that the icing specifications are given in terms of flight conditions. Since the flow conditions at the compressor face are rarely the same as the flight conditions, the air having been accelerated or diffused before entering the engine, it is necessary to relate the engine inlet conditions to the free-stream conditions. This is discussed further in the following sections. The problem of establishing and monitoring the liquid water content and mean effective droplet size of the spray cloud in the test cell is considered in the following section.

3.2 RELATION BETWEEN FREE-STREAM AND ENGINE COMPRESSOR INLET CONDITIONS

For purposes of discussion, flow from the free stream to the engine compressor inlet is assumed to be one-dimensional and isentropic. This is a good assumption for a pod-mounted engine. The validity of the assumption for an engine having a long inlet duct depends on the duct shape and flow conditions.

To simulate the free-stream temperature, pressure, and flight velocity in the test cell, the total pressure and total temperature at the compressor inlet are set equal the total pressure and total temperature computed from the altitude static pressure and static temperature and the flight Mach number. Based on results to be discussed later, it has been found that flow from the free stream to the compressor inlet occurs at essentially constant specific humidity. Hence, the specific humidity at the compressor inlet in the test cell should be set equal to the specific humidity of the air at the flight conditions

being simulated. In a natural icing cloud, it is expected that the supercooled liquid is in equilibrium with its saturated vapor at the local ambient temperature. That is, the relative humidity in the cloud is 100 percent. The specific humidity (ω) at the compressor is given by

$$\omega = \frac{\overline{M}_v}{\overline{M}_a} \frac{p_{v_\infty}}{p_\infty} = 0.622 \frac{p_{v_\infty}}{p_\infty}$$

where p_{v_∞} is the saturation pressure of supercooled liquid at the free-stream static temperature (T_∞), and p_∞ is the free-stream static pressure, i.e., altitude pressure. The relative humidity at the compressor will be 100 percent only if the compressor inlet flow velocity equals the flight speed. Thus, the flow entering the engine will generally not be in thermal equilibrium since equilibrium can exist only at 100-percent relative humidity. The importance of humidity on the icing problem is that humidity affects the heat and mass transfer from droplets in the spray and the heat and mass transfer from exposed surfaces within the engine inlet. These effects are analyzed and illustrated quantitatively in the following sections.

Acceleration or deceleration of the flow from the free stream to the compressor inlet results in a change in the liquid water content. Two separate phenomena are involved. One is the compressibility of the gas. The second phenomenon is droplet inertia and the inability of the droplets to follow streamlines exactly. This problem is discussed in detail in a following section. It is sufficient to remark here that the liquid water content generally changes by less than 30 percent from free stream to engine face. In Section VI, it is shown that the power required to maintain an anti-icing condition is not highly dependent on liquid water content. Thus a 30-percent correction to the liquid water content may not be an important consideration for icing cloud simulation.

3.3 MEAN EFFECTIVE DROPLET DIAMETER DETERMINATION

During engine icing tests in propulsion facilities, it is necessary to ensure that the water spray cloud is characterized by the desired mean effective drop diameter. One established method to measure drop sizes is to capture a sample of drops from the spray cloud on an oil-film covered slide. The slide is usually exposed to the water-air mixture for a short time at some flow station downstream of the water spray station. Then the slide water droplet sample is analyzed to determine the droplet size-frequency distribution. From this distribution, the mean effective diameter can be calculated. Unfortunately, this method, while simple and convenient, is not accurate. Correction factors must be introduced into the analysis of the droplet distribution because of droplet evaporation after being captured, because the drops may not be spherical in form in the oil film but may flatten, and because the slide samples only a very small portion of the air-water mixture flowing through the duct. A much more accurate and modern technique for determining conditions in the water spray cloud utilizes laser holography. With a laser-holographic camera system such as described by Gall and Floyd (Ref. 9) a three-dimensional photograph of any point in the duct flow can be obtained. From the

photograph, an analysis of the number of drops, their size, and free-flight shape can be made. With a sufficiently varied sampling across the entire duct, an accurate analysis of the spray cloud can be obtained. This process can be done "on-line" during the icing test, using an electronic scanning device to count only those water droplets whose form is clearly in focus in the hologram.

3.4 TECHNIQUE FOR SETTING LIQUID WATER CONTENT

The proper liquid water content of the air-water mixture is maintained by metering the airflow and the water flow, and adjusting the water flow rate to the desired amount. The relationship between the liquid water content (L or ℓ) and the actual water loading factor (f_c) in lbm of water per lbm of air can be obtained from considering the flow in a stream tube in the free stream.

$$f_{c_\infty} = \frac{W_{w_\infty}}{W_{a_\infty}} = \frac{\ell_\infty A V_w}{\rho_{a_\infty} A V_a} = \frac{\ell_\infty}{\rho_{a_\infty}} = \frac{\ell_\infty R_u T_\infty}{\bar{M}_a p_\infty} \tag{1}$$

or in particular where the liquid water content is in gm/m^3, T in °R, and p in psf:

$$f_{c_\infty} = 3.326 \times 10^{-3} \frac{L_\infty T_\infty}{p_\infty} \tag{2}$$

Since L is usually specified for free-stream icing conditions, T and p are the free-stream static temperature and pressure, respectively. The engine mass flow in the test facility is metered, often using a critical-flow venturi. In this case,

$$W_a = \frac{0.532\, C_{d,f}\, p_{t_\infty} A_t}{\sqrt{T_{t_\infty}}} \tag{3}$$

for mass flow metering venturis operating at a critical (choked) condition; $C_{d,f}$ represents a known discharge or flow coefficient. By using this equation and Eq. (2) for f_c, the water flow rate can be written as

$$W_{w_\infty} = \frac{0.532\, C_{d,f}\, p_{t_\infty} A_t}{\sqrt{T_{t_\infty}}} \left[3.326 \times 10^{-3} \frac{L_\infty T_\infty}{p_\infty}\right] \tag{4}$$

Since T_∞ and p_∞ are related to the total conditions (T_{t_∞} and p_{t_∞}) through the isentropic Mach number relations, the equation for W_w can be written:

$$W_w = 1.77 \times 10^{-3}\, C_{d,f} L_\infty A_t \sqrt{T_{t_\infty}} \left(1 + \frac{\gamma - 1}{2} M_\infty^2\right)^{\frac{1}{\gamma - 1}} \tag{5}$$

where M_∞ is the free-stream flight Mach number for the icing condition being simulated.

Equation (1) is valid so long as the water in the streamtube remains constant. In flight, the engine often causes the flow upstream of the inlet to accelerate or decelerate depending on the particular flight condition (see Fig. 6). If the water droplets have sufficient inertia, it is possible that they would not follow streamlines entering the engine. For this case, Eq. (1) does not give the correct loading factor. The amount by which Eq. (1) would have to be corrected when the droplet inertia is important can be quantitatively estimated as follows: The basic equation for the loading factor was

$$f_c = \frac{W_w}{W_a} \tag{6}$$

The amount of water (W_w) to be sprayed in the test cell is related to the conditions in the atmosphere encountered by the engine during its operation. Clearly, W_w thus depends on the free-stream liquid water content (ℓ_∞), the flight velocity, and whether droplets follow streamlines or not. When the engine is operating under static conditions, it is quite reasonable to expect that the amount of water ingested is equal to the liquid water content (ℓ_∞) times the air volumetric flow rate through the engine. Hence,

$$f_{c_{\substack{\text{static ambient} \\ \text{condition}}}} = \frac{\ell_\infty V_\infty}{W_a} = \frac{\ell_\infty}{\rho_a} = \frac{R_u \ell_\infty T_\infty}{\bar{M}_a p_\infty} \tag{7}$$

Therefore, it is not necessary to consider droplet inertia for the static ambient icing conditions, and this case is identical to the case where droplets follow streamlines.

The other case to consider is where droplets follow straight paths, i.e., their trajectories are not influenced by the disturbed flow field upstream of the engine inlet. In this case, the water flow rate is given by

$$W_w = A_p V_\infty \ell_\infty = A_{cf} V_\infty \ell_\infty \tag{8}$$

On the other hand, the airflow rate is given by

$$W_a = \rho_\infty A_\infty V_\infty = \rho_{cf} A_{cf} V_{cf} \tag{9}$$

Therefore,

$$f_c = \frac{W_w}{W_a} = \frac{A_{cf} V_\infty \ell_\infty}{\rho_\infty A_\infty V_\infty} = \frac{\ell_\infty A_{cf}}{\rho_\infty A_\infty} \tag{10}$$

But since f_{c_∞} can be defined by

$$f_{c_\infty} = \frac{\ell_\infty}{\rho_\infty} = \frac{R_u \ell_\infty T_\infty}{\bar{M}_a p_\infty} \tag{11}$$

as the free-stream loading factor, then

$$f_c = f_{c_\infty} \frac{A_{cf}}{A_\infty} \tag{12}$$

This is the required loading factor when droplets are not influenced by streamlines. To put this in a more precise form, the flow from the free stream to the compressor face is approximately isentropic, in which case

$$\frac{A_{cf}}{A_\infty} = \Gamma = \frac{M_\infty}{M_{cf}} \left[\frac{\left(1 + \frac{\gamma-1}{2} M_{cf}^2\right)}{\left(1 + \frac{\gamma-1}{2} M_\infty^2\right)} \right]^{\frac{\gamma+1}{2(\gamma-1)}} \tag{13}$$

Thus,

$$\frac{f_c}{f_{c_\infty}} = \Gamma \tag{14}$$

This relation has been evaluated for the military icing specifications, assuming two representative values of M_{cf}, and the results are presented in Fig. 7. The relationship is shown between the water loading factor which must be established in the test cell to the free-stream water loading factor based on free-stream liquid water content, pressure, and temperature. The two curves represent limiting cases for establishing the water loading factor for icing tests. Where droplets follow streamlines exactly and for static environment icing conditions, $f_c = f_{c_\infty}$. Where droplets are not influenced by streamlines, $f_c = \Gamma f_{c_\infty}$, where Γ must be determined by the values of M_∞ and M_{cf}.

A question arises as to which limiting case is more realistic for evaluating f_c for testing purposes; that is, do droplets follow streamlines or not? To estimate representative values of Γ, an average Γ value can be defined as

$$\bar{\Gamma} = \frac{\Gamma + 1}{2} \tag{15}$$

and the following table was devised:

M_∞	M_{cf}	$\Gamma = f_c/f_{c_\infty}$	$\bar{\Gamma}$
0.32	0.25	1.25	1.125
0.71	0.25	2.21	1.605
0.32	0.50	0.70	0.85
0.71	0.50	1.23	1.115

It is evident from this table that, on the average for military testing purposes, the highest amount of additional water which must be injected into a test cell to simulate correctly the proper engine ingestion of water is about 60 percent greater than the free-stream water loading. This pertains to the case where the engine is throttled back, yet the airspeed remains fairly high during aircraft descent. This result compares with the "scoop factor" of 1.33 presented in Ref. 10 for the same kind of flight condition called the "idle descent" mode. For the majority of the test points, however, as indicated by the average Γ factor, the test cell loading factor (f_c) is approximately equal to the free-stream loading factor. The next important question is to determine how sensitive the engine anti-icing power requirements are to variations in liquid water content, hence to f_c. If they are relatively insensitive, then it is reasonable to establish $f_c = f_{c_\infty}$ (Eq. (2)) for all icing tests defined in the military specifications.

3.5 SUMMARY

The air at the inlet of the bellmouth connecting the test facility plenum to the engine inlet must have the correct total pressure, total temperature, and humidity such that the condition of the water-air mixture at the engine compressor face simulates the flight condition. In general, the water loading factor (f_c) should be established equal to the water loading factor of the free-stream icing conditions.

SECTION IV
ANALYSIS OF MULTIPHASE FLOW WITH APPLICATION TO AN ICING TEST CELL

4.1 INTRODUCTION

In this section, an analysis of a typical direct-connect type of turbine engine icing test cell is presented. Through a number of simplifying assumptions, the problem is reduced to an analysis of one-dimensional flow in a variable area duct. The analysis provides a means for predicting the thermodynamic and kinetic state of the air-water mixture at the test section. It is useful in determining the test cell inlet conditions required to simulate a given icing condition.

The analysis parallels the analysis of exhaust gas spray coolers by Pelton and Willbanks (Ref. 11).

4.2 THE BASIC ASSUMPTIONS USED FOR DEVELOPING THE MATHEMATICAL MODEL OF THE MULTIPHASE AIR-WATER DUCT FLOW

Figure 8 shows a schematic of the icing test facility being considered. The duct has an arbitrary cross-sectional area, and water is injected parallel to, and in the direction of, the gas flow at some location along the duct. The analysis is based on overall conservation of species, mass, momentum, and energy both globally and in each phase.

The mathematical model for flow in the duct is based on the following assumptions:

1. All gases including water vapor are treated as ideal gases.

2. One-dimensional flow.

3. The gas phase is homogeneous at any axial station except in the boundary layers of the droplets.

4. The drop-size distribution of the spray can be characterized by discrete drop sizes.

5. Drops are injected parallel to and in the direction of the gas flow and remain entrained in the gas stream throughout the duct. That is, de-entrainment by gravity and turbulent diffusion is considered negligible.

6. Each drop injected maintains its identity through the duct. Hence, collisions, agglomeration, and drop breakup are considered negligible.

7. The drops are uniformly distributed at any cross section of the duct.

8. Internal resistance to heat transfer within a drop is much lower than external or film resistance to heat transfer. Thus, the internal temperature of a drop is uniform at any instant of time.

9. Heat transfer and friction at the duct walls are negligible.

10. Cross-sectional area of the duct is a prescribed function of axial location.

11. The drops are spherical in shape.

12. Drops can be supercooled to a critical temperature which is a prescribed function of drop diameter.

13. Upon reaching the critical temperature, the drop temperature suddenly rises to the freezing point and becomes a homogeneous equilibrium mixture of solid and liquid. The drop remains at the normal freezing point until enough heat has been removed to completely freeze the drop.

14. Vaporization and condensation are occurring at any instant at equilibrium rates. That is, at any instant, the drop surface vapor pressure is equal to the saturation pressure corresponding to drop temperature. The droplets of interest in icing problems are large enough for the effect of surface tension on vapor pressure to be negligible.

4.3 THE BASIC EQUATIONS OF CONSERVATION

Based on the assumptions of the previous section, the following global conservation equations can be written:

Conservation of Mass

$$\mathbb{W}_v + \mathbb{W}_{nc} + \sum_i \mathbb{W}_{c_i} = \mathbb{W} = \text{Constant} \tag{16}$$

Conservation of Water (Condensed Phase + Vapor)

$$\mathbb{W}_v + \sum_i \mathbb{W}_{c_i} = \mathbb{W}_\omega = \text{Constant} \tag{17}$$

Conservation of Noncondensable Gas

$$\mathbb{W}_{nc} = V_g \rho_g (1 - C_v) A = \text{Constant} \tag{18}$$

Conservation of Momentum

$$V_g^2 \frac{dC_v}{dx} + (1 - C_v) V_g \frac{dV_g}{dx} + V_g (1 - C_v)^2 \sum_i \left(V_{c_i} \frac{df_{c_i}}{dx} + f_{c_i} \frac{dV_{c_i}}{dx} \right) + \frac{1 - C_v}{\rho_g} \frac{dp}{dx} = 0 \tag{19}$$

Conservation of Energy

$$\frac{\left(h_v + V_g^2/2\right)\frac{dC_v}{dx}}{(1 - C_v)^2} + \frac{C_v}{1 - C_v}\left(\frac{dh_v}{dx} + V_g \frac{dV_g}{dx}\right) + \frac{dh_{nc}}{dx} + V_g \frac{dV_g}{dx} + \sum_i \left(h_{c_i} + \frac{V_{c_i}^2}{2}\right)\frac{df_{c_i}}{dx} + \sum_i f_{c_i}\left(\frac{dh_{c_i}}{dx} + V_{c_i}\frac{dV_{c_i}}{dx}\right) = 0 \tag{20}$$

Mass, momentum, and energy transfer between phases can be treated by first considering these processes for a single droplet. For droplet of class i, the following conservation equations apply:

Conservation of Mass

$$V_{c_i} \frac{dM_{d_i}}{dx} = k_{x_i} \pi d_i^2 \overline{M}_v \frac{x_v - \left(x_{v_s}\right)_i}{1 - \left(x_{v_s}\right)_i} \tag{21}$$

Conservation of Momentum

$$M_{d_i} V_{c_i} \frac{dV_{c_i}}{dx} + \left(V_{c_i} - V_g\right) V_{c_i} \frac{dM_{d_i}}{dx} = \rho_g \frac{\pi d_i^2}{4} C_D \frac{\left|V_g - V_{c_i}\right|\left(V_g - V_{c_i}\right)}{2} \tag{22}$$

Conservation of Energy

$$V_{c_i} \frac{dE_{c_i}}{dx} = \bar{h}_i \pi d_i^2 [T_\infty - (T_s)_i] + h_v|_{T_{s_i}} V_{c_i} \frac{dM_{d_i}}{dx} \tag{23}$$

By considering all droplets of class i,

$$\frac{df_{c_i}}{dx} = \frac{f_{c_i}}{M_{d_i}} \frac{dM_{d_i}}{dx} \tag{24}$$

and

$$\frac{d(h_{c_i} W_{c_i})}{dx} = \frac{\dot{W}_{c_i}}{M_{d_i}} \frac{dE_{d_i}}{dx} \tag{25}$$

The equation of state is

$$p = \frac{R_u \rho_g T_g}{x_v \bar{M}_v + (1 - x_v) \bar{M}_{nc}} \tag{26}$$

The molar fraction and mass fraction of vapor are related by

$$x_v = \frac{C_v / \bar{M}_v}{C_v / \bar{M}_v + (1 - C_v) / \bar{M}_{nc}} \tag{27}$$

Droplet diameter and mass are related by the expression:

$$d_i = \left(\frac{6 M_{d_i}}{\pi \rho_c} \right)^{1/3} \tag{28}$$

The molar fraction of vapor at a droplet surface is related to saturation pressure and static pressure by

$$\left(x_s \right)_i = p_v|_{T_{s_i}} / p \tag{29}$$

For low rates of mass transfer, the heat and mass transfer coefficients for spherical droplets can be obtained from the semi-empirical equation of Ranz and Marshall (Ref. 12). Thus,

$$k_x = \frac{\mu}{dScM}(2.0 + 0.6\ Re^{1/2}Sc^{1/3}) \tag{30}$$

and

$$\bar{h} = \frac{\mu C_p}{d\ Pr}(2.0 + 0.6\ Re^{1/2}Pr^{1/3}) \tag{31}$$

where the Reynolds number is given by

$$Re = \frac{|V_g - V_c|\rho_g d}{\mu} \tag{32}$$

Carlson and Hoglund (Ref. 13) determined the following semi-empirical equation for the drag coefficient of a solid sphere in low-speed flow and in the absence of mass transfer:

$$C_D = \frac{24}{Re}(1 + 0.15\ Re^{0.687}) \tag{33}$$

This relation is assumed to be valid for low rates of surface mass transfer as well. The above transport equations are used in the present study although the rates of mass transfer immediately following droplet injection may be high. Since the rate of mass transfer drops off to a low value very rapidly, the error introduced by omitting corrections to $\bar{h}$, k_x, and C_p for high rates of mass transfer is believed to be small.

4.4 A MODEL FOR DROPLET FREEZING

Many experiments have confirmed the fact that liquid water can exist in a supercooled state (Ref. 14). However, the results of the many studies are not completely in agreement with regard to the parameters governing the maximum degree of supercooling. Factors affecting maximum supercooling to some degree include: rate of cooling, concentration of impurities, and drop size (Refs. 14 through 16).

In the present study, the following simple model is proposed for freezing a droplet. It will be assumed that the maximum degree of supercooling is a known function of only the droplet diameter. Thus, a drop of given diameter can be supercooled to some critical temperature. Upon reaching the critical temperature, the temperature of the drop suddenly rises to the normal freezing point and becomes a homogeneous equilibrium mixture of solid and liquid. The relative fractions of solid and liquid are governed by the initial degree of supercooling. The drop remains at the freezing point until enough heat has been removed to completely freeze the drop.

A curve of critical temperature as a function of drop diameter was deduced from data given in Ref. 15 and is illustrated in Fig. 9. The data can be correlated by the following equations:

$$T_{sf} = 463.2 + 16.32\,\ell n\,(0.0333d) \qquad d \leq 300 \qquad (34)$$

and

$$T_{sf} = 463.2 \qquad 300 \leq d \leq 1000$$

where T_{sf} is in °R and d is the droplet diameter in microns. This relationship represents the average critical temperature for a large number of drops of given diameter. The variation in critical temperatures of individual drops from the average may be quite large. For purposes of the present study, it is assumed that all of the drops of a given diameter freeze upon reaching the critical temperature in the manner given above.

4.5 THERMODYNAMIC PROPERTY DATA

It is necessary to specify the thermodynamic property data including enthalpy, specific heat, and vapor pressure of each constituent as a function of temperature. The following equations serve this purpose.

4.5.1 Property Data for Air

For air, the enthalpy and specific heat data given in Ref. 17 are satisfactorily correlated by

$$C_{p_{nc}} = 0.2318 + 0.1040 \times 10^{-4}T + 0.7166 \times 10^{-8}T^2$$

and

$$h_{nc} = 0.2318T + 0.0520 \times 10^{-4}T + 0.2389 \times 10^{-8}T^3 - 127.064$$

where T is in °R, $C_{p_{nc}}$ is in Btu/lbm-°R, and h is in Btu/lbm. This correlation is valid for $400 \leqslant T \leqslant 1700$. The subscript nc is used since air is the noncondensable species in the flow.

4.5.2 Property Data for Water Vapor

For water vapor, the enthalpy and specific heat data of Ref. 18 are satisfactorily correlated by

$$C_{p_v} = 0.4304 + 0.1678 \times 10^{-4}T + 0.2781 \times 10^{-7}T^3$$

and

$$h_v = 0.4304T + 0.0839 \times 10^{-4}T^2 + 0.0927 \times 10^{-7}T^3 + 806.6$$

where T is in °R, C_{p_v} is in Btu/lbm-°R, h_v is in Btu/lbm, and $400 \leq T \leq 1700$.

4.5.3 Property Data for the Condensed Phases

The specific heat of the liquid phase was taken to be 1 Btu/lbm-°R, and the specific heat of the solid phase was taken to be 0.485 Btu/lbm-°R.

4.5.4 Vapor Pressure of the Condensed Phase

The following equation is a reasonably good correlation of the vapor pressure of liquid water as given in Ref. 11 over the temperature range $492 \leq T \leq 672$:

$$p_v = 2117.0\left(\frac{672}{T}\right)^{5.19} \exp\left\{-9.06\left(\frac{h_{fg}}{T} - 1.4525\right)\right\}$$

where T is in °R, p_v is in psfa, and h_{fg} is the latent enthalpy of evaporization given by

$$h_{fg} = 1352.3 - 0.5696T + 0.0839 \times 10^{-4}T^2 + 0.0927 \times 10^{-7}T^3$$

The vapor pressure in psfa of supercooled liquid, that is, liquid at a temperature less than 492°R, is given by the following equation as taken from Ref. 14:

$$p_v = 2117.0 \exp\left\{2.3\left[A_1 + \frac{B_1}{t} + \frac{C_1(t^2-K)}{t}\left[10^{(D_1(t^2-K)^2)} - 1\right] + E_1\left[10^{(F_1(374.11-t)^{5/4})}\right]\right]\right\}$$

where

t (= T/1.8) is the absolute temperature in degrees Kelvin, and A_1, B_1, C_1, D_1, E_1, F_1, and K are constants whose values are:

$A_1 = 5.4266514$

$B_1 = -2005.1$

$C_1 = 1.3869 \times 10^{-4}$

$D_1 = 1.1965 \times 10^{-11}$

$E_1 = -4.4 \times 10^{-3}$

$F_1 = -5.7148 \times 10^{-3}$

$K_1 = 2.937 \times 10^{5}$

The equation for the vapor pressure of ice in psfa as given in Ref. 14 is

$$p_v = 2.7845 \exp \{2.3[A_2/t + 0.4343B_2 \ell n(t) + C_2 t + D_2 t^2 + E_2]\}$$

where

t (= T/1.8) is the absolute temperature in degrees Kelvin and A_2, B_2, C_2, D_2, and E_2 are constants whose values are:

$A_2 = -2.4455646 \times 10^3$

$B_2 = 8.2312$

$C_2 = 1.677006 \times 10^{-2}$

$D_2 = 1.20514 \times 10^{-5}$

$E_2 = -6.757169$

4.6 THE COMPUTER PROGRAM

The system of equations is closed and can be integrated for specified initial conditions to give the variation in thermodynamic and kinetic states along the duct. The equations were programmed in FORTRAN IV language for solution on a digital computer. A program listing is given in Appendix III. The computer program developed in connection with a study of spray coolers and reported in Ref. 11 was used as the basis for the program in Appendix III.

The program has the capability to handle multiple water spray stations at arbitrary locations along the duct. The drops originating at any station must have uniform diameters. The drop diameter may, however, vary from station to station. With this capability, a spray with a distribution of drop sizes can be treated, providing the distribution can be characterized by a finite number of discrete drop sizes. To accomplish this, each drop-size class (i) is assigned to an individual injection station (i). From a given distribution of drop sizes, the fraction of injected liquid containing droplets in size class (i) can be determined. This fraction corresponds to the fraction of the total liquid injection rate to be assigned to injection station (i).

In the computer program, droplet freezing is handled in the following way: The temperatures of drops originating at each injection station are monitored, and when the temperature of a droplet reaches its freezing temperature defined by Eq. (34), then the droplet is considered to start freezing. An energy balance predicts the state of the droplet at each step in the flow while the droplet temperature is held constant at 492°R (32°F). After sufficient energy is lost from the droplet by conduction and evaporation to turn the droplet completely to ice, the droplet model is replaced by an ice particle model, and its temperature is allowed to vary. For the rest of the calculations, the particular size drop that has frozen is treated as a spherical particle of ice, and its temperature is again determined by energy and mass transfer at the ice particle surface.

4.7 SUMMARY

An analysis of the multiphase flow phenomena occurring in a typical turbine engine icing test cell duct flow was presented. The analysis was based on one-dimensional flow of a mixture of air, water vapor, liquid water, and ice in a variable area duct.

In the following section, the analysis and computer program are used to make calculations for a typical icing test cell. A parametric study is performed to determine the influence of the initial conditions on the final thermodynamic and kinetic states.

SECTION V
APPLICATION OF THE MULTIPHASE FLOW ANALYSIS: A PARAMETRIC STUDY

5.1 INTRODUCTION

In this section, results obtained with the multiphase flow analysis for flow in an icing test facility under typical operating conditions are reported and discussed. A parametric study was performed to determine the influence of the inlet conditions on the kinetic and thermodynamic flow properties at the test section.

The particular duct geometry chosen for the study is shown in Fig. 10. The bellmouth entrance approximates the inlet section of the AEDC Propulsion Engine Test Cell (J-1) and typifies many other installations. The inlet parameters which were used are:

1. The primary thermodynamic and kinetic state variables such as pressure, temperature, bellmouth inlet velocity, and humidity

2. The water loading factor (f_c) which gives the mass of liquid water sprayed into the airflow at the duct inlet per unit mass of air

3. The water injection velocity

4. The mass median water droplet diameter

5.2 THE EFFECT OF MATHEMATICALLY SIMULATING THE WATER SPRAY CLOUD WITH A DISTRIBUTION OF DROPLETS AS COMPARED WITH SIMULATING THE WATER SPRAY CLOUD WITH A SINGLE-SIZE DROPLET

The analysis was first applied to study the effect of a spray cloud with a droplet distribution on the kinetic and thermodynamic state of flow through the duct in comparison with the effects of a spray having only a single-sized drop. For the latter spray, the drop size was equal to the mass median diameter of the given distribution. The distribution was obtained from Ref. 9 and is a measured distribution from an icing

simulation test utilizing such a duct flow. The mass median diameter was approximately 25 microns, and the mass mean diameter was approximately 18 microns. Figure 11 shows three drop-size distributions that were presented in Ref. 9. The distribution utilized in this study is distribution A-3 of Fig. 11. The specific purpose of this mathematical experiment was to determine theoretically if the practice of characterizing an engine icing condition by the liquid water content of the flow and a mean effective drop diameter in the spray cloud is a valid method for correlating the final state of the water-airflow at the engine station with the given duct inlet conditions. If not, then it is necessary to take into account the actual distribution of droplet sizes produced in the spray cloud by the atomizing nozzle system when trying to correlate engine icing conditions with duct inlet conditions. Thus, another possible effect of the droplet distribution, other than on the capture efficiency of the component parts of the engine inlet, may be to affect the thermodynamic and kinetic state of the multiphase duct flow.

The results of the calculations made with the droplet distribution mathematical simulation and the mean effective diameter simulation are shown and compared in Figs. 12, 13 and 14. The other initial conditions assumed are presented in these figures. In Fig. 12, the local static gas temperature (T_g) is plotted versus length from the duct inlet. The gas temperature is not highly dependent on whether the spray cloud is characterized by having a distribution of droplet sizes or a single uniform drop size. Figure 13 shows the liquid droplet temperatures for each size drop in the distribution plotted against length from the duct inlet. Again, while the larger droplets in the spray cloud required greater length of flow before reaching a quasi-equilibrium temperature, all size droplets have reached approximately the same temperature at the engine station, and this is the same temperature reached by the mass median drop (Fig. 14). Therefore, for typical icing conditions, the characterization of the icing conditions by liquid water content and mean effective drop diameter is sufficiently accurate for testing purposes. The engine icing conditions can be correlated in terms of these two parameters.

By using the droplet freezing model in the program, a comparison was made with the same model droplet distribution spray cloud mentioned earlier and the single uniform size spray cloud of the mean effective diameter of the distribution. The computations showed that for the typical icing test conditions, the freezing model chosen, and droplet sizes for icing, there was no droplet freeze-out. The droplets remain subcooled and unfrozen for duct lengths of up to 40 ft from inlet to engine station. Thus, the icing conditions defined by the military specifications for engine testing can be characterized by liquid water content and mass median diameter, and for these conditions there should be no change in the liquid water content because of droplet freeze-out. It should be noted, of course, that in a real test facility, droplet freeze-out may occur when there is contamination of the spray water with particles that enable ice nucleation and crystal formation. However, this problem was not considered in this study.

5.3 PARAMETRIC STUDY OF THE EFFECTS OF THE THERMODYNAMIC AND KINETIC DUCT INLET PARAMETERS ON THE STATE OF THE FLOW AT THE TEST SECTION

5.3.1 Description of the Baseline Values of the Duct Inlet Parameters

For the duct geometry previously discussed, a parametric study was carried out by varying the duct inlet properties one at a time. The inlet variables that were studied are given below along with their baseline values. The baseline values of the duct inlet (initial) parameters are as follows:

1. Liquid water initial temperature, T_s (632°R or 172°F)
2. Liquid water content, L (1 gm/m^3 or 6.234 x 10^{-5} lbm/ft^3)
3. Inlet air specific humidity, ω_∞ (3.715 x 10^{-3} lbm H_2O/lbm air)
4. The mass median drop diameter, d_m (3.175 x 10^{-4} ft or 96.8 microns)
5. The water injection velocity, V_s (8.35 ft/sec)
6. Air inlet velocity, V_g (80.6 ft/sec)
7. Duct radius at constant area section, R (3.8 ft)

The reason d_m was chosen at approximately 100 microns rather than a more representative value of, say, 25 microns is simply that small drops cool faster than larger drops. Thus, for the larger baseline droplet chosen, the axial variations of the other properties were more clearly defined when the baseline drop diameter was 100 microns than if it were 25 microns. This effect will be evident in the figure to be presented showing effects of varying drop diameter. The results of the parametric study are discussed in the following sections.

5.3.2 The Effect of Variation of Initial Water Temperature

The effect of the temperature variation of the water spray into the bellmouth was negligible; that is, the final state of the air-water mixture at the engine station did not depend significantly on the temperature of the injected water. These results are shown in Figs. 15 and 16 where the temperature difference (ΔT) is plotted versus length from the duct entrance. The obvious explanation of these results is that the amount of water being sprayed into the bellmouth in an icing simulation (and hence the amount of energy carried into the bellmouth by the water) is extremely small compared with the mass flow (or the energy flow) of air. Thus, the process in the duct for icing simulation is nearly a constant energy flow, not considering heat transferred through the duct walls. The gas temperature at the engine station depends primarily on the gas total temperature and

the Mach number of the flow at the engine station. The water droplets cool quickly down to approximately the same quasi-equilibrium temperature which, it was found later, could be predicted in terms of the air temperature and humidity at the engine station. It should be emphasized that this conclusion applies only for small liquid water loading typical of icing simulations.

5.3.3 The Effect of Variation of Initial Liquid Water Content (Loading Factor)

The effect of the variation of the liquid water content (L) from about 1 to 10 gm/m^3 on the final temperature of the airflow is shown in Fig. 17 to be small. Again, the reason for this small effect is that the absolute quantity of water sprayed into the duct flow is very small compared with the mass flow of air. The variation of L from 1 to 10 gm/m^3 caused only a minor variation in the gas temperature at the engine station (4°R) and extremely small effect on pressure and velocity of the airflow at the engine station. Also, the temperature of the liquid water at the engine station did not change significantly with variation of the liquid water content. This is shown in Fig. 18 where ΔT is plotted versus duct length. In this figure, there is, at most, two degrees difference between the water temperature at the engine station over this range of liquid water content.

5.3.4 The Effect of Variation in Mass Median Droplet Diameter

The effect of varying the mean effective diameter is shown in Fig. 19. As stated previously and shown in Fig. 19, small drops cool down faster than large drops. As Fig. 19 indicates, a spray cloud of uniform sized drops of 25-micron diameter cools down at a much faster rate than a spray cloud of 100-micron diameter drops. The 25-micron drop temperature drops below the gas temperature but then recovers and approaches the gas temperature. Droplets of 200 microns and larger will be substantially out of equilibrium with the gas temperature at 25 ft from the duct inlet. This size of droplets requires a duct length substantially longer than 25 ft before their temperature would come to within a few degrees of the gas temperature. The water spray system must produce only a very small number of drops larger than, say, 200 microns to minimize their effect on the icing simulation.

5.3.5 The Effect of Variation in Inlet Air Humidity

The effects of varying the inlet air relative humidity from zero (completely dry air) to 100 percent (completely saturated air) are shown in Fig. 20. It can be noted that the inlet humidity is very important in determining the temperature of the water droplets. The reason is that evaporation and condensation at the droplet surface play major parts in determining droplet temperature. In general, the rate of surface mass transfer is highly dependent on the humidity of the air surrounding the droplet. By controlling the inlet humidity, it is, therefore, possible to have some degree of control over the thermal state in the test section.

5.3.6 The Effect of the Difference between Inlet Airflow Velocity and Inlet Water Velocity

The effect of the variation of the water injection velocity on the water temperature at the engine station is shown in Fig. 21. This figure shows that as the velocity difference between the water spray cloud and the airflow is decreased, a greater length of flow is required before the water temperature approaches the air temperature; that is, increasing the relative velocity increases the heat and mass transfer from the drops. The coefficients of mass and heat transfer are defined by Eqs. (24) and (25), respectively. These coefficients are dependent on a Reynolds number based on the relative velocity or velocity difference between the airflow and the water drops. Thus, heat and mass transfer increase as the relative velocity between air and the water drops increases. Hence, control of the initial velocity difference between the sprayed water and the airflow at the duct inlet may provide a method for controlling the flow conditions at the engine face. Note that this comparison was computed with d_m = 15 microns because the effect of inlet velocity difference was more pronounced than a calculation made with d_m = 96.8 microns.

5.3.7 Discussion

After injection of a droplet into an air stream, the velocity of the droplet tends to approach the velocity of the air. The temperature of the droplet approaches the wet bulb temperature of the air; hence, unless the air is saturated, the droplet and air temperature will not become equal. In a duct flow, equilibrium can be achieved in a sufficiently long duct since droplet evaporation or condensation leads to saturation of the air. The duct length for this to occur is several orders of magnitude greater than the length available for a practical test cell. Figures 12 through 17 show this effect. It can be noted that the droplet temperature usually becomes essentially constant only a few feet downstream of the injection station. This distance is, of course, a function of the inlet flow conditions and the droplet diameter.

The steady-state droplet temperature (T_s) (wet bulb temperature) can be calculated from the relation:

$$T_g - T_s = -h_{f_g} \frac{Pr}{Sc} \frac{\bar{M}_v}{\bar{M} C_p} \left(x_v - p_v|_{T_s}/p \right)$$

where T_g is the local gas temperature, C_p is the specific heat of air, x_v is the mole fraction of water vapor in the gas phase, $p_v|_{T_s}$ is the saturation vapor pressure of water at temperature T_s, and p is the local static pressure. This equation can be used to estimate the temperature nonequilibrium in the test section. An accurate value of x_v can be obtained only by calculating the entire duct flow. However, for many flow conditions of interest in icing simulation, the specific humidity (ω), and therefore x_v, is essentially constant along the duct. Thus for an estimate, x_v can be taken to be equal to the vapor content upstream of the spray bank.

It is very difficult to obtain an accurate measurement of the humidity under icing conditions. If accurate knowledge and control of humidity is important in an icing test, it may be desirable to circumvent the difficult problem of humidity measurement by creating known humidity in the test cell. This can be accomplished by supplying the test cell with very dry air and mixing the required amount of superheated steam with the air to create the desired humidity. It is important for the mixing to be essentially complete by the time the flow reaches the water sprays. Very good humidity control should be possible with this system.

5.3.8 Summary

A summary of the results of this section of the report follows. First, for the flow conditions assumed, it was found that the thermodynamic and kinetic state of the air and water mixture at the test section of a typical direct-connect icing facility duct is not dependent on the drop-size distribution. The analysis showed that after about 25 ft downstream of the inlet, the spray cloud can be satisfactorily modeled with two parameters, the mass median drop diameter and the liquid water content. The droplet size distribution used in the calculation was a measured distribution from an icing test cell. Second, the temperature of the air, water vapor, and water mixture 25 ft downstream of the inlet was practically independent of the initial temperature of the spray water. The reason is that the liquid water contents are extremely small. Third, the effect of varying the liquid water content between 1 and 10 on the thermal and kinetic states at the test section is small. Fourth, the effect of inlet air humidity upstream of the water spray station is relatively important in determining the test section's thermal state and a substantial degree of control over the thermal state at the test section is possible through humidity control. Fifth, the temperature of relatively small (5 to 25 microns) droplets approaches the air temperature at a greater rate than that of the relatively large (100 to 1000 micron) droplets because their mass is considerably less. Hence, the small droplets are effectively at the air temperature in a much shorter length of duct than the relatively large droplets, and for this reason, the test facility water spray systems must not produce a significant fraction of water drops greater than 100 microns if effective simulation is to be provided. Sixth, the water spray velocity should be substantially different from the surrounding airflow velocity in order to increase the rate of heat and mass transfer from the drop and the approach to equilibrium. That is, a large initial degree of kinetic nonequilibrium between the injected liquid and air helps to promote a more rapid approach to thermal equilibrium.

SECTION VI
CONSIDERATION OF SOME FACTORS AFFECTING ICING SIMULATION

6.1 INTRODUCTION

Since most ground test facilities cannot duplicate all of the flow conditions experienced by an engine in flight, it is necessary to determine which of the icing variables are relatively most important in determining engine icing behavior. In this section of the

report, the effect of droplet-size distribution on capture efficiency is discussed. In addition, an analysis of the heating rate required to maintain an anti-icing condition on a surface in an icing environment is provided. The relative importance of correctly simulating the specific humidity, liquid water content, and mass median droplet diameter for simulating icing conditions in a propulsion engine test facility is illustrated quantitatively.

6.2 THE EFFECT OF DROPLET-SIZE DISTRIBUTION ON CAPTURE EFFICIENCY

In Section V, the effects of a water spray cloud with a distribution of droplet sizes were compared with the effects of a spray cloud with a uniform droplet size on the final thermodynamic and kinetic state of a flowing mixture of water and air. The effects were shown to be equivalent for a typical icing situation.

There are, however, other possible effects which the drop-size distribution might have which must be considered when simulating icing in ground test facilities. For example, a given drop-size distribution might affect ice accumulation rates on the exposed surfaces of components of the engine inlet by affecting the capture efficiency of these surfaces. Capture efficiency is defined here as follows. Consider the volume swept by the projected area of a surface moving through a uniform stream. For a uniform stream laden with particles, the hypothetical maximum particle impingement rate is simply the product of the particle concentration per unit volume times the volume flow swept by the surface; that is,

$$W_{IMP,\,max} = L_\infty \times A_p \times V_\infty \tag{35}$$

where A_p is the projected area of the surface. In general, however, since the surface disturbs the flow field ahead of it, the particles lying in the path of the surface will be influenced by the disturbed flow. Depending on particle inertia, the particles will follow or at least be sufficiently influenced by the streamlines of the airflow to take curved trajectories, and some particles in the path of the surface will pass over the surface without impinging. The two possibilities are shown in Fig. 22; the larger droplets in the stream will be least likely to follow streamlines because of their inertia. It is possible to define the absolute rate of impingement of particles on a surface by analyzing the action of the particles in the disturbed flow field about the surface. For a given size particle, a limiting trajectory can be found which is just tangent to the surface. The tangential trajectory is used to find the cross-sectional area of the streamtube far upstream of the surface which contains all of the particles of a given size that will impinge on the surface. Particles outside this streamtube will be swept over the surface and will not impinge. Hence, the actual impingement rate is

$$W_{IMP} = L_\infty \times A_{d_T} \times V_\infty \tag{36}$$

where A_{d_T} is the cross-sectional area of the streamtube defined by the tangential trajectory (Fig. 22). This analysis assumes that, for the small stream loadings typical of icing

conditions, the flow field over the surface is not influenced or modified by the presence of the water droplets. The flow field is determined only by the surface geometry.

The capture efficiency of a surface can now be defined as

$$E_c = \frac{W_{IMP}}{W_{IMP,\,max}}$$

For a given surface in an icing condition, each size water droplet in the free stream will have a characteristic tangential trajectory because of its inertia; the capture efficiency (E_c) of a surface refers to a specified drop size. The overall capture efficiency of a body in a stream laden with particles depends on the distribution of drop sizes in the stream. It is of interest to this study to determine, at least qualitatively, if the overall capture efficiencies of the engine inlet components are sensitive to drop-size distributions. If so, then this may be an important parameter to simulate, or duplicate if possible, in the ground test facility for the following reason.

If the capture efficiencies of surfaces within an engine are dependent on the drop-size distribution, then it is possible that power requirements for keeping a surface inside the engine inlet ice free would depend not only on cloud liquid water content and mass median droplet diameter, but also on the icing cloud drop-size distribution. In this event, it would be necessary to duplicate both the mass median diameter and the drop-size distribution to simulate the icing environments in the propulsion test facility. For this reason, the variation of capture efficiency of typically sized surfaces to different measured drop distributions was investigated. In addition, the sensitivity of anti-icing power requirements of exposed surfaces to variations in stream liquid water content was analyzed assuming a surface capture efficiency of unity.

6.3 SURFACE CAPTURE EFFICIENCY FOR DROP DISTRIBUTIONS TYPICAL OF ICING CONDITIONS

6.3.1 Introduction

The problem is to estimate capture efficiencies for typically sized engine inlet components for droplet sizes representative of icing environments and, from these calculations, to determine if these capture efficiencies are sensitive to droplet distributions typical of icing conditions in the atmosphere and in a ground test facility. The principal inlet components of the high-bypass turbofan-type engine considered in this study are the spinner bullet nose on the compressor axis, the compressor inlet guide vanes, and the first-stage blades. The capture efficiencies of the guide vanes and the compressor blades may be very crudely obtained by analogy to equivalent cylinders. The thickness of the guide vanes and compressor blades define the diameter of equivalent cylinders. The spinner hub capture efficiency can be estimated directly from known analytical and experimental results for bodies of revolution.

The work of Langmuir (Ref. 19) can be used to determine the capture efficiencies of right circular cylinders in incompressible flow, given the cylinder diameter, the temperature and density of the air, and the density of the droplets and their diameter. The effect of compressibility has been found to be negligible (Ref. 20); hence, Langmuir's work also applies with sufficient accuracy to compressible flow over cylinders. Langmuir defined two correlation parameters which enable the capture efficiency of a given cylinder/airflow/drop combination to be estimated from his analytical results presented in Ref. 19. These two parameters are the inertia parameter (K) where

$$K = \frac{2}{9} \frac{\rho_c d^2 V_\infty}{\mu D}$$

and the parameter (ϕ) called the altitude parameter in Ref. 19 as defined by

$$\phi = \frac{9 \rho_g^2 D V_\infty}{\mu \rho_c}$$

By using the given information on a particular cylinder/airflow/drop combination, K and ϕ can be evaluated, and the capture efficiency of the cylinder under the given conditions can be obtained from Fig. 1 or 2 of Ref. 19. Thus, for a given distribution of droplet sizes, a mass fraction (of the total water content, per unit volume of gas) can be calculated for each droplet-size class. From this, the mass fraction of liquid water impinging on the cylinder from each droplet-size class can be determined. Thus, an overall mass-weighted capture efficiency of a cylinder for a given drop-size distribution can be calculated. It should be mentioned here that Langmuir found that, for his assumed droplet-size distributions, one can equate the overall capture efficiency of a cylinder for a distribution of droplets to the capture efficiency of the cylinder for the mass median droplet. On the other hand Dorsch, et al. (Ref. 21), show that the capture efficiency of a 5 to 1 ellipsoid of revolution for a given drop distribution was not equal to the capture efficiency of the ellipsoid for the mass median drop. Thus, to clarify the problem for simulated icing testing, these effects were reinvestigated during this study.

6.3.2 Droplet-Size Distributions in Icing Conditions

The first problem was to find reported drop-size distributions in the natural atmospheric environment. Distributions typical of conditions in cumulus clouds are reported by Battan and Reitan (Ref. 22) and in fog conditions by Eldridge (Ref. 23). In these references, the distributions were presented in terms of frequency of occurrence (number of drops of a given size per sample) versus drop diameter. The resulting mass fraction distributions are shown in Fig. 23. Distribution N-1 is the mass fraction distribution for icing conditions in fogs, reported in Ref. 23. Distribution N-2 corresponds to conditions in tropical cumuliform clouds, and distribution N-3 corresponds to the conditions in cumuliform clouds over the USA; both of these distributions were reported in Ref. 22. In this study, these distributions were reduced to and presented in the form of mass fraction of total liquid water content (per drop size class per sample) versus drop diameter.

Drop distributions that were measured in an icing test in a ground test facility are reported by Gall and Floyd (Ref. 9). These distributions were also reduced in this study to mass fraction (of total liquid water content per drop-size class) versus drop diameter. These distributions are presented in Fig. 11 of this report. The mass median and mass mean diameters of these distributions are also presented in Fig. 11 with sufficient supplementary data to identify each distribution in its original form as given in Fig. 23 of Ref. 10.

A comparison of Figs. 10 and 23 of this report shows that the drop distributions in the icing facility are fairly similar to drop distributions in cumuliform clouds. To compare these distributions with the distributions utilized by Langmuir and Blodgett (Ref. 19), the original forms of the distributions (number frequency versus drop diameter) were replotted in this study in the form of number frequency of occurrence versus a reduced droplet diameter which was the form favored by Langmuir and Blodgett. The reduced diameter (d_R) is defined as

$$d_R = \frac{d}{d_m}$$

Comparisons are shown in Figs. 24 and 25. In Fig. 24, the cumuliform distributions of Ref. 22 and the artificial distribution of Ref. 10 are compared, whereas in Fig. 25 the distributions of Ref. 22 are compared with the Langmuir distributions which are denoted as B, C, D, and E in Ref. 19. Because the Langmuir distributions were suggested by data from cloud measurements made by Houghton and Radford (Ref. 24) and by Radford (Ref. 25), the favorable comparison in Fig. 25 is not surprising. The important point to be made from these comparisons is that the test facility spray system, like that described by Gall and Floyd, is capable of simulating the droplet size and water mass distributions which occur in natural icing and cloud conditions in the atmosphere.

6.3.3 Effect of Drop Distributions on Capture Efficiency

The question previously posed was whether the capture efficiency of typical engine inlet surfaces was dependent on drop distributions in icing conditions. Since natural and artificial icing cloud drop distributions were shown to compare favorably, it may seem irrelevant to pursue the question of the relation between capture efficiency and drop distribution. Nevertheless, the values of these estimated capture efficiencies are important for estimating water impingement rates, and in addition, while the drop-size distributions compared favorably, they were not identical. For these reasons, overall capture efficiencies for two different diameter cylinders and a 5:1 ellipsoid of revolution were computed for distributions N-2, N-3, A-1, A-2, and A-3.

The stream conditions were the same for each case, defined by

$$V_\infty = 440 \text{ ft/sec}$$

$$p = 1932 \text{ psfa}$$

$$T = 480°R$$

For the circular cylinders, the inertia parameter (K) and the altitude parameter (ϕ) were used together with the results in Figs. 1 and 2 of Ref. 19, to obtain, for each droplet distribution, a mass-weighted overall capture efficiency (E_{co}). The results of these computations are presented in the following table:

CYLINDER DIAMETER: 0.04166 ft (1/2 in.)

Distribution	d_m, microns	Capture Efficiency, E_{co} Based on Distribution	Capture Efficiency, E_{co} Based on Mass Median Diameter
N-2	40.0	0.928	0.962
N-3	26.5	0.923	0.925
A-1	38.0	0.950	0.958
A-2	30.0	0.938	0.942
A-3	22.0	0.909	0.912

CYLINDER DIAMETER: 0.25 ft (3 in.)

Distribution	d_m, microns	Capture Efficiency, E_{co} Based on Distribution	Capture Efficiency, E_{co} Based on Mass Median Drop
N-2	40.0	0.770	0.805
N-3	26.5	0.690	0.680
A-1	38.0	0.773	0.892
A-2	30.0	0.725	0.732
A-3	22.0	0.632	0.630

Essentially the same procedure was followed for computing the overall capture efficiency of the 5:1 ellipsoid of revolution. The method for computing ellipsoid capture efficiency is outlined by Dorsch, et al. (Ref. 21). For this study, an ellipsoid with a midsection diameter of 2 ft was chosen; hence the major diameter (axis) was ten feet. For the same free-stream condition, the computed capture efficiencies of the ellipsoid are shown in the following table:

5:1 ELLIPSOID (10-FT MAJOR AXIS)

Distribution	d_m, microns	Capture Efficiency, Overall, E_{co} Based on Distribution	Based on Mass Median Drop
N-2	26.5	0.107	0.079
N-3	40.0	0.180	0.160
A-1	38.0	0.156	0.140
A-2	30.0	0.119	0.110
A-3	22.0	0.072	0.055

From the data in the previously shown tabulations, the following conclusions can be drawn. First, with only one exception, the calculated overall capture efficiencies for both cylinders and the ellipsoid of revolution which were based on droplet-size distributions are approximately equal to capture efficiencies based on the mass median diameter of each distribution. The exception is for the distribution N-3 for both the 1/2-in. and 3-in. circular cylinders. Second, in general, as the mass median diameter is increased, the capture efficiency increases, and as the cylinder diameter increases, the capture efficiency decreases. Third, as stated, for the ellipsoid of revolution the capture efficiency based on the droplet-size distribution compares reasonably close to the capture efficiency based on the mass median drop diameter. This agrees with the Langmuir predictions (Ref. 26). It is pertinent to point out that Lewis and Ruggeri (Ref. 27) provide experimental data on capture efficiency for four different bodies of revolution which they compared with the theoretical prediction. They point out that, in general, fairly good agreement exists between experimental and theoretical impingement characteristics. Fourth, the most important point for this study is that the results of the capture efficiency calculation showed that the capture efficiency of the bodies was about the same for drop distributions produced in the icing facility as for natural cloud icing conditions when the mass median diameters for these distributions were approximately equal. However, the capture efficiencies based on the test cell distributions were slightly greater than those based on natural distributions but not significantly so. Thus, the capture efficiencies of the engine inlet components under simulated icing conditions should be approximately equal to capture efficiencies which occur during flight. This means that if the ground test icing facility provides a spray cloud with the correct mass median drop size and of the correct liquid water content, then the absolute rates of impingement of subcooled water on the engine inlet components should correspond very nearly to in-flight water impingement rates. Thus, it is possible to provide very good icing simulation, in principle, in the ground test facility for turbofan and turbojet engines of the type which are typically pod mounted.

An important point to resolve is the degree of approximation which is acceptable when providing simulation of the icing conditions in the ground test facility. That is, how accurately in practice must the free-stream liquid water content, humidity, and other

parameters be simulated in the icing facility in order to achieve good simulation, and hence, accurate experimental evaluation of anti-icing power requirements. In the following sections of this report, the sensitivity of anti-icing power requirement of a surface to variations in stream liquid water content and humidity is analyzed. This analysis is then used to define the kind of accuracy required in ground testing for providing these parameters in order to obtain good icing simulation.

6.4 HEATING RATE REQUIRED TO MAINTAIN AN ANTI-ICING CONDITION ON A SURFACE IN AN ICING ENVIRONMENT

The purpose of this section is to analyze the effect of humidity, liquid water content, and liquid capture rate on the heating rate required to maintain an anti-icing condition on engine components. The analysis parallels the analysis given in Ref. 28. The degree of importance of duplicating in the test cell the values assumed by these variables under actual flight conditions is discussed. The flow over the component surface is assumed to have been accelerated or diffused from some prescribed free-stream conditions. Thus, the fact that the Mach number of the flow entering an engine compressor is generally different from the flight Mach number can be recognized. Flow from the free stream to a component surface is assumed to occur isentropically and at constant specific humidity. The validity of the latter assumption can be inferred from calculations made with the computer program discussed in Section IV. For prescribed free-stream conditions, the conditions at the edge of the gas boundary layer on the surface are determined by the local static pressure or Mach number. Since some of the droplets cannot follow streamlines, a certain portion of them will impinge on the surface and form a liquid film. The rate of impingement depends on the liquid water content, the surface capture efficiency, and the flow conditions. It is assumed that the surface is maintained at the freezing point (492°R) and that enough heat is supplied to prevent any ice formation. Vaporization from the liquid film into the adjacent gas boundary layer will occur.

In the absence of radiation heat transfer, a heat balance at the surface yeilds

$$\underset{\text{I}}{\dot{q}''_w = \bar{h}(T_w - T_{aw})} + \underset{\text{II}}{w_v\left(h_{f_g}\right)} + \underset{\text{III}}{w_c C_c\left(T_w - T_{c_\infty}\right)} - \underset{\text{IV}}{w_c V_\infty^2/2} \tag{37}$$

where $\dot{q}''_w$ is the anti-icing heating rate, $\bar{h}$ is the gas side heat transfer coefficient, w_v is the rate of vaporization from the film, w_c is the flux of subcooled liquid entering the film, T_w is the wall or film temperature, T_{c_∞} is the subcooled liquid temperature, and T_{aw} is the adiabatic wall temperature. In this heat balance, it is tacitly assumed that the liquid in the film is at a uniform temperature. A few remarks about the individual terms in Eq. (31) are in order.

Term (I) is the rate of heat loss from the liquid film to the air by convection. The adiabatic wall temperature is given by

$$T_{aw} = T_e\left(1 + r\,\frac{\gamma-1}{2}\,M_e^2\right) \tag{38}$$

where r is the recovery factor and M_e is the Mach number at the edge of the gas boundary layer.

Term (II) is the rate of heat loss due to evaporation of the liquid film. In terms of the mass transfer coefficient (k_x), the rate of evaporation is approximately

$$w_v = \bar{M}_v k_x\left(p_{v_w} - p_{v_e}\right)/p_e \tag{39}$$

where p_{v_w} is the saturation pressure of water at the freezing point. By the analogy between heat and mass transfer on a flat plate,

$$k_x = \frac{\bar{h}}{C_p \bar{M}}\left(\frac{Pr}{Sc}\right)^{0.67} \tag{40}$$

Term (III) is identified with the sensible heating of the supercooled liquid droplets to the film temperature from their temperature before impingement. The droplets are assumed to pass through the gas boundary layer with no temperature or mass change.

Term (IV) reflects the flux of kinetic energy contained in the droplets entering the film. It is assumed that the droplets are in velocity equilibrium with the gas at the gas boundary layer edge and that the droplets do not slow down as they pass through the gas boundary layer.

It is convenient to introduce the parameter ($b = w_c C_c/\bar{h}$) and rewrite Eq. (31) in the form

$$Q = \frac{\dot{q}_w''}{\bar{h}\left(T_w - T_{aw}\right)} = 1 + \frac{\dfrac{h_{fg}\bar{M}_v}{C_p \bar{M}}\left(\dfrac{Pr}{Sc}\right)^{0.67}\dfrac{\left(p_{v_w} - p_{v_e}\right)}{p_e} + b\left(T_w - T_{c_\infty}\right) - bT_e\,\dfrac{\gamma-1}{2}\,\dfrac{C_p}{C_c}\,M_e^2}{T_w - T_{aw}} \tag{41}$$

It can be noted that the parameter on the left-hand side (Q) is the ratio of heating rate required in an icing environment to the heating rate required to maintain the surface temperature at T_w in a dry environment. The parameter (b) is approximately the ratio of the sensible heat transfer to the impinging liquid to the heat loss from the film by convection. It reflects the effect of liquid water content and the liquid capture rate on the heating rate. In particular, b is directly proportional to the liquid water content and surface capture efficiency. The humidity is reflected in the partial pressure (p_{v_e}).

Based on calculations made with the computer program, it can be inferred that the supercooled droplets are in quasi-equilibrium with the gas phase locally along the path

from the free stream to the compressor inlet and icing surface. The process occurs at substantially constant specific humidity, and depending on the engine inlet ducting, the flow may be isentropic to a good approximation.

Thus, for given free-stream pressure (p_∞) (or altitude), temperature (T_∞), and velocity (V_∞) or Mach number (M_∞), the heating rate parameter (Q) can be determined as a function of local icing surface pressure (p_e) or Mach number (M_e), the parameter (b), and the humidity. The subscript (e) denotes conditions at the outer edge of the gas boundary layer. From the constant humidity assumption,

$$p_{v_e}/p_e = p_{v_\infty}/p_\infty$$

Figure 26 shows the effects of boundary layer edge Mach number (M_e) and the parameter (b) on the heating rate parameter (Q) for the high altitude test conditions of the military specification given in Table I. Calculations have shown that, for icing surfaces in a turbine engine, b generally will not exceed 2.0. It can be observed that Q is relatively independent of the free-stream Mach number. If M_∞ is increased from 0 to 2, Q only increases by a factor of two. This is an important result since b is directly proportional to the liquid water content and has some dependence on the droplet size distribution. If b is approximately 0.5, a 50-percent variation in b results in about a 10-percent variation in Q. It can be concluded that exact duplication of the liquid water content or droplet size distribution is not too important in conducting anti-icing tests. It should be pointed out that this conclusion may not be applicable for conducting icing tests without anti-icing heat or for testing de-icing equipment. The rate of ice accretion on an unheated surface is highly dependent on liquid water content, liquid capture rate, and the frequency of operation; therefore, the heating load of a de-icing system is proportional to the rate of ice accretion.

In Fig. 27, the effect of humidity on the heating rate parameter (Q) is shown. It can be noted that, for the particular flow conditions for which the calculations were made, the heating rate parameter is relatively insensitive to the humidity. This effect can be attributed to the low partial pressure of water vapor at the edge of the boundary layer compared with the partial pressure at the surface of the liquid film. The partial pressure difference across the boundary layer, of course, determines the rate of evaporative cooling. Large variations in the small partial pressure at the boundary layer edge do not significantly affect the partial pressure difference.

It is important to have approximately the correct humidity, however. Icing tests have been conducted in which the air was essentially saturated at the total conditions of the stream corresponding to a large degree of supersaturation in the free stream, which implies that the airflow into the engine compressor was supersaturated in the test. This procedure cannot produce the desired degree of simulation, especially for flight Mach numbers above 0.5.

The effect of humidity on the heating rate parameter becomes more pronounced as the air temperature is increased, although the absolute heating load diminishes. This

effect deserves detailed consideration if anti-icing tests are to be conducted at temperatures much above the -4°F specified in Table I.

6.5 EVAPORATION FROM THE SPRAYBANK

In order to prevent freezing in the water spray system, the water must be sprayed into the cold air stream at a temperature exceeding the freezing point. Thus, evaporation of the spray will occur. Net condensation may occur if the air is greatly supersaturated. The extent of evaporation is governed principally by the air temperature and humidity and the temperature of the water at injection. The initial rate of evaporation from a droplet may be very high; however, evaporative cooling and convective heat transfer from the droplet bring the droplet rapidly to the local wet bulb temperature and a correspondingly low evaporation rate.

There are two primary effects of spray evaporation to be considered. The first effect is humidification of the air stream. As discussed in Section 5.4.6, it may be desirable to create the desired humidity by mixing steam with the air upstream of the spraybank. Thus it is important to know how the spray evaporation affects humidity. Based on calculations made with the computer program discussed in Section V, it appears that spray evaporation is not too important. If the air stream is nearly dry, evaporation from the spray may more than double the humidity. However, since the evaporative cooling contribution to the heating load for anti-icing is not highly dependent on humidity for nearly dry air, a relatively large change in humidity will not seriously affect the anti-icing heating rate. On the other hand, if the humidity is large, the percent change in humidity resulting from the spray evaporation is small. For high humidity condition, the evaporative cooling contribution to the anti-icing heat load is small; thus, the additional humidification from the spray should have but a small influence on the anti-icing heating rate. The second effect is the change in the liquid water content due to spray evaporation. The average liquid water content in an icing tunnel is usually determined from measurements of the air and water flow rates. Results of calculations made with the computer program show that the liquid water content may decrease by about 10 percent because of evaporation for liquid water contents on the order of 1 gm/m^3. If the spray vaporization rate can be calculated accurately for a particular system, then the effect of evaporation can be accounted for by increasing the water flow from the sprays. In view of the relative insensitivity of the anti-icing heating rate on liquid water content as discussed in the previous section, this effect is probably negligible. An upper bound on the evaporation can be obtained by determining the amount of liquid necessary to saturate the air stream at the stagnation conditions.

SECTION VII
CONCLUDING REMARKS

A study of icing simulation in altitude test cells was made. A mathematical model for the flow in a typical icing test cell was developed, and the governing equations were programmed for computer solution. A parametric study was performed to determine the effects of test cell inlet and water spray conditions on the thermodynamic and kinetic

state of the flow at the test section or test article. The importance of correctly simulating droplet size distribution, mean effective droplet diameter, liquid water content, and humidity was investigated analytically.

The results of the parametric study made with the mathematical model of the icing test cell indicate that simulated flight conditions at the face of an engine compressor can be obtained through proper selection of the test cell inlet conditions and water spray settings. The model can be used to determine the required test cell inlet conditions for proper simulation. The thermodynamic state at the engine was found to be very sensitive to inlet air temperature, pressure, and humidity and insensitive to the inlet water temperatures, droplet size distribution and velocity, and liquid water content. The velocity difference between the inlet airflow and the water from the spray system was relatively important, however.

In general, the total pressure and temperature at the test cell inlet should be set equal to the total pressure and temperature of the free flight condition being simulated. While there is some humidification from the water spray system, this influence can usually be ignored. The test cell inlet specific humidity should be set equal to the specific humidity corresponding to saturation at the static pressure (altitude) and static temperature being simulated. The test article should be located sufficiently far downstream of the spray section to ensure that the required near-equilibrium thermal state is obtained in the test section. The required distance can be calculated using the mathematical model and computer program developed in this study. For the system considered in this study, the distance is approximately 20 ft.

It is very difficult to make accurate humidity measurements under conditions prevailing in the test cell under icing conditions. This difficulty can be circumvented by mixing superheated steam in correct proportion with dry air entering the test cell. The mixing process should occur well upstream of the water spray section. Thus, the desired test cell humidity can be created and direct measurement with its attendant difficulty and uncertainty is avoided.

An analysis of the heating rate required to maintain an anti-icing condition on a surface was made. From the analysis, it was determined that the heating rate is relatively insensitive to droplet size distribution and liquid water content and only moderately sensitive to humidity. It can be concluded that exact duplication of these variables is not required for adequate testing of an anti-icing system. Icing tests in the absence of anti-icing heat and the testing of de-icing systems will generally require better simulation of the environment than testing under anti-icing conditions.

The military specifications for conducting icing tests were found to be inexplicit. There is ambiguity associated with the temperature and mean effective droplet size and complete absence of a humidity specification. A wide range of test conditions is possible within the framework of the specifications as formulated. In order to be definitive, icing test specifications should include the conditions in the atmosphere to be simulated including

the ambient temperature and pressure, the humidity, the liquid water content, and the mass median or mass mean droplet diameter.

From a simplified analysis of droplet capture efficiency on bodies which represent various turbine engine components, it was found that the overall capture efficiencies are relatively insensitive to droplet distribution when the majority of drops are greater than five microns in diameter. The capture efficiency (scoop factor) for the engine was found to be near unity.

It appears that current capability to provide icing environments for turbine engine testing in altitude test cells is quite good. These facilities can provide the correct spray cloud, that is, one with the proper mean effective drop diameter and a sufficiently correct drop size distribution, at the required thermal state. In principle, control over the pertinent flow variables such as humidity, temperature, pressure, liquid water content and velocity is excellent.

This ability to define and control the simulated environment gives altitude test cells a distinct advantage over testing in natural icing environments or artificial environments created by tanker aircraft.

REFERENCES

1. Kissling, H.H. "Aircraft Engine Anti-Icing Test and Evaluation Technology." Paper presented at AIAA 10th Aerospace Sciences Meeting, San Diego, California, January 1972.

2. Lewis, W. "Icing Properties of Noncyclonic Winter Stratus Clouds." NACA TN 1391, September 1947.

3. Jones, A.R. and Lewis, W. "Recommended Values of Meteorological Factors to be Considered in the Design of Aircraft Ice-Prevention Equipment." NACA TN 1855, March 1949.

4. Hacker, P.T. and Dorsch, R.G. "A Summary of Meteorological Conditions Associated with Aircraft Icing and a Proposed Method of Selecting Design Criteria for Ice-Protection Equipment." NACA TN 2569, November 1951.

5. Lewis, W. and Bergrum, N.R. "A Probability Analysis of the Meteorological Factors Conducive to Aircraft Icing in the United States." NACA TN 2738, July 1952.

6. "Airworthiness Standards: Transport Category Airplanes; Appendix C." Federal Aviation Regulations, Part 25, Federal Aviation Administration.

7. Lewis, W. "Review of Icing Criteria." Paper presented in Aircraft Ice Protection - Report of Symposium held April 28-30, 1969, Federal Aviation Administration, Washington, D.C. (AD690469).

8. "Military Specifications for Turbojet and Turbofan Testing." MIL-E-5007C, December 1965.

9. Gall, E.S. and Floyd, F.X. "Icing Test Capability of the Engine Test Facility Propulsion Development Test Cell (J-1)." AEDC-TR-71-94 (AD729205), August 1971.

10. Striebel, E.E. "Ice Protection for Turbine Engines in Aircraft Ice Protection." Report of Symposium April 28-30, 1969, Federal Aviation Administration, Washington, D.C. (AD690496).

11. Pelton, J.M. and Willbanks, C.E. "A Kinetic Model for Two-Phase Flow in High Temperature Exhaust Gas Coolers." AEDC-TR-72-89 (AD744514), June 1972.

12. Ranz, W.E. and Marshall, W.R. "Evaporation from Drops - Part II." Chemical Engineering Progress, Vol. 48, No. 4, April 1952.

13. Carlson, D.J. and Hoglund, R.F. "Particle Drag and Heat Transfer in Rocket Nozzles." AIAA Journal, Vol. 2, 1964.

14. Dorsey, N.E. Properties of Ordinary Water Substance. American Chemical Society Monograph, Series 81, Reinhold Publishing Company, New York, 1940.

15. Heverly, J.R. "Supercooling and Crystallization." Transactions of American Geophysical Union, Vol. 30, No. 2, April 1949.

16. Gokhale, N.R. "Dependence of Freezing Temperature of Supercooled Water Drops on the Rate of Cooling." Journal of the Atmospheric Sciences, Vol. 22, March 1955.

17. Keenan, J.H. and Kaye, J. Gas Tables. John Wiley and Sons, Inc., New York, 1961.

18. Keenan, J.H. and Keyes, F.G. Thermodynamic Properties of Steam. John Wiley and Sons, Inc., New York, 1961.

19. Langmuir, 1. and Blodgett, K. "A Mathematical Investigation of Water Droplet Trajectories." Air Material Command Technical Report No. 5418, Army Air Force. February 1946.

20. Brun, R.J., Serafini, J.S., and Gallagher, H.M. "Impingement of Cloud Droplets on Aerodynamic Bodies as Affected by Compressibility of Air Flow Around the Body." NACA TN 2903, March 1953.

21. Dorsch, R.G., Brun, R.J., and Gregg, J.L. "Impingement of Water Droplets on an Ellipsoid with Fineness Ratio 5 in Axisymmetric Flow." NACA TN 3099, March 1954.

22. Battan, L.J. and Reitan, C.H. "Droplet Size Measurements in Convective Clouds." Proceedings of the First Conference on the Physics of Clouds - Artificial Stimulation of Rain, 1958.

23. Eldridge, R.G. "The Relationship between Visibility and Liquid Water Content in Fog." Journal of the Atmospheric Sciences, Vol. 28, October 1971.

24. Houghton, H.G. and Radford, W.H. "On the Measurement of Drop Size in Liquid Water Content in Fogs and Clouds." Papers in Physical Oceanographic Institute and Meteorology. Published by M.I.T. Press and Woods Hole Oceanographic Institute, Vol. 4, November 1938.

25. Radford, W.H., Reprint No. 152, Massachusetts Institute of Technology, 1939.

26. Langmuir, I. "Super-Cooled Water Droplets in Rising Currents of Cold Saturated Air." Collected Works of Irving Langmuir, Vol. 10, pp. 316-318, Pergamon Press, 1961.

27. Lewis, J.P. and Ruggeri, R.S. "Experimental Droplet Impingement on Four Bodies of Revolution." NACA TN 4092, December 1957.

28. Neel, C.B., Jr., Bergum, N.R., Jukoff, D., and Schlaff, B.A. "The Calculation of the Heat Required for Wing Thermal Ice Prevention in Specified Icing Conditions." NACA TN 1472, December 1947.

APPENDIXES

I. ILLUSTRATIONS
II. TABLE
III. COMPUTER PROGRAM

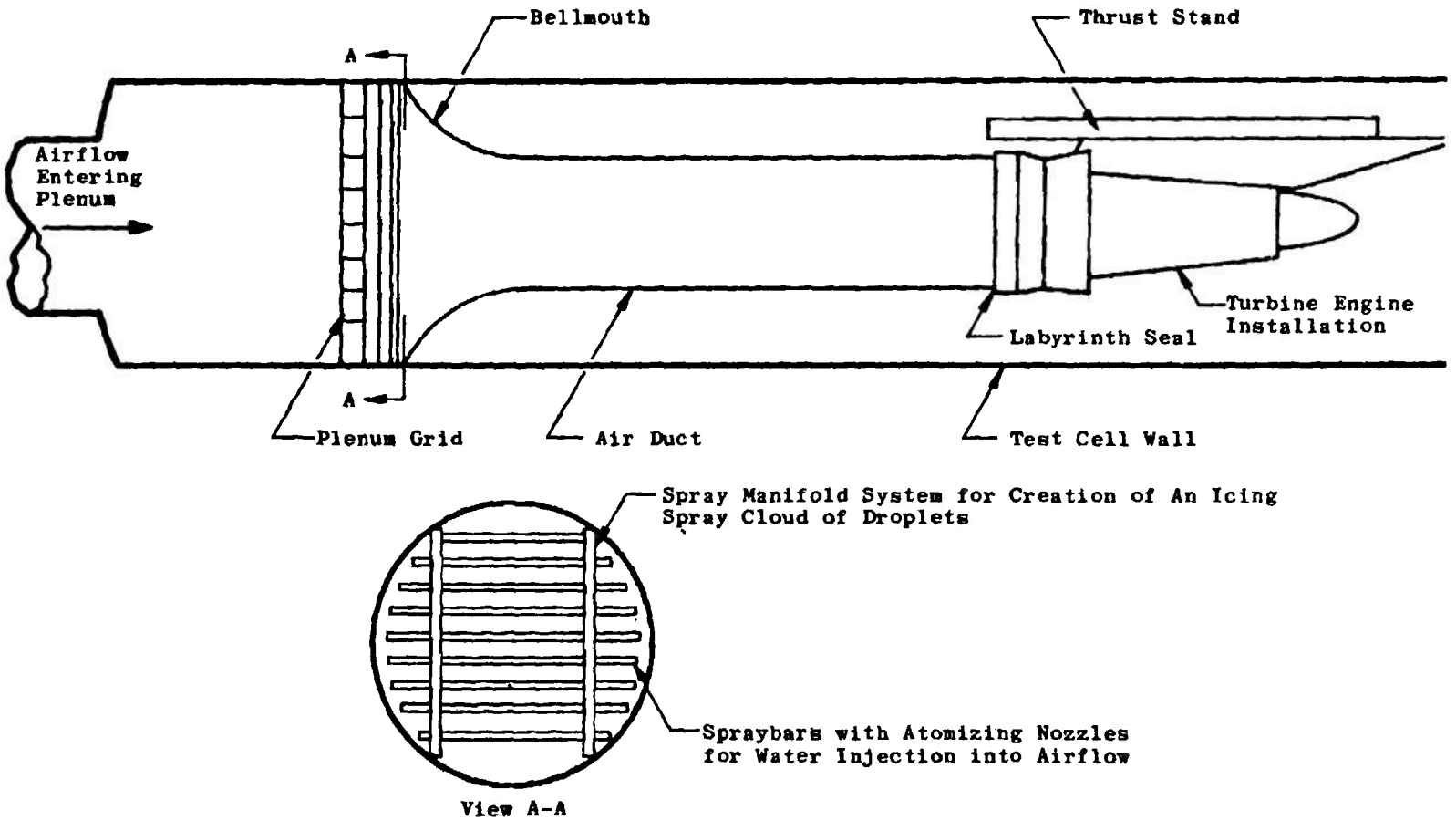

Fig. 1 Typical Propulsion Engine Altitude Test Cell Configuration

1. Pressure Altitude Range, Sea Level to 22,000 ft
2. Maximum Vertical Extent, 6,500 ft
3. Horizontal Extent, Standard Distance of 17.4 nautical miles

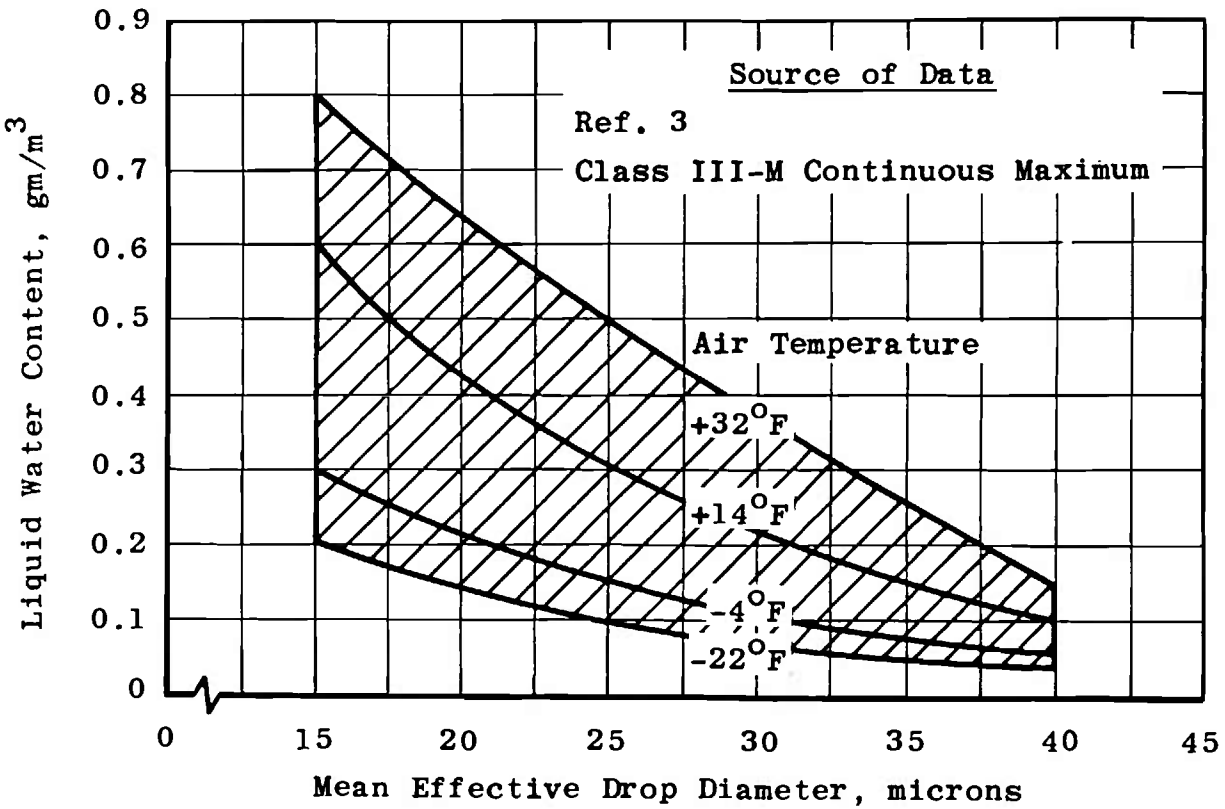

Fig. 2 Liquid Water Content versus Mean Effective Drop Diameter, Stratiform Clouds

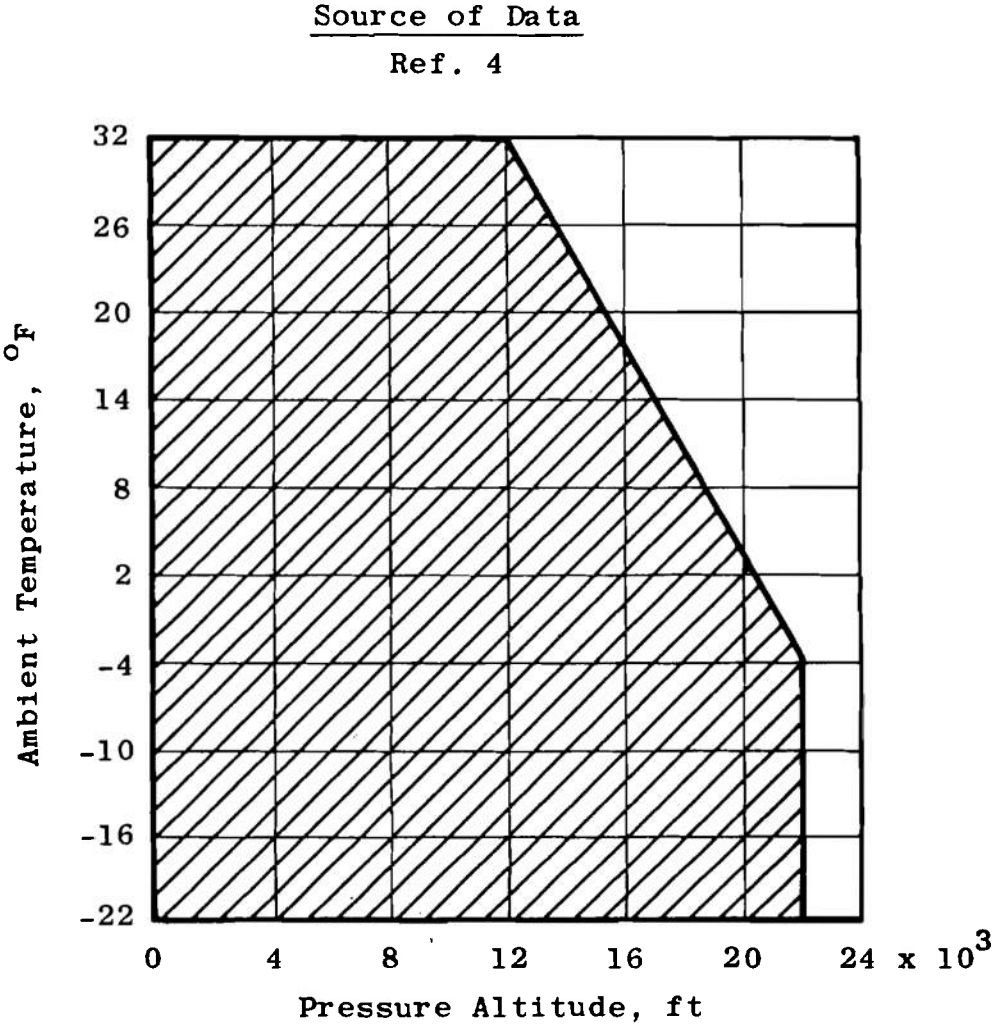

Fig. 3 Static Temperature versus Static Pressure for Stratiform Cloud Icing Conditions

1. Pressure Altitude Range, 4,000 to 22,000 ft
2. Horizontal Extent, Standard Distance of 2.6 nautical miles

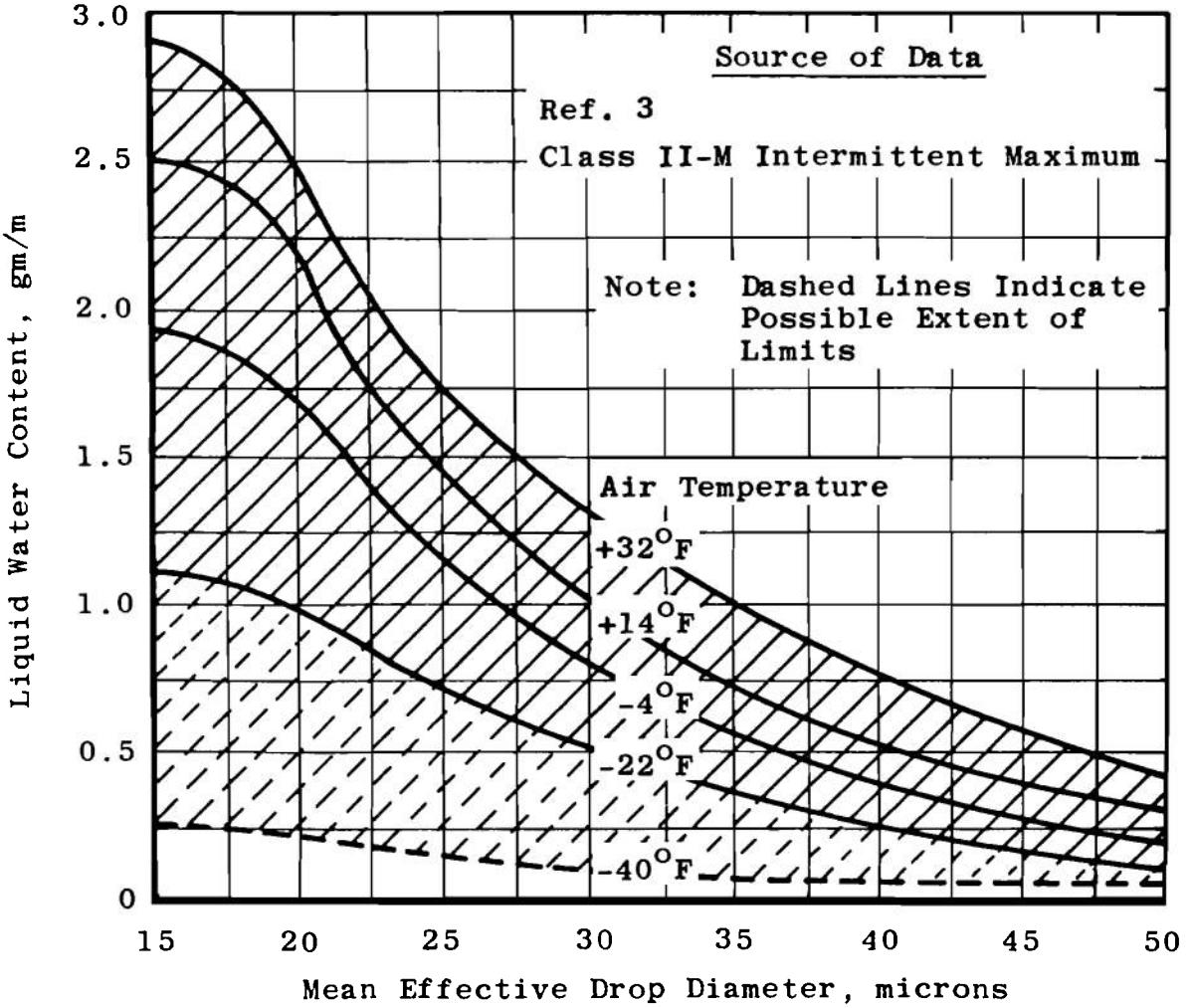

Fig. 4 Liquid Water Content versus Mean Effective Drop Diameter, Cumuliform Clouds

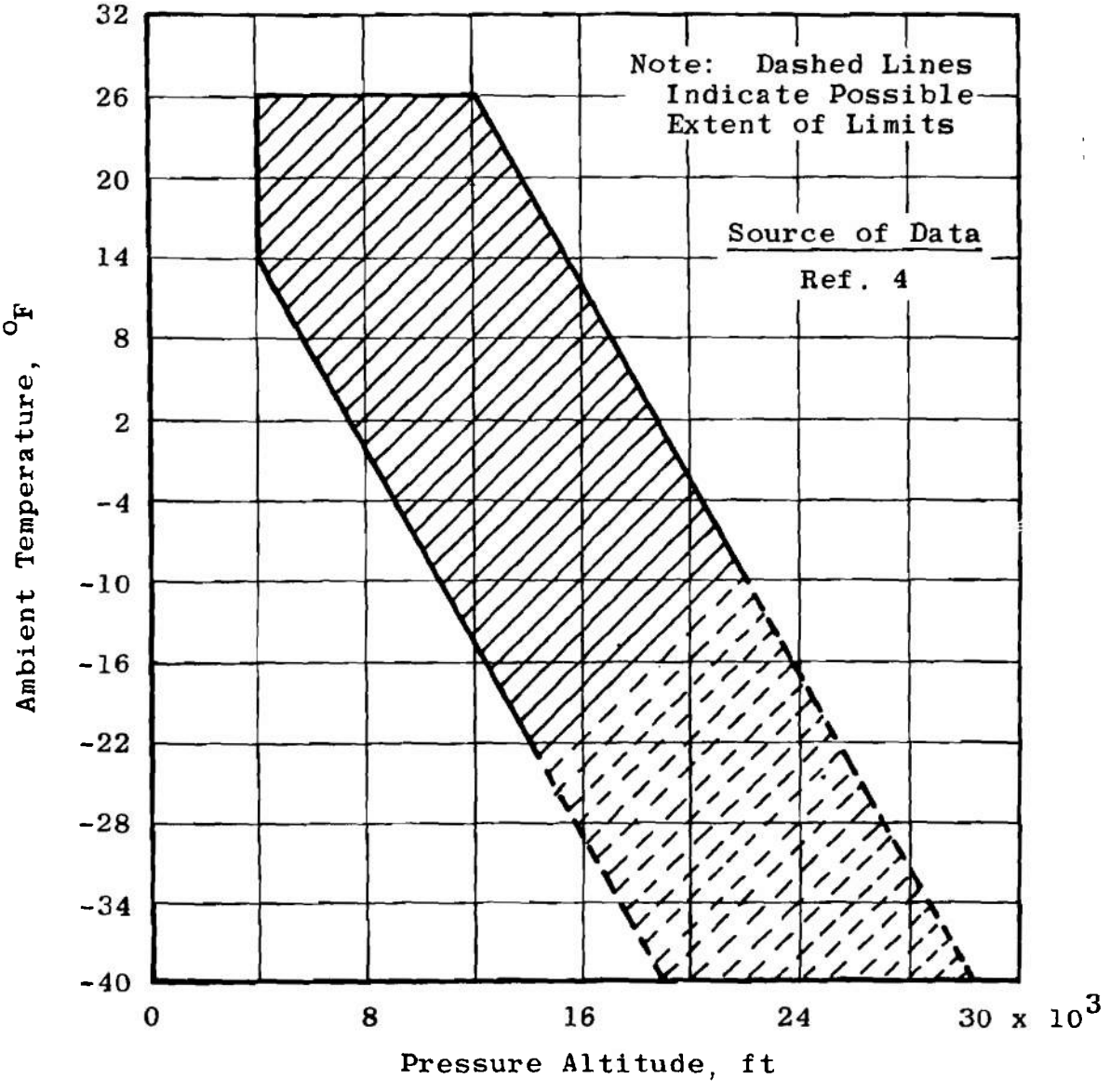

Fig. 5 Static Temperature versus Static Pressure for Icing Conditions in Cumuliform Clouds

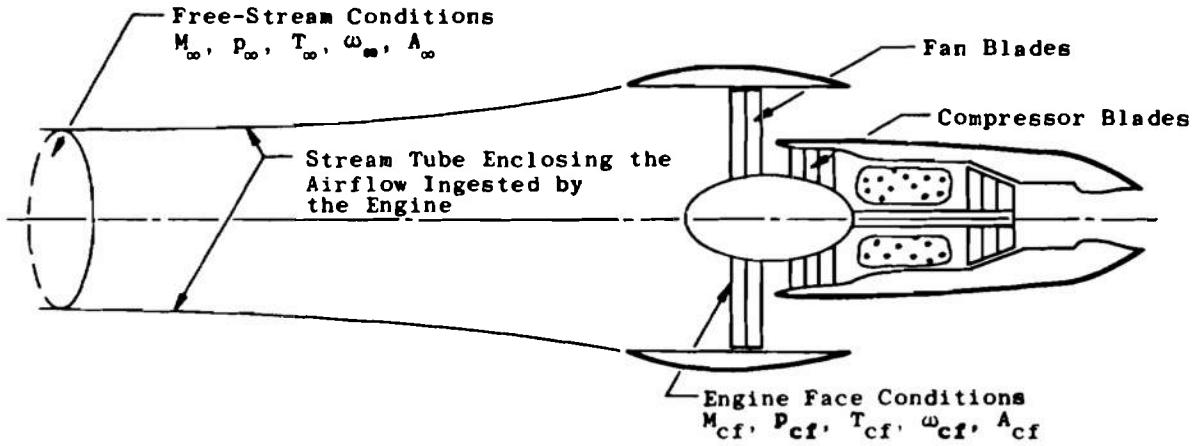

a. Inlet Mach Number Less Than Flight Mach Number

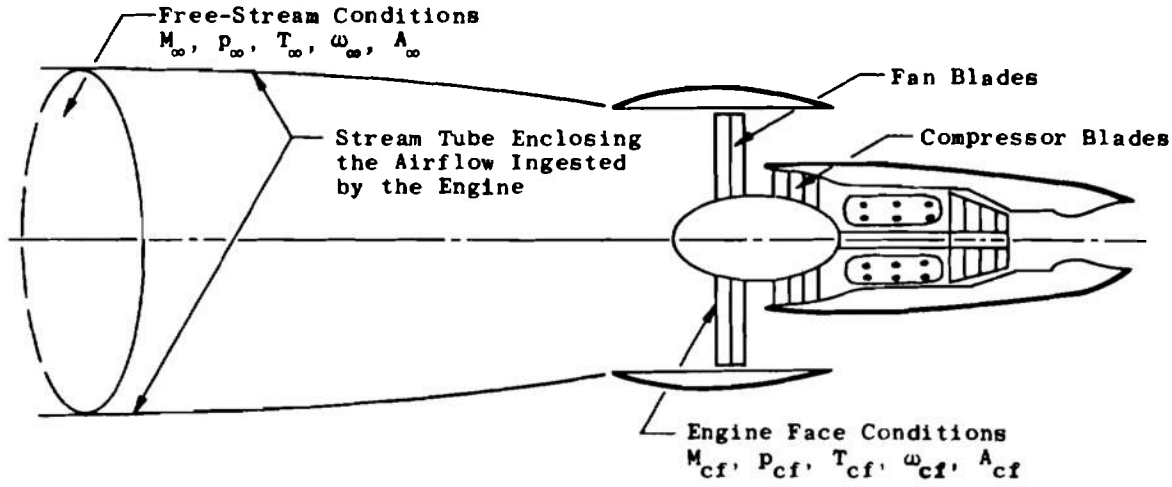

b. Inlet Mach Number Greater Than Flight Mach Number

Fig. 6 Schematic Showing Possible Streamtube Configurations for Turbofan Icing Conditions

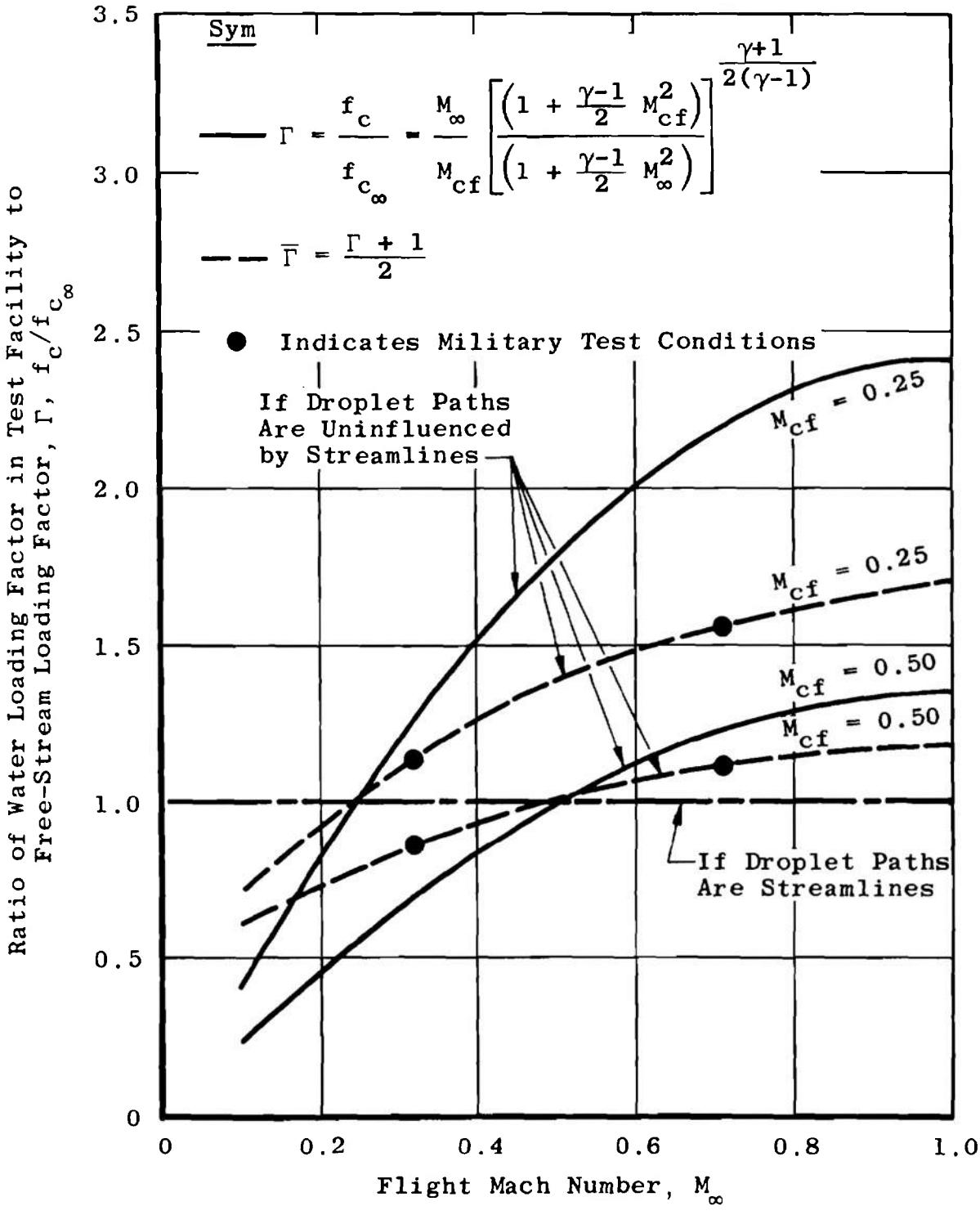

Fig. 7 Variation of Loading Factor Ratio with Flight Mach Number and Engine Compressor Face Mach Number

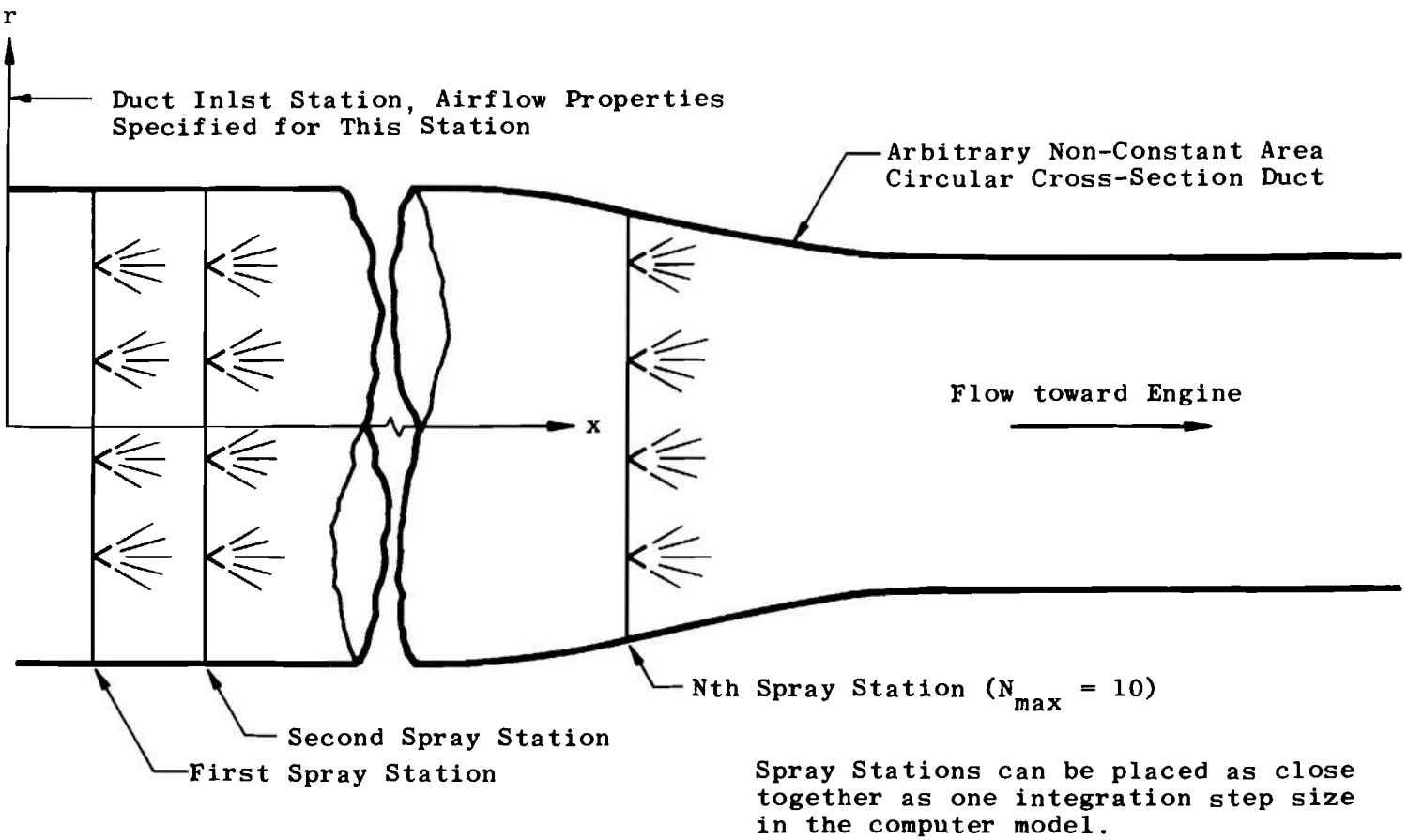

Fig. 8 Simplified Schematic of Duct Geometry for Analysis

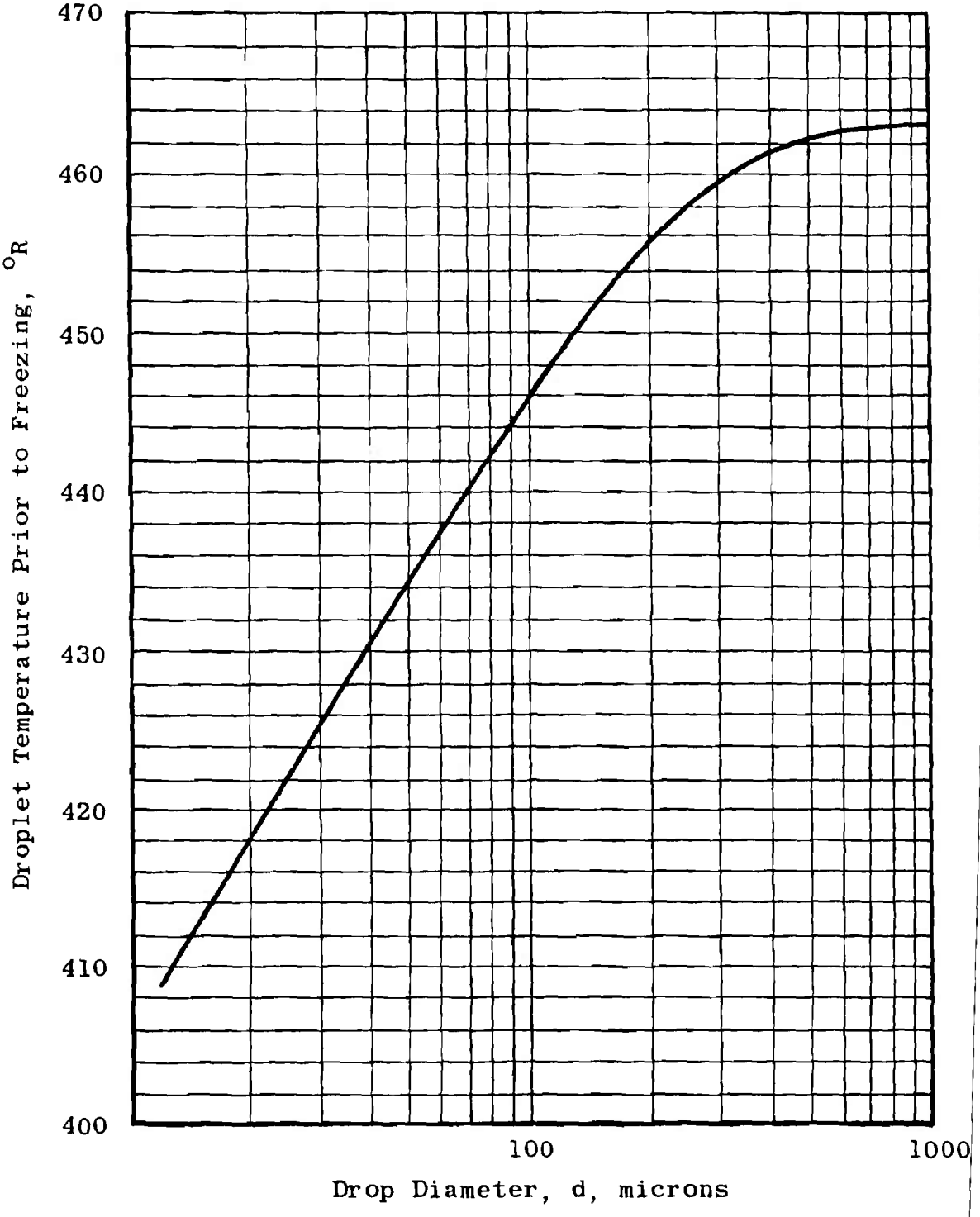

Fig. 9 Supercooled Droplet Freezing Temperature as a Function of Droplet Diameter

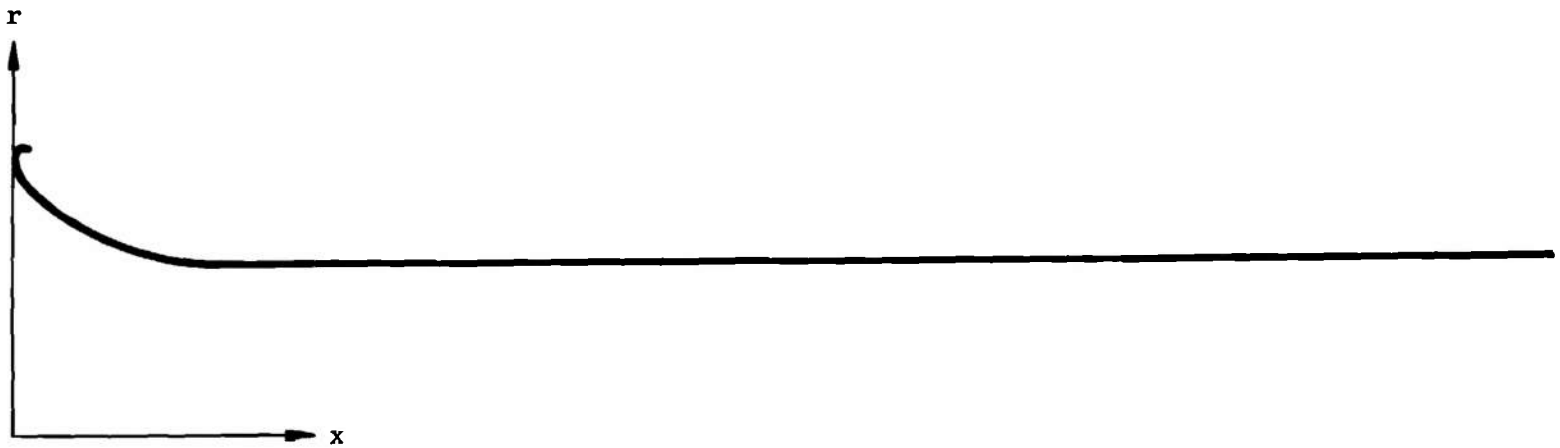

x/R	r/R	p_g	T_g	M_g
0	1.575	1355.0	486.00	0.074
0.064	1.492	1353.7	486.98	0.083
0.128	1.419	1352.2	485.85	0.092
0.270	1.288	1348.4	485.48	0.112
0.339	1.238	1346.3	485.27	0.121
0.524	1.129	1340.0	484.63	0.146
0.593	1.099	1337.6	484.38	0.155
0.708	1.059	1333.9	484.00	0.167
0.916	1.011	1328.5	483.44	0.184
1.10	1.000	1327.2	483.31	0.188
↓	↓	↓	↓	↓
10.00	1.00	1327.2	483.31	0.188

Note:

Computer program requires geometry input as dimensional quantities, that is, x and r are input in units of feet. To convert to dimensional quantities, R = 3.9 feet.

Fig. 10 Duct Geometry Used in the Parametric Study of This Report

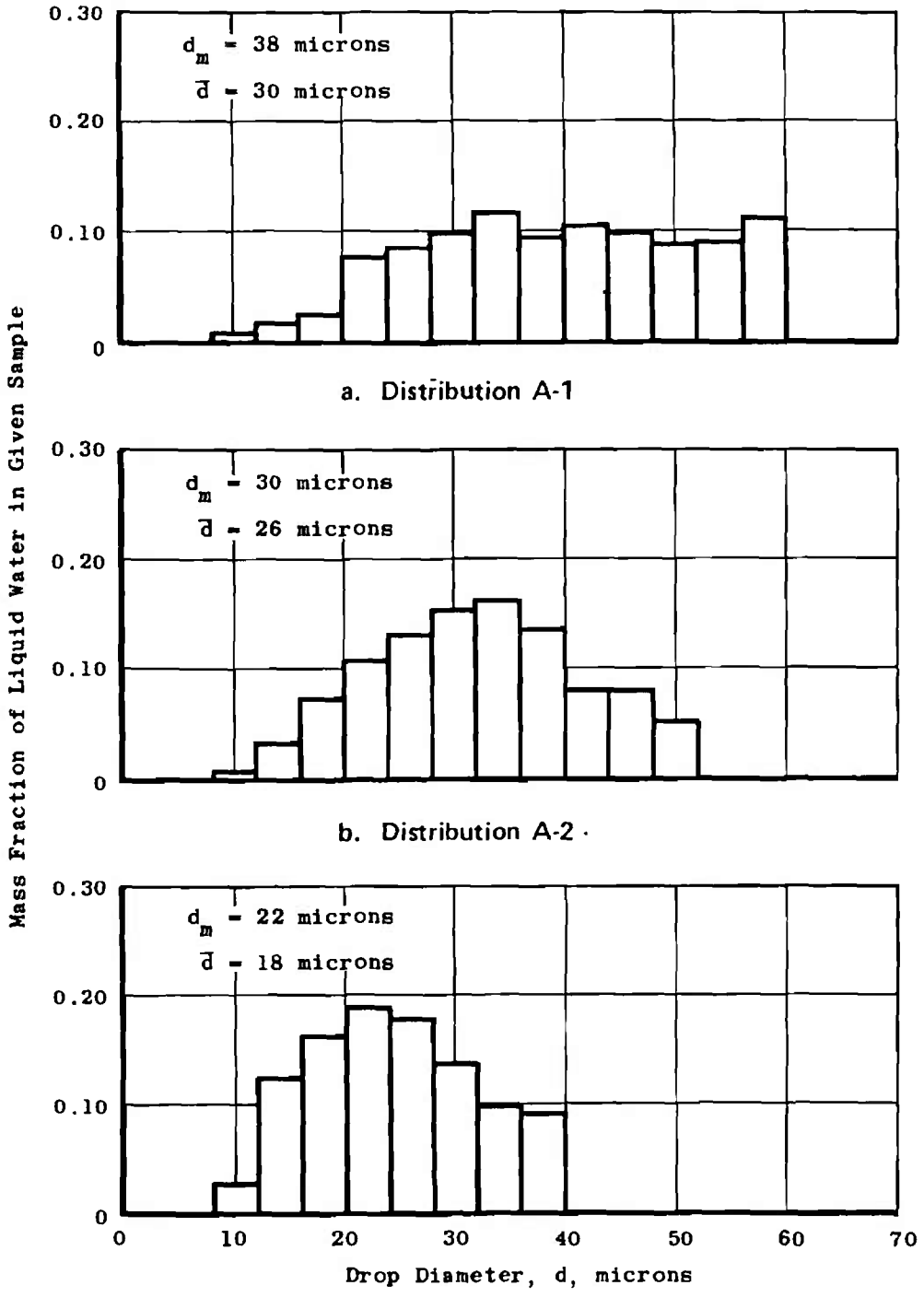

Fig. 11 Mass Fraction of Water in Spray Cloud Contained in Drops of Given Size Class

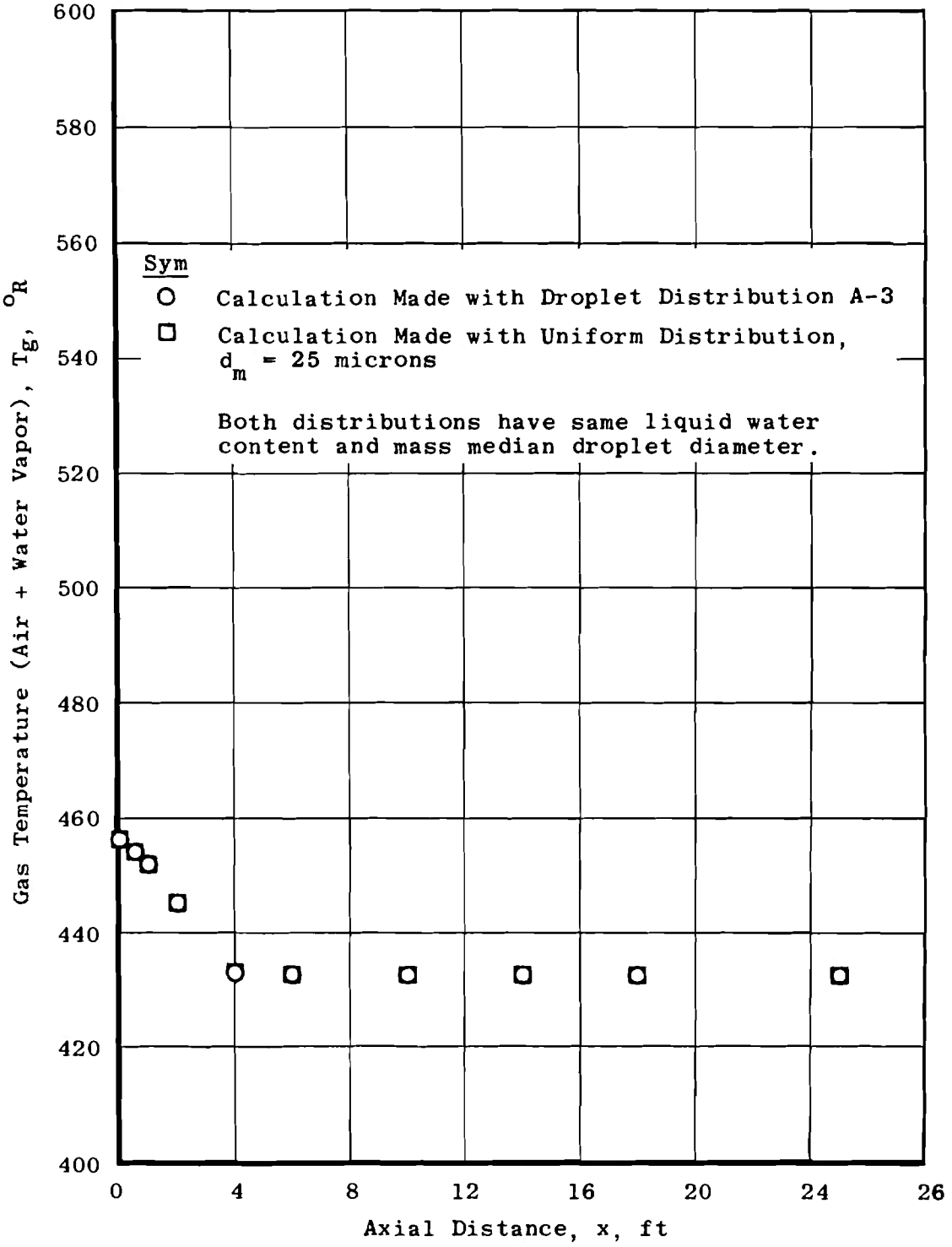

Fig. 12 Gas Temperature versus Axial Location: The Effect of Typical Drop Distribution Compared with Uniform Drop Distribution Having the Same Liquid Water Content and Mass Median Diameter

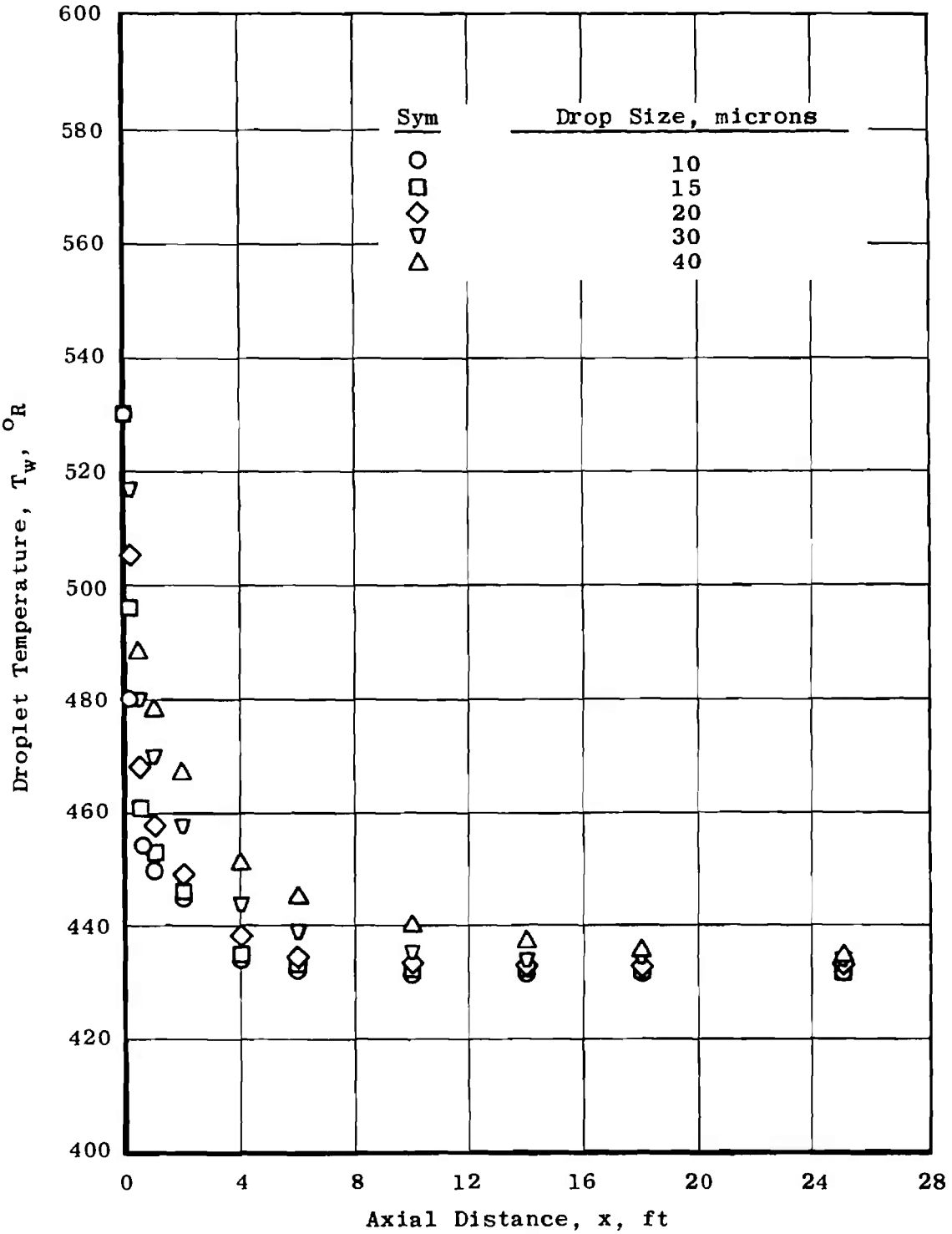

Fig. 13 Droplet Temperature versus Axial Location: The Effect of Droplet Size on Droplet Temperature

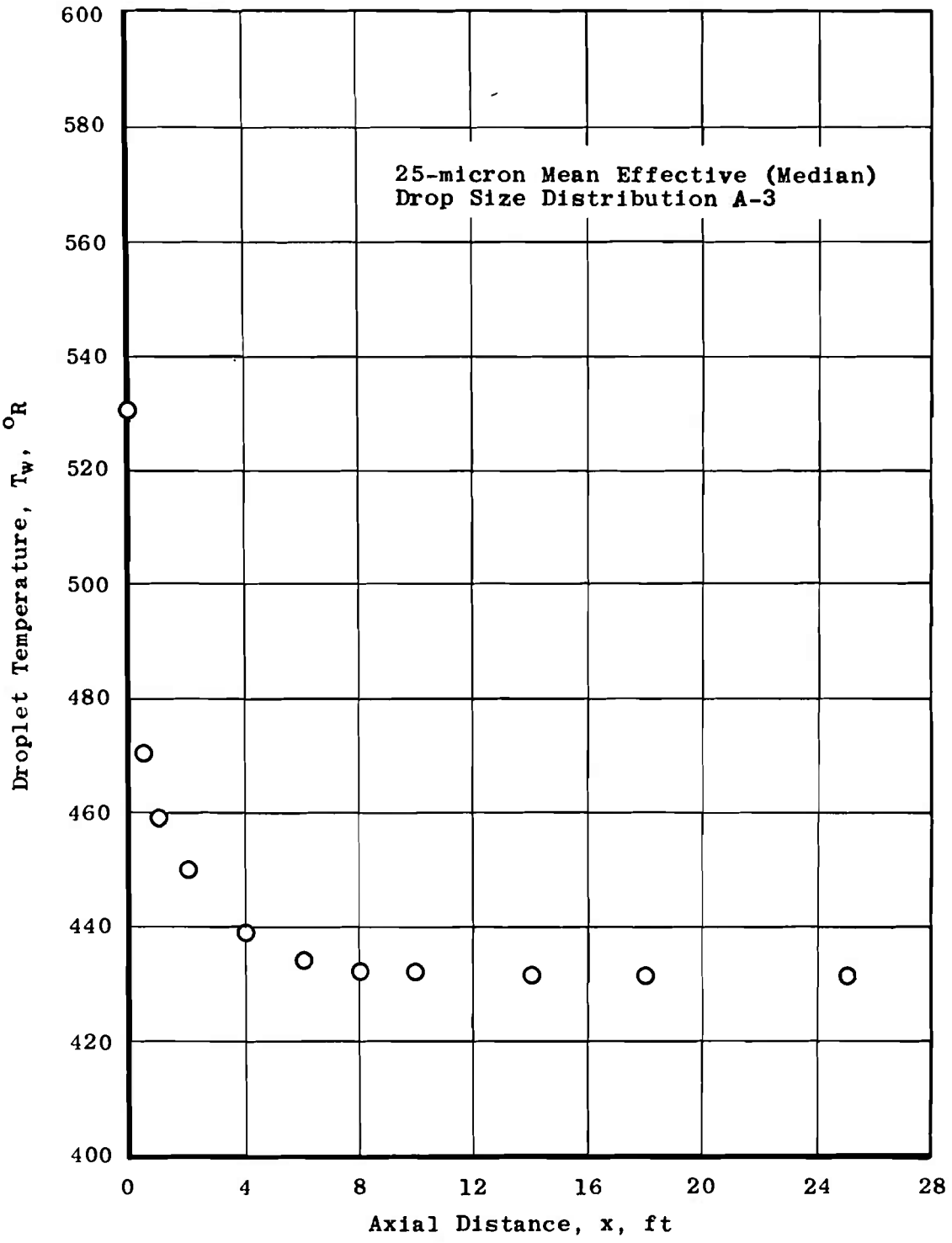

Fig. 14 Droplet Temperature versus Axial Location: Single Size Drop, 25-micron Diameter

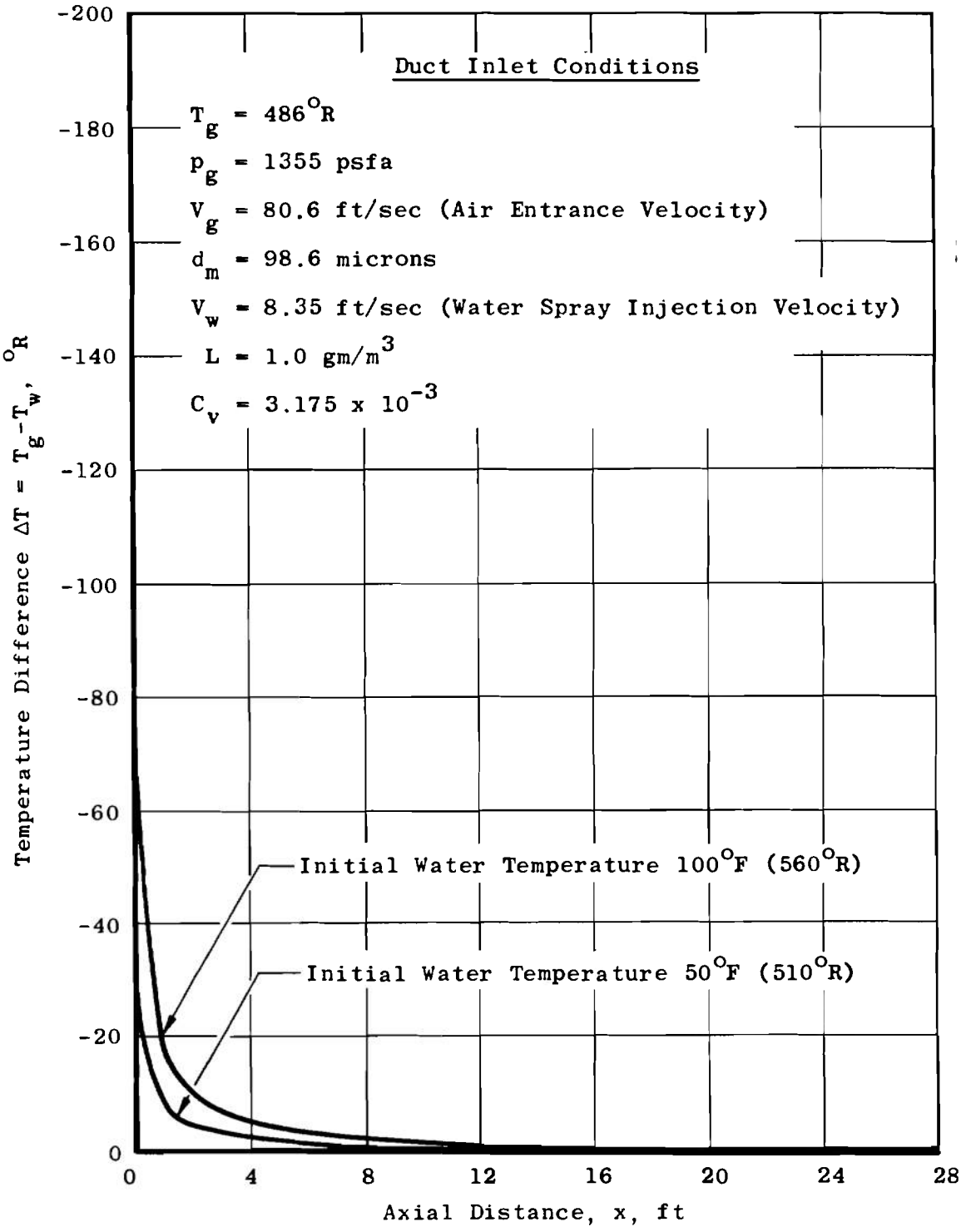

Fig. 15 Temperature Difference between Gas and Water Droplets versus Axial Location: The Effect of Initial Water Spray Temperature

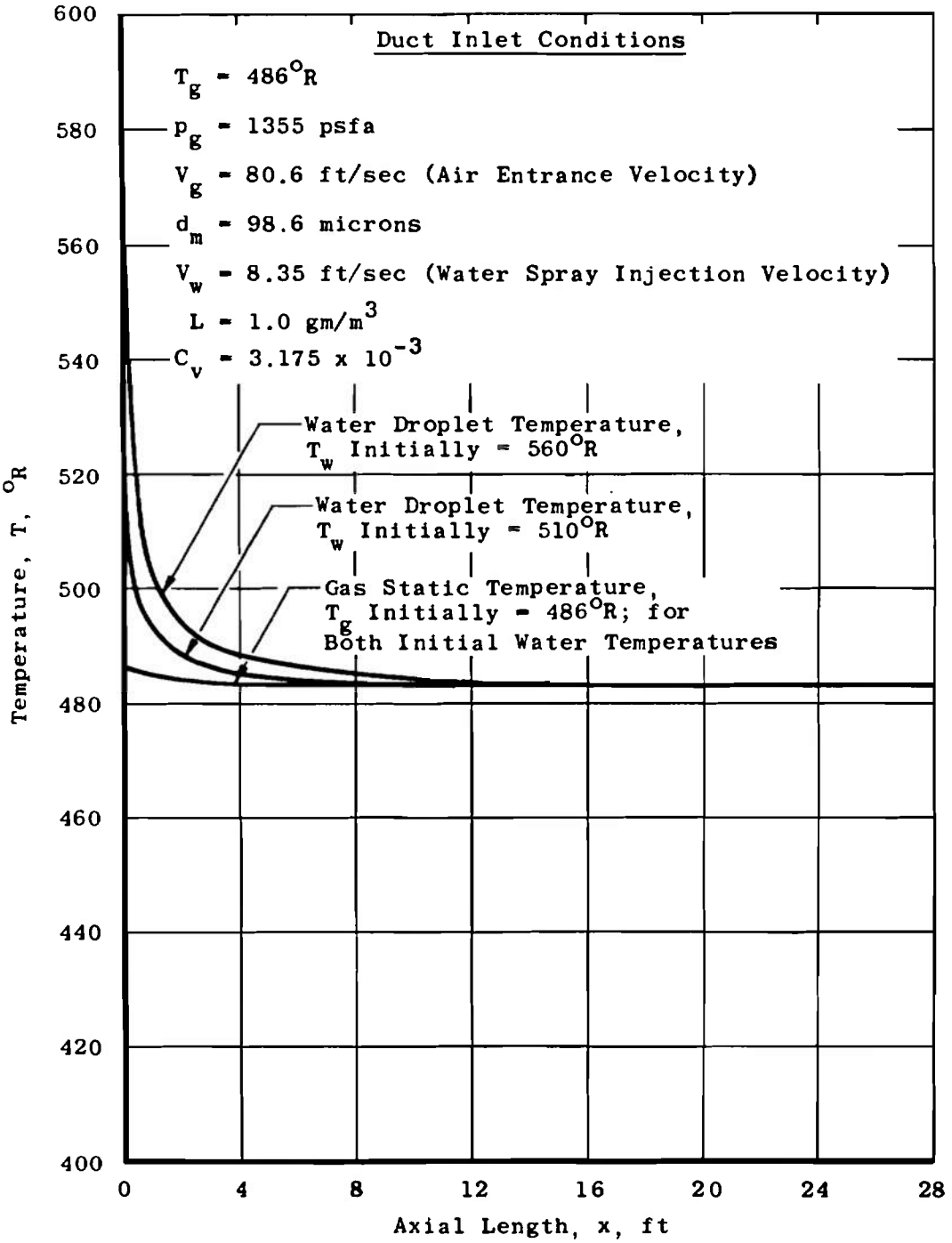

Fig. 16 Temperature versus Axial Location: A Comparison between Water Droplet Temperature and Gas Static Temperature for Two Different Initial Water Spray Temperatures

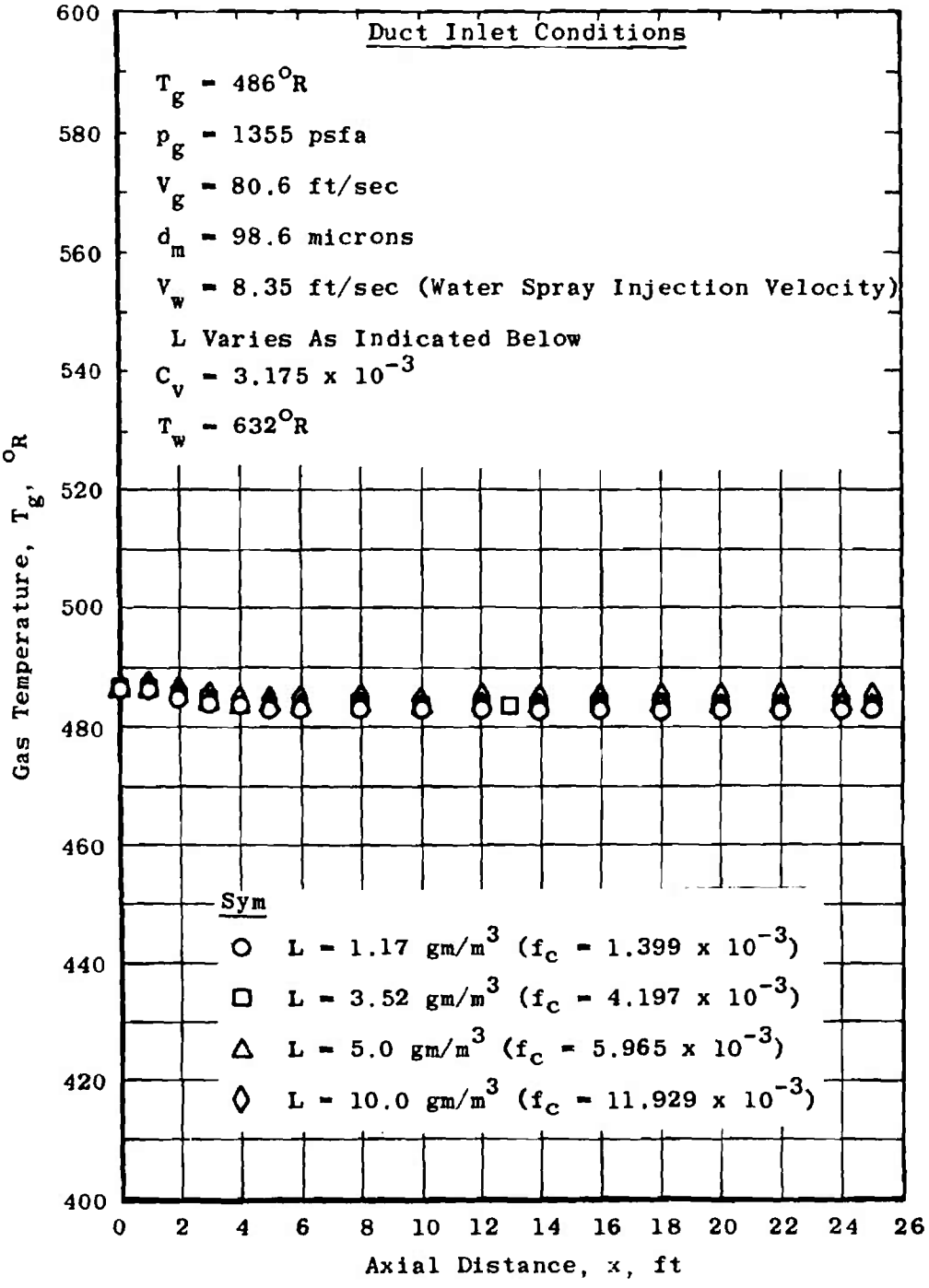

Fig. 17 Gas Static Temperature versus Axial Location: The Effect of Liquid Water Content on Gas Static Temperature

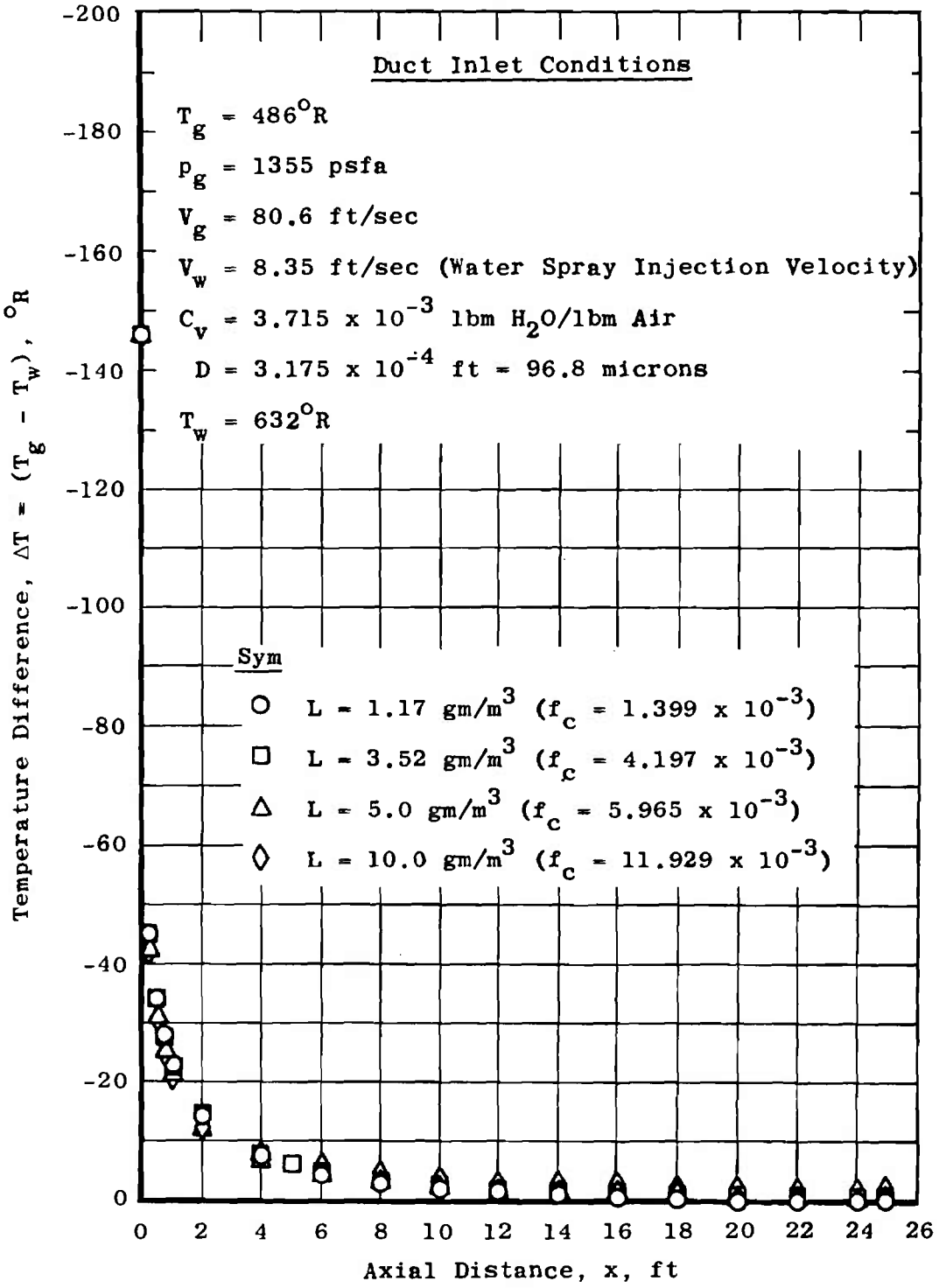

Fig. 18 Temperature Difference between Gas and Water Droplets versus Axial Location: The Effect of Liquid Water Content on Temperature Difference

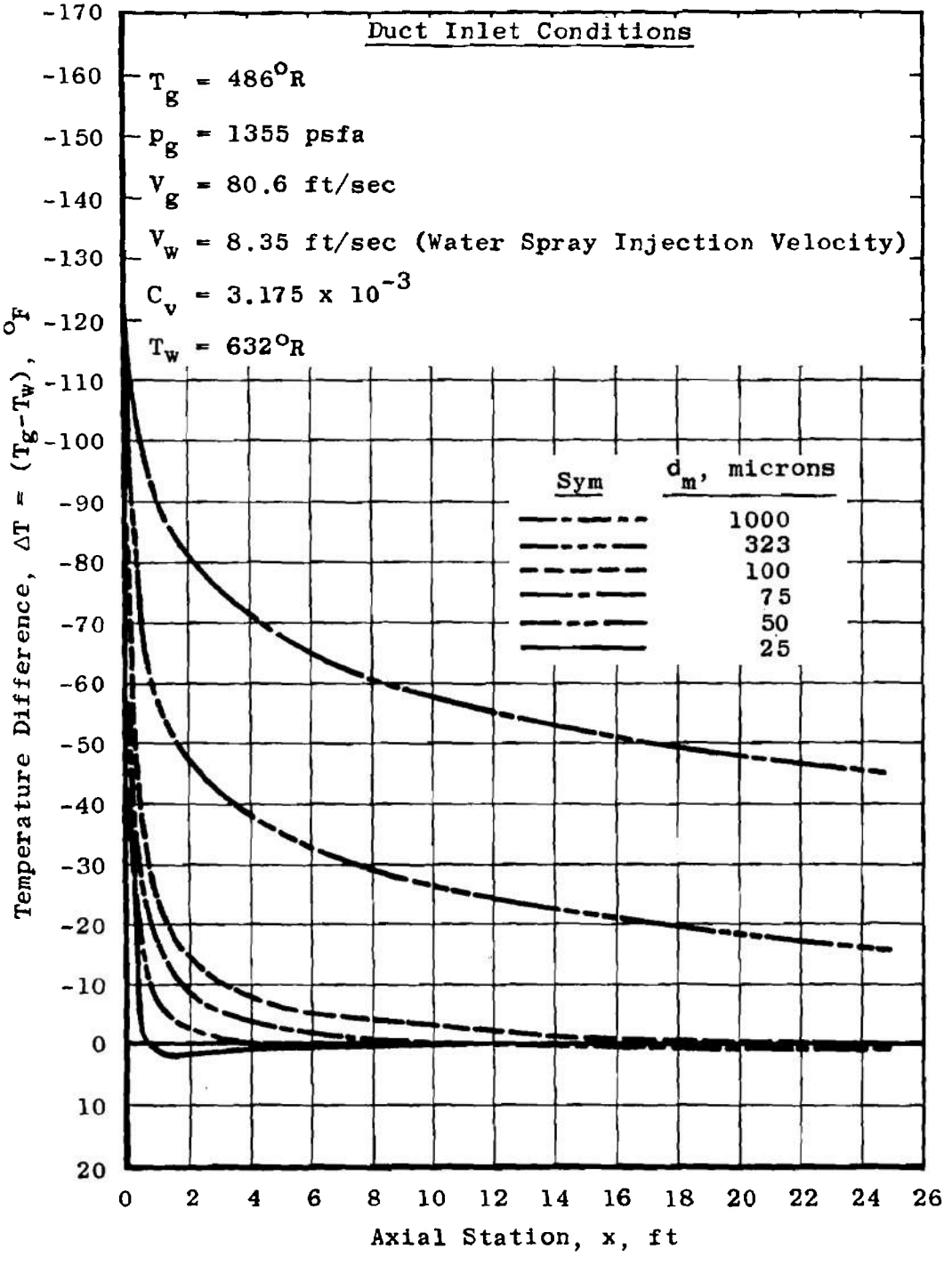

Fig. 19 Temperature Difference between Gas and Water Droplets versus Axial Location: The Effect of Droplet Diameter on Temperature Difference

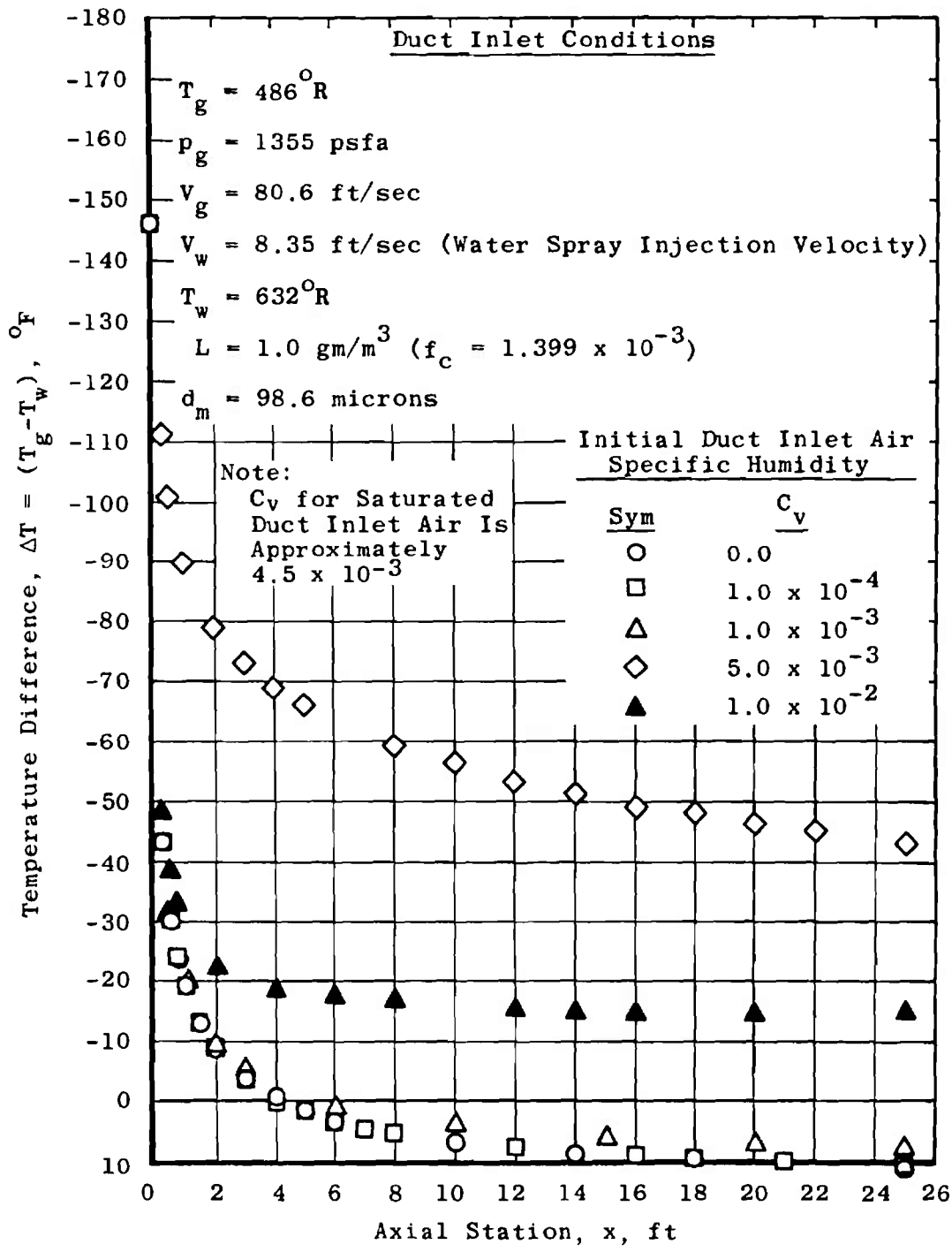

Fig. 20 Temperature Difference between Gas and Water Droplets versus Axial Location: The Effect of Duct Inlet Air Specific Humidity

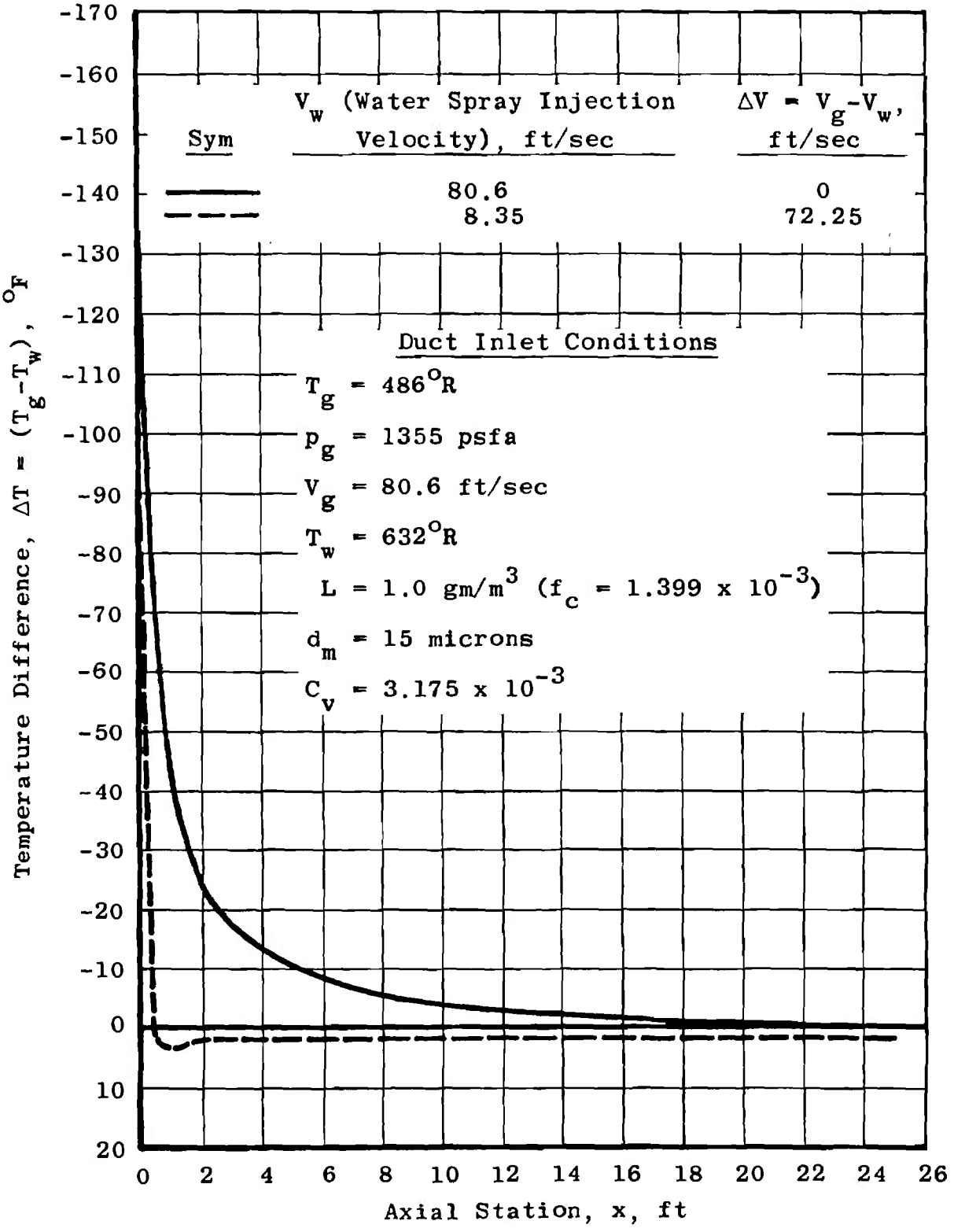

Fig. 21 Temperature Difference between Gas and Water Droplets versus Axial Location: The Effect of the Initial Velocity Difference between Phases

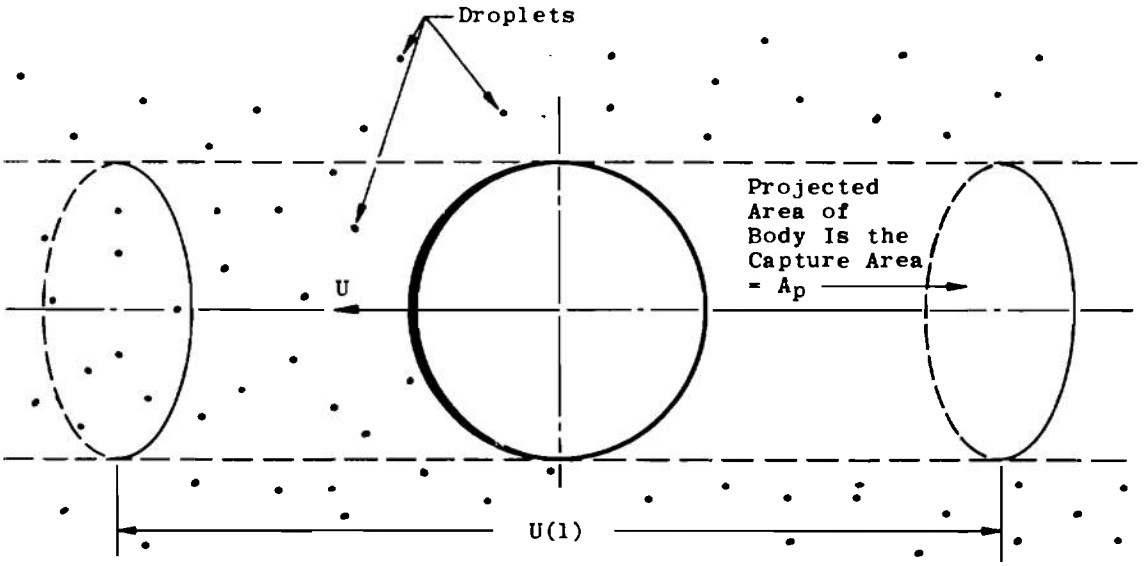

a. Capture Process for Droplets Not Influenced by Streamlines, Idealized Process

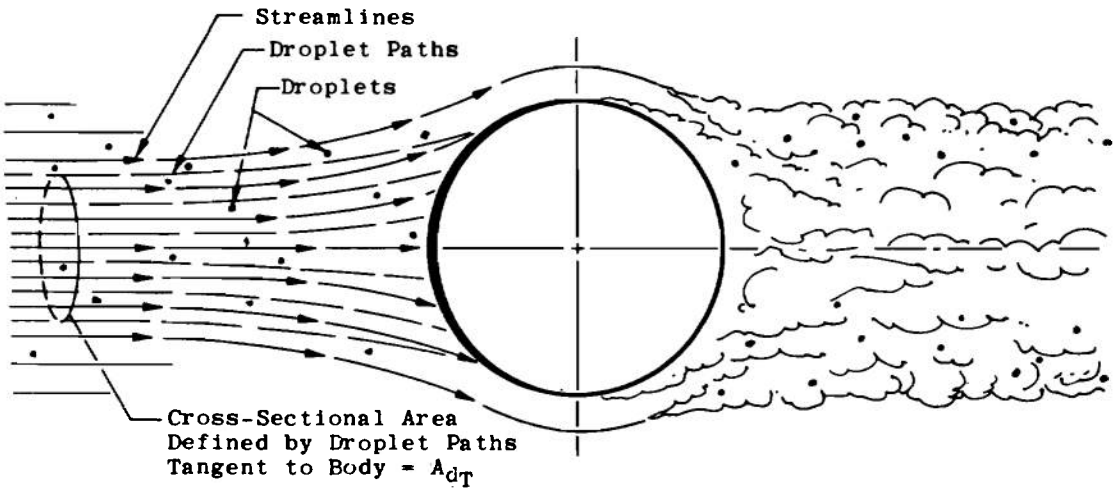

b. Capture Process for Droplets Influenced by Streamlines, Actual Process

Fig. 22 Schematics Illustrating Droplet Capture: The Impingement Process

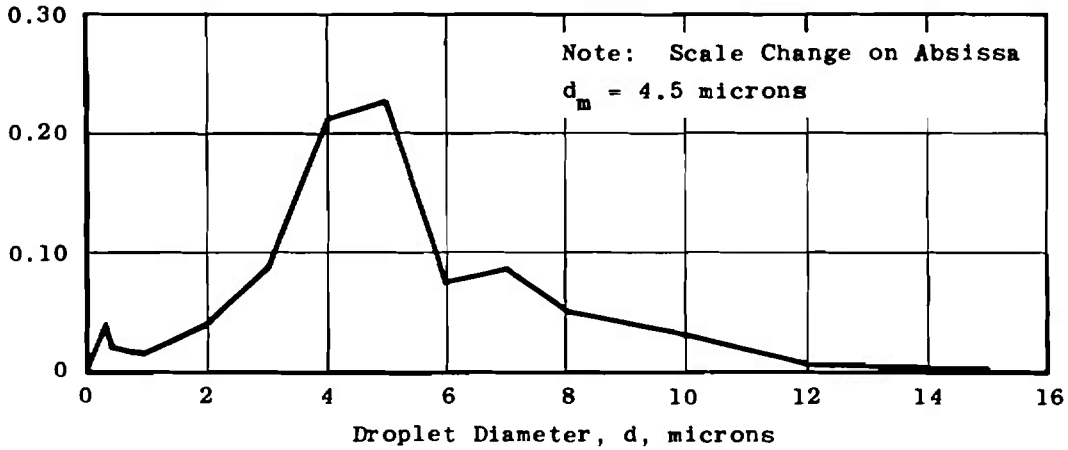

a. Distribution N-1: For Stable Fogs

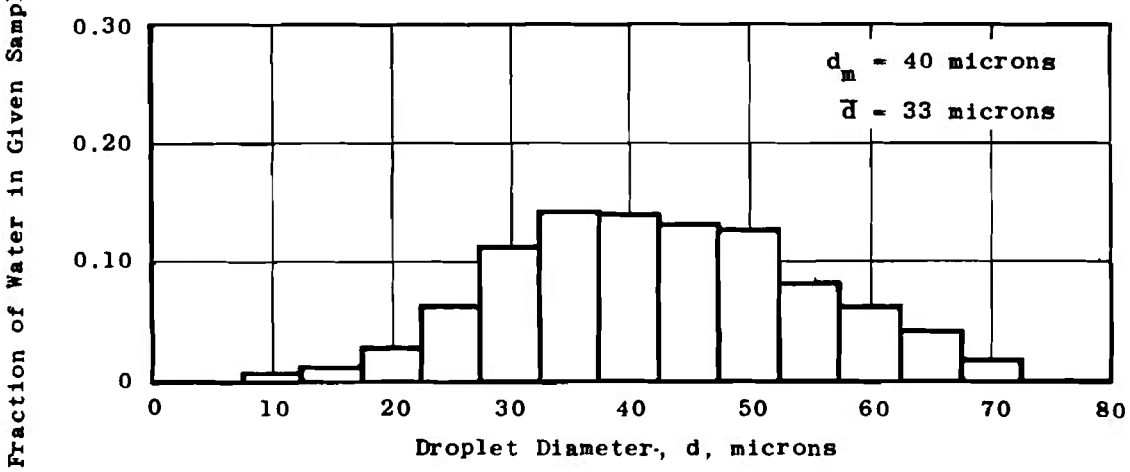

b. Distribution N-2: For Tropical Cumuli

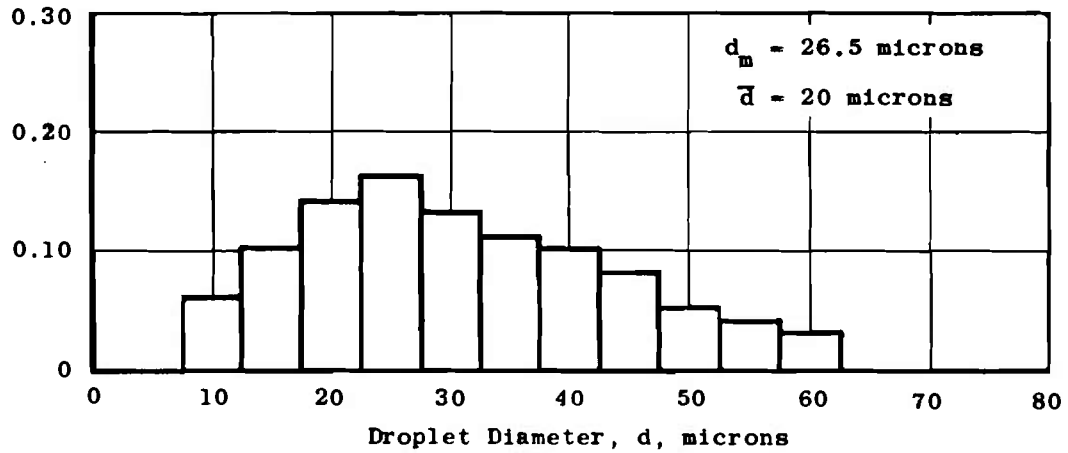

c. Distribution N-3: For Cumuli over Continental U. S.

Fig. 23 Mass Fraction of Water Contained in Drops of Given Size Class: Natural Environment

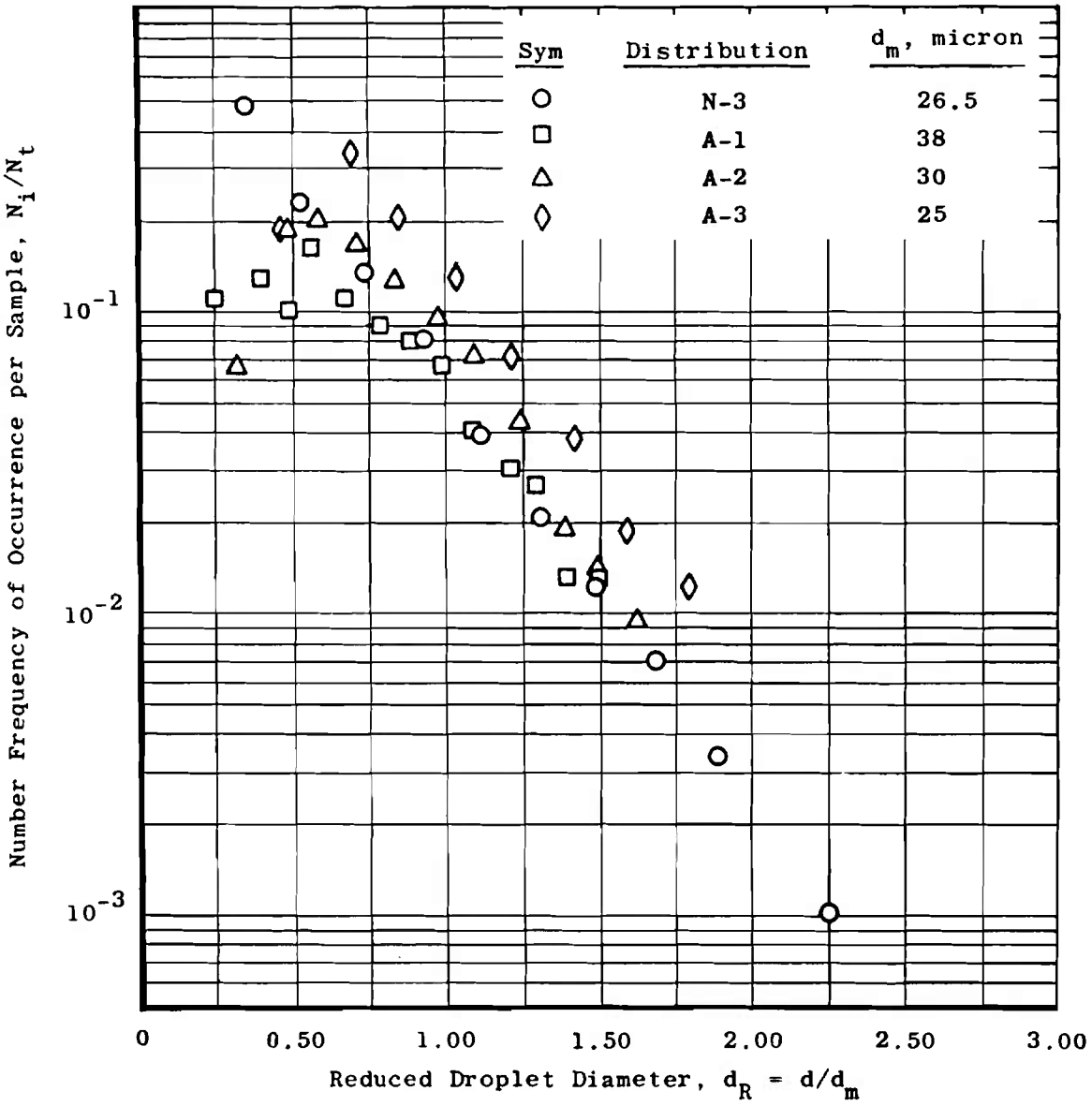

Fig. 24 Droplet Size Class versus Number Frequency of Occurrence: Comparison of Artificial and Natural Distributions

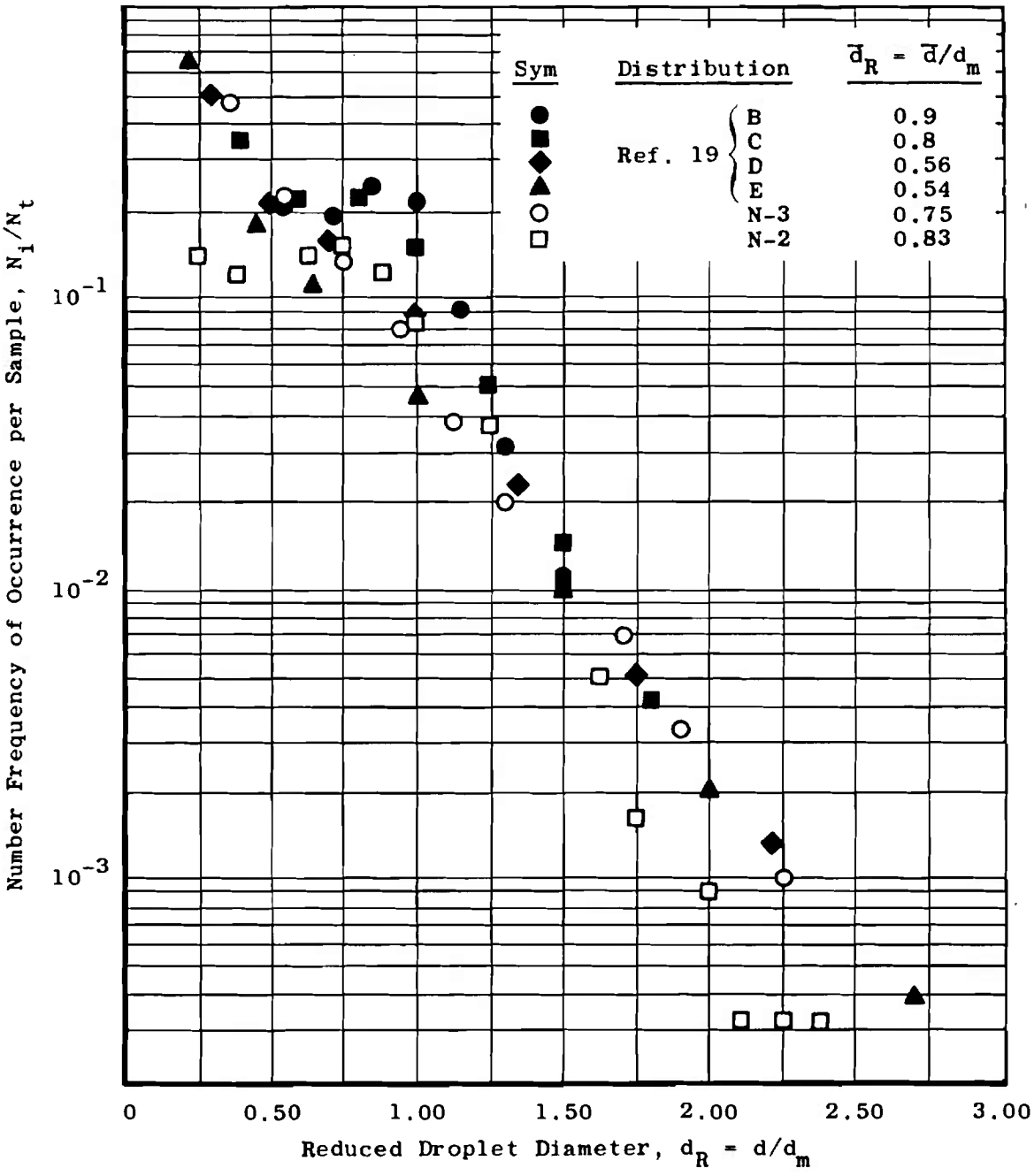

Fig. 25 Droplet Size Class versus Number Frequency of Occurrence: Comparison of Natural Distribution to Langmuir's Distributions

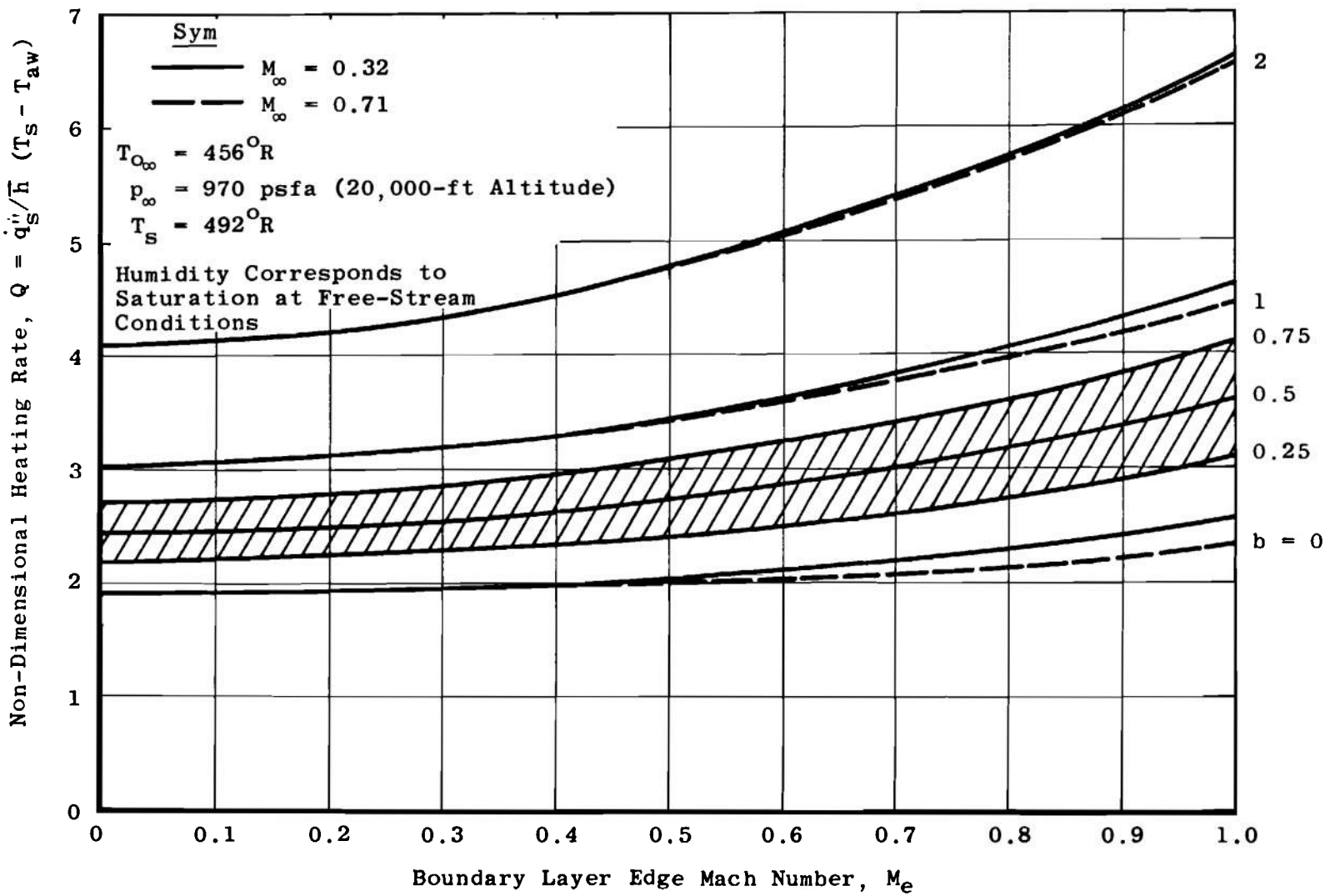

Fig. 26 Sensitivity of Nondimensional Heating Rate (Q) to Sensible Heat Parameter (b)

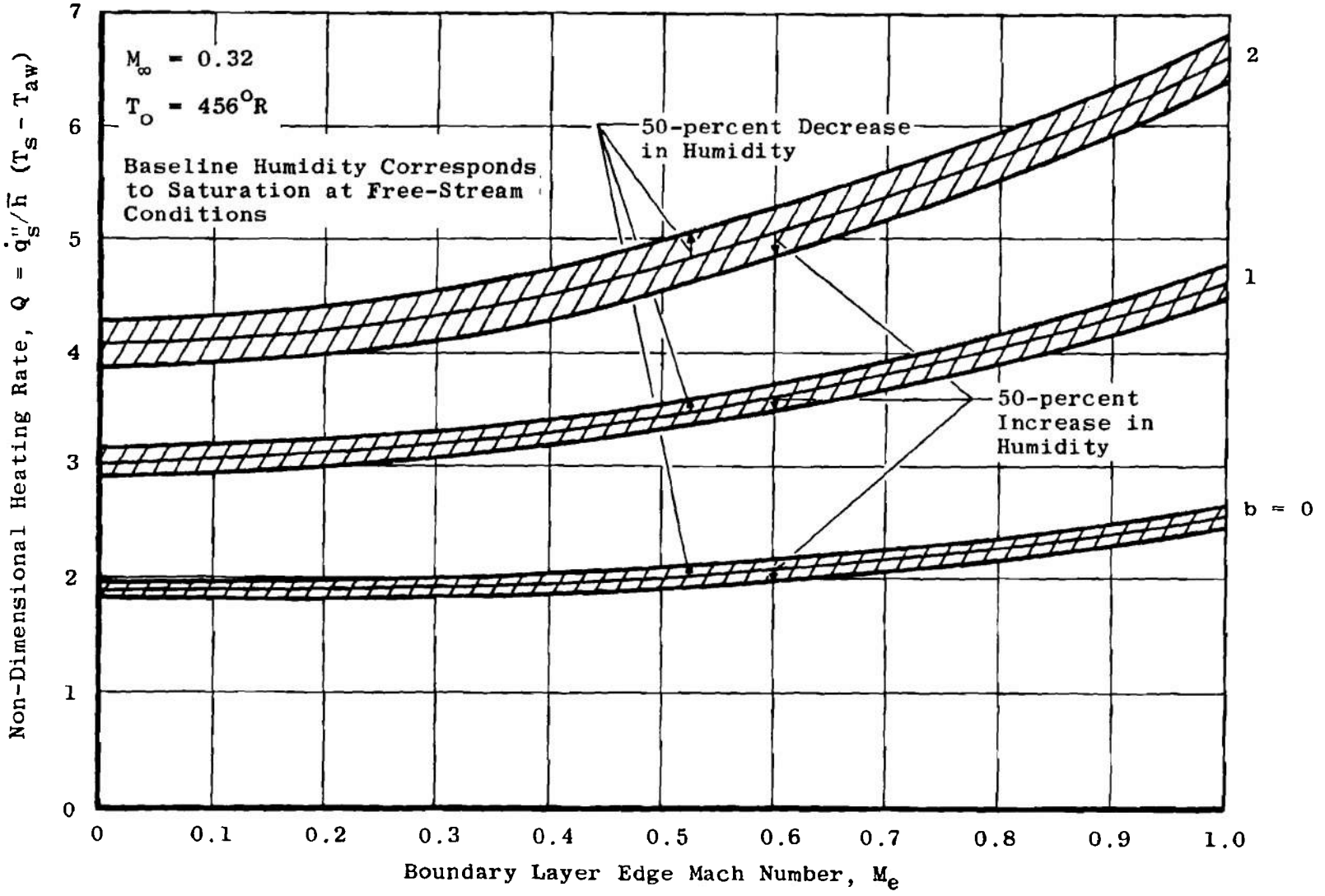

Fig. 27 Sensitivity of Nondimensional Heating Rate (Q) to Humidity for Different Values of the Sensible Heat Parameter (b)

TABLE I
ICING CONDITIONS SPECIFIED IN THE MILITARY SPECIFICATIONS FOR TURBOJET AND TURBOFAN TESTING

I. SEA-LEVEL ANTI-ICING CONDITIONS

ATTRIBUTE	CONDITION I	CONDITION II
Liquid Water Content	1 gm/m^3	2 gm/m^3
Atmosphere Air Temperature	-4°F (-20°C)	+23°F (-5.0°C)
Flight Velocity	Static	Static
Altitude	Sea Level	Sea Level
Mean Effective Drop Diameter	15 microns	25 microns

II. ALTITUDE ANTI-ICING CONDITIONS

ATTRIBUTE	CONDITION I	CONDITION II
Liquid Water Content	0.5 gm/m^3	0.5 gm/m^2
Inlet Air Temperature	-4°F (-20°C)	-4°F (-20°C)
Flight Velocity (Mach Number)	0.32	0.71
Altitude	20,000 ft	20,000 ft
Mean Effective Drop Diameter	15 microns	15 microns

APPENDIX III
COMPUTER PROGRAM

A listing of the computer program used to integrate the equations governing flow in a typical icing test facility are given in this Appendix along with a sample calculation made with the program. The capabilities of the program have been discussed in Section IV of the text.

INPUT AND OUTPUT

The English system of units is used in the program with lengths, including droplet diameter, in feet, pressure in pounds of force per square foot, temperatures in degrees Rankine, mass in pounds, and time in seconds. Almost all input data are punched on cards and read into the program. An exception to this is the initial integration step size DX in feet, which is specified in the main program. The procedure for preparation of input cards is illustrated below. The input data required are as follows:

1. A table of duct radius versus axial position
2. Gas properties
   a. Static temperature
   b. Static pressure
   c. Mass fraction of water vapor
   d. Velocity
3. Total number of injection stations
4. Water properties for each injection station
   a. Temperature
   b. Loading fraction (mass rate of water injection divided by mass flow rate of dry air through the duct)
   c. Droplet diameter
   d. Velocity

The input data cards are prepared as follows:

Card 1

Cols. 1-2 Number of points describing duct geometry (NXY)

A constant area duct can be treated by specifying three points along the duct, including the beginning and end points.

Cards 2 to NXY + 2

These cards specify the duct geometry.

Cols. 1-12	Axial location
Cols. 13-24	Corresponding duct radius

Card NXY + 3

Cols. 1-80	Title identification

Card NXY + 4

Cols. 1-2	Number of injection stations, NSTA

Card NXY + 5

Cols. 1-10	Axial location of first injection station
Cols. 11-20	Axial location of second injection station
Cols. 1 + 10(I-1) through 10I	Axial location of Ith injection station

A fictitious injection station at the end of the duct must be indicated on this card. For example, if only one injection station is used, the location of the end of the duct must be entered in Cols. 11-20.

Card NXY + 6

Cols. 1-10	Mass fraction of water vapor
Cols. 11-20	Gas velocity
Cols. 21-30	Gas temperature
Cols. 31-40	Pressure

Card NXY + 7

Cols. 1-10	Mass flow rate of water from first injection station divided by mass flow rate of dry air through duct
Cols. 11-20	Mass flow rate of water from second injection station divided by mass flow rate of dry air through duct

Cols. 1 + 10(I-1) through 10I	Mass flow rate of water from Ith injection station divided by mass flow rate of dry air througn duct

Card NXY + 8

Cols. 1-10	Water injection velocity for first injection station
Cols. 11-20	Water injection velocity for second injection station
Cols. 1 + 10(I-1) through 10I	Water injection velocity for Ith injection station

Card NXY + 9

Cols. 1-10	Temperature of water injected at first injection station
Cols. 11-20	Temperature of water injected at second injection station
Cols. 1 + 10(I-1) through 10I	Temperature of water injected at Ith injection station

Card NXY + 10

Cols. 1-10	Droplet diameter of water injected at first injection station
Cols. 11-20	Droplet diameter of water injected at second injection station
Cols. 1 + 10(I-1) through 10I	Droplet diameter of water injected at Ith injection station

In cards NXY + 7 to NXY + 10, it is necessary to make entries for only the number of injection stations being considered.

It has been found that the most common cause of program failure is use of an improper integration step size. No criterion has been developed for step size selection; however, through experience with the program the user may develop a "feel" for selecting a satisfactory step size. Difficulties are to be expected in getting solutions for initial conditions corresponding to an extremely high degree of nonequilibrium.

The program output includes the following: axial location (X), mass fraction of water vapor (CV), area ratio (A/AO), gas velocity (VG), condensed phase velocity (VL), condensed phase loading fraction (FL), gas temperature (TG), condensed phase temperature (TS), static pressure (P), and droplet diameter (D). The first line of values of FL, VL, TS, and D at a particular value of X are values corresponding to water that originated at the first injection station. The second line of values of FL, VL, TS, and D corresponds to the water from the second injection station, and so on.

PROGRAM LISTING

The program listing is presented on the following pages.

```
C      MAIN PROGRAM FOR SPRAY COOLER AND DRYER  PROBLEM
C IF THIS PROGRAM SHOULD STOP BEFORE THE REQUIRED LIMIT ON X IS MET
C WITH A PRINTOUT OF 'TEMP-FI- IS OUT OF RANGE  TG=XXX , TS=XXX 'AT THE
C END OF THE OUTPUT, WE SHOULD INCREASE THE AMOUNT OF WATER TO BE
C      INJECTED (FL).
C
C
C
C
C
C
C
      DIMENSION ROL(10),CPL(10)
      DIMENSION FL(10),VL(10),TS(10),D(10),STA(11)
      DIMENSION Y(90)
      DIMENSION YP(60)
      DIMENSION BUFF(1000)
      COMMON BA
      COMMON ROL,VW,GW,GC,RV,CJ,WNCA0,B(4),ISTA,ISET,KKK,
     1KOUNT,NSTA,IDUM
      COMMON /ICEE/CPI,ROI,SUMJ(10),DELE(10),SUM9(10),NF(10),NG(10)
      COMMON /XYN/ XS(99),YS(99),NXY
      COMMON/LOW/ MICH
      COMMON /DDXX/ DX
      COMMON /RSQR/ R2
      COMMON /ROYS/ ALP(10),JECT,INIT
      CALL LUNITS
      LCR=29
      LPR=21
      M=0
      READ (LCR,102)NXY
      READ(LCR,104)(XS(I),YS(I),I=1,NXY)
  104 FORMAT (2E12.0)
      R2=YS(1)*YS(1)
      NXY=NXY-2
  200 M=M+1
      BA = 0.05
      MICH=0
      READ(LCR,51015)ALP
51015 FORMAT(20A4)
      READ(LCR,102)NSTA
      NS1= NSTA+1
      READ(LCR,101)(STA(I),I=1,NS1)
      READ(LCR,100)CV,VG,TG,P
      READ(LCR,101)(FL(I),I=1,NSTA)
      READ(LCR,101)(VL(I),I=1,NSTA)
      READ(LCR,101)(TS(I),I=1,NSTA)
      READ(LCR,101)(D(I) ,I=1,NSTA)
  100 FORMAT(4E10.2)
  101 FORMAT (8E10.0)
  102 FORMAT( I2)
  103 FORMAT(15H1 BEGIN STATION ,I4,12X,16H RUN INFORMATION ,20A4)
      CJ=778.0
      GC= 32.2
      ISET = 9
      GW=29.0
      VW=18.0
      RV= 1.986* 778.0
      DO 20 I=1,10
      NG(I)=0
```

```
      NF(I)=0
      ROL(I)=62.400
      CPL(I)=1.00
      SUM9(I)=0.0
   20 SUMJ(I)=0.D0
      ROI=ROL(1)*0.91700
      CPI=CPL(1)*0.48500
      THEF = 540.0
      ISTA=1
      NEQ=8
C     THE ARRAYS USED IN DIFFE ARE NOW SET UP
      Y(1)=CV
      Y(2)=VG
      Y(3)=TG
      Y(4)=P
      Y(5)=FL(1)
      Y(6)=VL(1)
      Y(7)=TS(1)
      Y(8)= D(1)
      WNCAO= Y(2)*(1.0-Y(1))*Y(4)/(Y(3)*RV*((1.-Y(1))/GW +Y(1)/VW))
      X=0.0
      WRITE(LPR,103) ISTA,ALP
      INIT=0
      JECI=4
3     CONTINUE
      DX=.0001
      KOUNT =0
      LIMIT=99999
      DO 1 I=1,LIMIT
      CALL DIFFE(X,Y,YP,DX,KKK,NEQ,I)
      IF(X.GE.STA(ISTA+1))GO TO 2
1     CONTINUE
      JJJ= JJJ+1
2     CONTINUE
C     WE WILL NOW PLOT THE STATION JUST FINISHED
      NP=KOUNT
      ISTA= ISTA+1
      ISET = 9
      IF(ISTA .GT. NSTA)GO TO 5
      WRITE(LPR,103) ISTA,ALP
C     SET UP  ARRAYS  FOR DIFFE
      Y(NEQ+1)=FL(ISTA)
      Y(NEQ+2)=VL(ISTA)
      Y(NEQ+3)=TS(ISTA)
      Y(NEQ+4)=D(ISTA)
      NEQ =NEQ+4
      KOUNT = 0
      GO TO 3
    5 CONTINUE
      GO TO 200
  222 STOP
      END
      SUBROUTINE DIFFE(X,Y,YP,DX,KK,NEQ,I)
      DIMENSION Y(50),YP(50),Z(50),ZP(50),ZN(50)
      COMMON HA
      COMMON ROL,VW,GW,GC,RV,CJ,WNCAO,B(4),ISTA,ISET,KKK,
     1KOUNT,NSTA,IDUM
      COMMON /XYN/ XS(99),YS(99),NXY
      COMMON /DDXX/ DXX
      COMMON /BARK/ BARM(10)
      CALL LUNITS
      LPR=21
      LCR=29
      CALL MONITR(X,Y)
      CALL YFUNC(X,Y,YP,1)
      DO 1 I=1,NEQ
```

This card establishes initial integration step size.

```
    1 Z(I)=Y(I)+DX*YP(I)
      X=X+DX
      DX2=.5D+0*DX
      DO 5 J=2,9999
      CALL YFUNC(X,Z,ZP,J)
      K=0
      DO 40 I=1,NEQ
      ZN(I)=Y(I)+DX2*(YP(I)+ZP(I))
      IF(DABS(ZN(I)-Z(I))-1.D-05*DABS(ZN(I)))4,4,3
    3 K=1
    4 KK=J
      Z(I)=ZN(I)
   40 CONTINUE
      IF(K)5,6,5
    5 CONTINUE
      WRITE(LPR,99)(ZN(I),I=1,NEQ)
      WRITE(LPR,90)KK
   90 FORMAT(I5)
   99 FORMAT(4E20.10)
      STOP
    6 DO 7 I=1,NEQ
    7 Y(I)=Z(I)
      IF(J .GE. 3 .AND. J .LE. 5)GO TO 1212
      IF(J .LT. 3)GO TO 2020
      DX=.5*DX
      DXX=DX
      GO TO 1212
 2020 DX=2.0*DX
      IF(DX .GT. 0.1) DX=0.1
      GO TO 1212
 1212 CONTINUE
      DXX=DX
      RETURN
      END
      SUBROUTINE YFUNC(X,Y,YP,K)
      DIMENSION ROL(10),CPL(10)
      DIMENSION  Y(50),YP(50),A5(10),A6(10),A7(10),A8(10),A10(10),XVS(10
     1),XML(10),XMEG(10),BARM(10),DM(10),AK(10),CD(10)
     2,XHV(10)
      COMMON BA
      COMMON ROL,VW,G,GC,RV,CJ,WNCA0,B(4),ISTA,ISET,KKK,
     1KOUNT,NSTA,IOUM
      COMMON /RSQR/ R2
      COMMON /DDXX/ DX
      COMMON /ROYS/ ALP(10),JECT,INIT
      COMMON /ICEE/CPI,ROI,SUMJ(10),DELE(10),SUM9(10),NF(10),NG(10)
      COMMON /BARK/ BARM
      COMMON /PLOTT/ XX(102),CV (102),VG (102),TG(102),P(102),FL(10,102)
     C,VL (10,102),TS (10,102),D (10,102)
      COMMON /AYE/ I
      CALL LUNITS
      LPR=21
      LCR=29
      PIE =3.1416
      SUM1=0.
      SUM2=0.
      SUM3=0.
      SUM4=0.
      SUM5=0.
      CALL ROBEE(ROG,Y(1),Y(2),X)
      DO 1 I=1,ISTA
      J= 8+4*(I-1)
      A5(I) = PIE*ROL(I)*Y(J)**2  /2.0
      CALL SUB1(Y(1),Y(3),Y(4),Y(J-1),XVS(I),XV,XK(I),Y(J),DM(I),CD(I),B
     1ARM(I),Y(J-2),Y(2))
      YP(J)= XK(I)*PIE*Y(J)**2.0*(XV-XVS(I))*VW/(A5(I)*Y(J-2)*(1.0-XVS(I
```

```
     1)))
      A6(I)= YP(J)
      YP(J-2)=((PIE/M.0)*ROG*(Y(J)**2    )*CD(I)*DABS(Y(2)-Y(J-2))*(Y(2)-
     1Y(J-2))-( Y(J-2)-Y(2))*Y(J-2)*A5(I)*A6(I))/(DM(I)*Y(J-2))
      A7(I)=YP(J-2)
      YP(J-3)= A5(I)*A6(I)*Y(J-3)/DM(I)
      A8(I)=YP(J-3)
      SUM1=SUM1+A5(I)*A6(I)*Y(J-3)/DM(I)
      CALL HLI(Y(J-1),XHL(I),XHFG(I),XHV(I))
      YP(J-1) =   BARH(I)* PIE * Y(J)**2 *(Y(3)-Y(J-1))/ (DM(I)*Y(J-2))-
     CXHL(I)*A5(I)*A6(I)/DM(I)+A5(I)*A6(I)*XHV(I)/DM(I)
      A10(I)= YP(J-1)
      SUM2 = SUM2 + Y(J-2)*A8(I)+ Y(J-3)*A7(I)
      SUM3 = SUM3 +A8(I)*(XHL(I)+Y(J-2)**2 /(2.0*GC*CJ))
      SUM4 = SUM4 +Y(J-3)* Y(J-2)*A7(I)/(GC*CJ)
      SUM5 = SUM5 + Y(J-3)*A10(I)
1     CONTINUE
      YP(1)=-SUM1*(1.0-Y(1))**2.0
      A9=YP(1)
      CALL AAA3(X,Y(1),Y(2),A3,AA0,DAA0,ROG)
      CALL DERT( ROG,Y(1),Y(2),Y(3),Y(4),A9,SUM2,SUM3,SUM4,SUM5,A0,A3,AI
     C1,A12,A13,A14,R,CPV,CPA,A2,A4,AA0,A)
      YP(3)= (A11*A14-A12*A13)/(A11*(CPV*Y(1)/(1.0-Y(1))+CPA)-A12*A0*ROG
     1*R)
      A15= YP(3)
      YP(2) = (A13-A0*ROG*R*A15)/A11
      A16=YP(2)
      CALL DERP(ROG,Y(1),Y(2),Y(3),R,A2,A3,A4,A9,A15,A16,DP,A)
      YP(4) = DP
      IF(K.GT. 1) GO TO 3
      IF(X .EQ. 0.0)GO TO 9999
      IF(X.LT.0.00051) GO TO 9999
      IF(X .LT. HA)GO TO 3
      IF (X.LT.1.0)  HA = HA + 0.05
      IF (X.GT.1.0)  HA = HA + 0.25
9999  CONTINUE
      CPG=Y(I)*CPV  +(1.D0-Y(1))*CPA
   20 FORMAT (1H ,3E20.9)
      CPG=CPG*778.00
      GAMG=CPG/(CPG-R)
      AMACH=DSQRT(GAMG*GC*R*Y(3))
      AMACH=Y(2)/AMACH
      POT=1.D0+(GAMG-1.D0)*0.5D0*AMACH*AMACH
      PO=Y(4)*POT**(GAMG/(GAMG-1.D0))
      TO=Y(3)*POT
   30 FORMAT(11H1STATION = ,I4,10X,16H RUN INFORMATION,20A4)
   31 FORMAT(15H0INITIAL AREA =,G16.6)
      AREAI=3.1415926D0*R2
      IF(INIT .EQ. 0) WRITE(LPR,31) AREAI
      INIT=INIT+1
      WRITE(LPR,4) X,AMACH,PO,TO
      IF(JECT .GE. 54) WRITE(LPR,30)ISTA,ALP
      IF(JECT.GE.54) JECT=0
      JECT=JECT+2
      WW= Y(I)/(1.0-Y(1))
    4 FORMAT(4H0X= ,G16.6,3X,4H MG=,G16.6,3X,4H PO=,G16.6,3X,4H TO=,
     1 G16.6)
      WRITE(LPR,5) AA0,WW
      IF(JECT .GE. 54) WRITE(LPR,30)ISTA,ALP
      IF(JECT.GE.54) JECT=0
      JECT=JECT+2
    5 FORMAT(8H0 A/A0= ,G16.6,3X,9H WV/WNC =,G16.6)
      WRITE(LPR,6)Y(1),Y(2),Y(3),Y(4)
      IF(JECT .GE. 54) WRITE(LPR,30)ISTA,ALP
      IF(JECT.GE.54) JECT=0
      JECT=JECT+2
```

```
    6 FORMAT(4H0CV=,G16.6,3X,4H VG=,G16.6,3X,4H TG=,G16.6,3X,3H P=,G16.6
     1 )
      DO 10 I= 1,ISTA
      J=B+4*(I-1)
      DELT=Y(3)-Y(J-1)
      WRITE(LPR,8)Y(J-3),Y(J-2),Y(J-1),Y(J),DELT
      IF(JECT .GE. 54) WRITE(LPR,30)ISTA,ALP
      IF(JECT.GE.54) JECT=0
      JECT=JECT+2
    8 FORMAT(4H0FL=,G16.6,3X,4H VL=,G16.6,3X,4H TS=,G16.6,3X,3H D=,
     1G16.6,1X,6H DELT=,F7.3)
      WRITE(LPR,9) YP(J-3),YP(J-2),YP(J-1),YP(J)
      IF(JECT .GE. 54) WRITE(LPR,30) ISTA,ALP
      IF(JECT.GE.54) JECT=0
      JECT=JECT+2
10    CONTINUE
    9 FORMAT(5H0FLP=,G16.6,3X,5H VLP=,G16.6,3X,5H TSP=,G16.6,3X,4H DP=,
     1G16.6)
      WRITE(LPR,7) YP(1),YP(2),YP(3),YP(4)
      IF(JECT .GE. 54) WRITE(LPR,30) ISTA
      IF(JECT.GE.54) JECT=0
      JECT=JECT+2
    7 FORMAT(5H0CVP=,G16.6,3X,5H VGP=,G16.6,3X,5H TGP=,G16.6,3X,4H PP=,
     1G16.6)
      IF(KOUNT .GE.100) GO TO 1000
      KOUNT = KOUNT +1
      XX(KOUNT) =X
      CV (KOUNT)= Y(1)
      VG (KOUNT)= Y(2)
      TG (KOUNT)= Y(3)
      P (KOUNT) = Y(4)
      DO 1001 I= 1,ISTA
      J= B+4*(I-1)
      FL (I,KOUNT) =Y(J-3)
      VL (I,KOUNT) =Y(J-2)
      TS (I,KOUNT) =Y(J-1)
      D (I,KOUNT) = Y(J)
1001  CONTINUE
1000  CONTINUE
3     CONTINUE
2     FORMAT(1H ,7E16.6)
      RETURN
      END
      SUBROUTINE MUNITR(X,Y)
      DIMENSION YP(50)
      DIMENSION XVS(10),XK(10),DM(10),CD(10)
      DIMENSION Y(50),B(10),CPL(10)
      COMMON BA,ROL(10),VM,GM,GC,RV,CJ,WNCA0,Z(4),ISTA
      COMMON /1CEE/CPI,RO1,SUMJ(10),DELE(10),SUM9(10),NF(10),NG(10)
      COMMON /DDXA/ DX
      COMMON /AYE/ I
      COMMON /BARK/ BARM(10)
      CALL LUNITS
      LPR=2
      LCR=29
      ENTLO=144.0
      CALL YFUNC(X,Y,YP,2)
      DO 10 I=1,ISTA
      B(I)=BARM(I)
   10 CONTINUE
      DO 1000 I=1,ISTA
      J=B+4*(I-1)
      A=(Y(J)/.001093)
      IF(Y(J) .LE. .00328D0 .AND. Y(J) .GT. .001093)TSF=463.2D0
      IF(Y(J) .LT..001093D0)TSF=(463.20+16.320*DLOG(A))
      ENTL=ENTLO+(TSF-492.0)
```

```
      IF(NG(I) - I)44,55,55
   44 IF(Y(J-1) .GT. TSF)GO TO 1000
   55 IF(NF(I) .EQ. I)GO TO 1000
      HVV=1349.60-.55*(4290*Y(J-1)
      SUM9(I)=SUM9(I)+((3.0/Y(J))*YP(J)*DX*HVV)
      SUMJ(I)=SUMJ(I)+6.D0*B(I)*(Y(J-1)-Y(3))*DX/(ROL(I)*Y(2)*Y(J))
      WRITE(LPR,100) SUM9(I),SUMJ(I),I
      WRITE(LPR,100) YP(J),HVV,ISTA
      WRITE(LPR,101) B(I)
  101 FORMAT(E20.10)
  100 FORMAT(2E20.10,I10)
      SUMJ(I)=SUMJ(I)-SUM9(I)
      WRITE(LPR,99) SUMJ(I)
      IF(DABS(SUMJ(I))-ENT(I)4,5,5
    4 Y(J-1)=492.00
      NG(I)=1
      GO TO 1000
    5 NF(I)=1
      ROL(I)=ROI
 1000 CONTINUE
   99 FORMAT(E20.10)
      IF(X .GT. 100.19)WRITE(LPR,99)SUMJ(I)
      RETURN
      END
      SUBROUTINE  SUM1( CV,TG,P,TS,XVS,XV,XK,D,DM,CD,BH,VL,VG)
      DIMENSION TT(2)
      DIMENSION ROL(10),CPL(10)
      COMMON HA
      COMMON ROL,VW,GW,GC,RV,CJ,WNCA0,B(4),ISTA,ISET,KKK,
     1KOUNT,NSTA,IDUM
      COMMON /ICEE/CP1,ROI,SUMJ(10),DELE(10),SUM9(10),NF(10),NG(10)
      COMMON /AYE/ I
      CALL LUNITS
      LPR=21
      LCR=29
      J=1
      IF(TS-492.0)5,5,4
    4 XV=(CV/VW)/(CV/VW +(1.-CV)/GW)
      X2=-3.06*((-.5696*TS+ .0639E-4 *TS**2 +.0927E-7 *TS**3+1352.3)/TS-
     C1.4525744)
      X1= 672.0/TS
      PVIS = 2117.0 *X1**5.19*DEXP(X2)
      GO TO 8
    5 IF(NF(I)-1)6,7,7
    6 A=5.4266514D0
      TT(J)=TS/1.80
      BB=-2005.1D0
      C=1.38690-4
      DD=1.1965D-11
      DK=293700.00
      E=-.004400
      F=-.0057148D0
      H=10.**((DD*(TT(J)**2.-DK)**2.0))-1.0
      R=C*(TT(J)**2-DK)/TT(J)
      G=10.0**((F*(374.11-TT(J))**1.25))
      RR=R*H
      S=A+BB/TT(J)+RR
      PVTS=2117.0*DEXP(2.3*(S+E*G))
      GO TO 8
    7 A=-2445.56540D0
      TT(J)=TS/1.80
      BB=8.231200
      C=-.01677006D0
      DD=.00001205140D0
      E=-6.75716900
      F=((A/TT(J))+.4343*BB*DLOG(TT(J)))+C*TT(J)+DD*TT(J)**2+E
```

```
      G=2.3*F
      PVIS=2.7845*DEXP(G)
    8 CONTINUE
      XVS = PVIS/P
      XVF =(XVS+XV)/2.0
      XM=XVF*VM +(1.-XVF)*GM
      TFI =(TS+TG)/2.0
      FMV=(10.6E-7 *DSQRT(TFI))/(1.+153B./TFI)
      FMNC= 7.5E-7 *DSQRT(TFI)/ (1.+216./TFI)
      FM  = XVF *FMV +(1.-XVF)*FMNC
      DAM = (.5375/P)*(TFI/491.0)**2.334
      ROF = P* XM/(RV*TFI)
      SCF=FM/(ROF*DAM)
      IF(VG .EQ. VL)VG=VG+.0000001
      RE  =DABS(VG-VL)*ROF*D)/FM
      ANN= 2.0+0.6*DSQRT(RE) * SCF** 0.3333
      AK  = ANN*FM/(D*SCF*XM)
      CM  = D**3  *3.1416 *ROL(I)/6.0
      CD  = 24.0/RE*( 1.0+.15*RE**0.687)
      IF( TFI .GT.1700.0 .AND. TFI .LT.4500.0) GO TO 221
      IF(TFI .LT. 400.  .OR. TFI  .GT. 4500. )GO TO 222
      CPVF =.4304 +.10/RE-4*TFI +0.2781E-7*TFI**2.0
      CPNCF = 0.2318 + 0.1040E-4 *TFI + 0.7166E-8 *TFI**2
      GO TO 102
  221 CPVF = .3319 +0.143RE-3 *TFI -0.1312E-7 *TFI**2.0
      CPNCF= 0.2214 + 0.4521E-4*TFI- 0.3776E-8 *TFI**2
      GO TO 102
  222 WRITE(LPR,101)
  101 FORMAT(25H TEMP=FI=IS OUT OF RANGE )
      WRITE(LPR,122)TG,TS
  122 FORMAT(5H0 TG=,E20.6,5X,4H TS=,E20.6 )
      STOP
  102 CONTINUE
      FKV = 0.432*FMV
      FKNC = 0.257 *(0.115+ 5.17*CPNCF)* FMNC
      FK = XVF *FKV +(1.-XVF)*FKNC
      CPF= XVF*(VM/XM)*CPVF +(1.-XVF)*CPNCF *GM/XM
      PVF = CPF *FM/FK
      FNU = 2. +0.6*DSQRT(RE) + PVF**0.3333
      HM =FNU *FM *CPF/(D*PVF)
      RETURN
      END
      SUBROUTINE  ROGEE(ROG,CV,VG,A)
      DIMENSION ROL(10),CPL(10)
      DIMENSION A(4,5)
      COMMON HA
      COMMON ROL,VM,GM,GC,RV,CJ,ANCAO,B(4),ISTA
      COMMON /XYM/ XS(99),YS(99),NXY
      COMMON /RSGR/ R2
      CALL LUNITS
      LPR=21
      LCR=29
      IF (X.LT.XS(1)) GO TO 10
      IF (X.LT.XS(2)) GO TO 20
      DO 5 I=1,NXY
      IF (X.GE.XS(I+1).AND.X.LE.XS(I+2)) GO TO 30
      IF (X.GT.XS(NXY)) GO TO 10
    5 CONTINUE
      WRITE(LPR,100)X
  100 FORMAT(17H X OUT OF RANGE,=,E16.7)
      STOP
   10 CONTINUE
      I=NXY-1
      GO TO 30
   20 I=1
   30 CONTINUE
```

```
      N=I-1
      DO 31 K=1,4
      KIK =1+K-1
      KN=K+N
      A(K,1)=1.
      A(K,5)=YS(KIK)
      DO 31 L=2,4
      IF(XS(KN) .EQ. 0.) A(K,L)=0.00
      IF(XS(KN) .EQ. 0.) GO TO 31
      A(K,L)=XS(KN)**(L-1)
   31 CONTINUE
      IRO=4
      ICL=5
      CALL CHOLES (A,IRO,ICL,0)
      IF(IRO .EQ. -1) WRITE(LPR,700)
  700 FORMAT(5HH THE MATRIX USED TO GET FIT OF DUCT GEOMETRY IS SINGULAR
     1)
      DO 60 I=1,4
   60 B(I)=A(I,5)
      AA0 =B(1) +B(2)*X +B(3)*X**2.0+ B(4)*X**3.0
      AA0=AA0*AA0/R2
      ROG = WNCA0/((1.-CV)*VG*AA0)
      RETURN
      END
      SUBROUTINE HLI(TS,AHL,AHFG,AHV)
      AHL =TS -540.0
      AHFG = -.5696*TS + .0839E-4 *TS**2 + 0.0927E-7 *TS**3.0+1352.3
      AHV=AHL+AHFG
      RETURN
      END
      SUBROUTINE AAA3(X,CV,VG,A3,AA0,DAA0,ROG)
      DIMENSION ROL(10),CPL(10)
      COMMON BA
      COMMON ROL,VG,GW,GC,RV,CJ,WNCA0,B(4),ISTA
      COMMON /RSQR/ R2
      AA0 = B(1) + B(2)*X +B(3)*X**2.0 +B(4)*X**3.0
      DAA0 = B(2) +2.0* B(3)*X +3.0*B(4)*X**2.0
      DAA0=2.00*AA0*DAA0/R2
      AA0=AA0*AA0/R2
      A3 = VG*(1.-CV)*DAA0/(VG*(1.-CV)*AA0)**2.
      RETURN
      END
      SUBROUTINE CHOLES(A,N,M,MATSYM)
      DIMENSION A(N,M)
      IF(A(1,1).NE.0.0) GO TO 47
      DO 37 J=2,N
      IF(A(J,1).EQ.0.0) GO TO 37
      IFLIP=J
      GO TO 27
   37 CONTINUE
      GO TO 54321
   27 DO 57 K=1,M
      TEMP=A(IFLIP,K)
      A(IFLIP,K)=A(1,K)
      A(1,K)=TEMP
   57 CONTINUE
   47 DO 2 J=2,M
      A(1,J)=A(1,J)/A(1,1)
    2 CONTINUE
      DO 6 I=2,N
      DO 7 J=2,M
      IF(MATSYM.EQ.0)GO TO 49
      IF(I-J)69,68,67
   49 IF(J.GT.I)GO TO 69
   68 K=J-1
      SUM=0.0
```

```
      DO 3 IR=1,K
      SUM=SUM+A(I,IR)*A(IR,J)
    3 CONTINUE
      A(I,J)=A(I,J)-SUM
      GO TO 7
   64 K=I-1
      SUM=0.0
      DO 4 IR=1,K
      SUM=SUM+A(I,IR)*A(IR,J)
    4 CONTINUE
      IF(A(I,I).EQ.0.0) GO TO 54321
      A(I,J)=(A(I,J)-SUM)/A(I,I)
      GO TO 7
   67 A(I,J)=A(J,I)*A(J,J)
    7 CONTINUE
    6 CONTINUE
      DO 52 K=2,N
      IEN=I-K
      SUM=0.0
      LL=I+1
      DO 51 IR=LL,N
      SUM=SUM+A(I,IR)*A(IR,M)
   51 CONTINUE
      A(I,M)=A(I,M)-SUM
   52 CONTINUE
      GO TO 12345
54321 K=-1
12345 RETURN
      END
      SUBROUTINE  DERIV(ROG,CV,VG,TG,P,AY,SUM2,SUM3,SUM4,SUM5,A0,A3,A11,
     1A12,A13,A14,R,CPV,CPA,A2,A4,AA0,A)
      DIMENSION ROL(10),CPL(10)
      COMMON BB
      COMMON ROL,VW,GW,GC,RV,CJ,WNCA0,H(4),ISTA,ISET,KKK
      IF(VG .LT. 0.0)GO TO 20
      R= P/(ROG* TG)
      A0 = GC*(1.-CV)/ROG
      AA = WNCA0/(VG**2.*(1.-CV)*AA0)
      A11 = (1.0-CV)*VG-TG*R*A0*A4
      A12= (1.+CV/(1.-CV))*VG/(GC*CJ)
      A1 = GW*CV +VW*(1.-CV)
      A  = AA*CA0/(VG*(1.-CV)**2.*AA0)
      AV= GW *CV/A1
      A2 = RV*VW*GW*(GW-VW)/(A1**2.*(AV*VW +(1.-AV)*GW)**2.)
      A13= A0*WNCA0*TG*R**3-A4*(VG**2.+ROG*TG*A2*A0+TG*R*A*A0)-VG*(1.-CV
     1)**2.*SUM2
      CALL MEEV (TG,XMV,CPV,CPA      )
      A14= -A4*(XMV*VG**2.0/(2.*GC*CJ))/(1.-CV)**2. -SUM3-SUM4-SUM5
      RETURN
   20 CALL LUNITS
      LPR=21
      LCR=29
      WRITE(LPR,31)VG
   31 FORMAT(E20.10)
      STOP
      END
      SUBROUTINE  MEEV(TG,XMV,CPV,CPA)
      DIMENSION ROL(10),CPL(10)
      COMMON BB
      COMMON ROL,VW,GW,GC,RV,CJ,WNCA0,H(4),ISTA,ISET,KKK
      IF( TG .GE.1700. .AND. TG .LE. 4500.)GO TO 222
      IF( TG .LT. 400. .OR.  TG .GT. 4500.)GO TO 221
      XMV = .4304*TG +.0839E-4*TG**2.0+0.0927E-7*TG**3.0-236.3161+1042.9
      CPV = .4304 + .1678E-4*TG+.2781E-7*TG**2.0
      CPA = .2318+ .1040E-4*TG+.7166E-8 *TG**2.0
      GO TO 100
```

```
222     ANV = .3319 *TG + .0719E-3*TG**2.0-.04373E-7*TG**3-185.381+1042.9
        CPV = .3319 + .143HE-3*TG- 0.1312E-7*TG**2.0
        CPA = .2214 +0.3521E-4*TG -0.3776E-8*TG**2.0
        GO TO 100
  221 CALL EXITS
        LPH=21
        LCK=29
        WRITE(LPH,99)
   99 FORMAT(24H TEMP-G IS OUT OF RANGE )
        WRITE(LPH,1)TG
    1 FORMAT(4HUTG=,F16.6)
        STOP
100     CONTINUE
        RETURN
        END
        SUBROUTINE DERP(ROG,CV,VG,TG,R,A2,A3,A4,A9,A15,A16,DP,A)
        DIMENSION ROL(10),CPL(10)
        COMMON HA
        COMMON ROL,VW,GA,GC,RV,CJ,WNCA0,H(4),ISTA
        DP= ROG*R*A15 +(ROG*TG*A2+TG*R*A )*A9-TG*R*A4*A16-4NCA0*A3*TG*R
        RETURN
        END
$EOF
23
0.0             6.14167
0.41667         5.62500
0.83333         5.20833
1.25000         4.87500
1.66667         4.62500
2.08333         4.38333
2.50000         4.21667
2.91667         4.08333
3.33333         3.99167
3.75000         3.91667
4.16667         3.90833
4.28333         3.9000
4.58333         8.9000
5.00000         3.9000
5.41667         3.9000
5.83333         3.9000
6.66667         3.9000
7.50000         3.9000
8.33333         3.9000
10.0000         3.9000
15.0000         3.9000
20.0000         3.9000
25.0000         3.9000
        SAMPLE CALCULATION : TWO INJECTION STATIONS USED
02
0.0             0.05            25.0
0.000122        184.            453.25          1330.0
0.0005          0.0005
75.             75.
600.            600.
0.00005         0.0001
```

SAMPLE CALCULATION

For purposes of illustration, selected pages of printout for a sample calculation are presented below. The duct geometry is given in Fig. 10, and two injection stations are considered. The initial conditions can be deduced from the printout, and the initial integration step size was 0.0001.

```
BEGIN STATION  1          RUN INFORMATION     SAMPLE CALCULATION : TWO INJECTION
INITIAL AREA =    118.501
X=     .000000     MG=     .176092     PO=    1359.18     TO=     456.089
A/AO=    1.00000     WV/WNC =     .122015-03
CV=    .122000-03   VG=     184.000     TG=    453.250     P=     1330.00
FL=    .500000-03   VL=     75.0000     TS=    600.000     D=     .500000-04  DELT==146.75
FLP=   -.737858-02   VLP=    3609.08     TSP=   -16694.2     DP=    -.245953-03
CVP=    .737678-02   VGP=    89.7051     TGP=    2.98843     PP=    -29.0501
X=     .100000-02   MG=     .176101     PO=    1359.18     TO=     456.090
A/AO=    .999955     WV/WNC =     .122729-03
CV=    .122714-03   VG=     184.009     TG=    453.250     P=     1330.06
FL=    .499256-03   VL=     75.3638     TS=    598.379     D=     .499782-04  DELT==145.12
FLP=   -.689509-02   VLP=    3666.41     TSP=   -13720.1     DP=    -.230055-03
CVP=    .689339-02   VGP=    89.4655     TGP=    2.77425     PP=    -28.9669
X=     .200000-03   MG=     .176109     PO=    1359.18     TO=     456.090
A/AO=    .999911     WV/WNC =     .123397-03
CV=    .123382-03   VG=     184.018     TG=    453.251     P=     1329.99
FL=    .499618-03   VL=     75.7326     TS=    596.850     D=     .499539-04  DELT==143.60
FLP=   -.646998-02   VLP=    3710.75     TSP=   -14859.6     DP=    -.216084-03
CVP=    .646836-02   VGP=    89.2535     TGP=    2.58243     PP=    -28.8924
X=     .300000-03   MG=     .176118     PO=    1359.18     TO=     456.091
A/AO=    .999866     WV/WNC =     .124025-03
CV=    .124010-03   VG=     184.027     TG=    453.251     P=     1329.99
FL=    .499990-03   VL=     76.1054     TS=    595.403     D=     .499329-04  DELT==142.15
FLP=   -.609291-02   VLP=    3744.51     TSP=   -14092.9     DP=    -.203643-03
CVP=    .609140-02   VGP=    89.0642     TGP=    2.40915     PP=    -28.8252
X=     .400000-03   MG=     .176126     PO=    1359.18     TO=     456.091
A/AO=    .999821     WV/WNC =     .124617-03
```

BEGIN STATION 2 RUN INFORMATION SAMPLE CALCULATION : TWO INJECTION

X=	.503000-01	MG=	.180252	PO=	1359.16	TO=	456.151		
A/AO=	.977904	WV/WNC =	.152594-03						
CV=	.152571-03	VG=	188.333	TG=	453.178	P=	1328.61		
FL=	.489420-03	VL=	150.347	TS=	506.901	D=	.489592-04	DELT=	-53.725
FLP=	-.100506-03	VLP=	594.916	TSP=	-488.390	DP=	-.349416-05		
FL=	.500000-03	VL=	75.6000	TS=	600.000	D=	.100000-02	DELT=	146.82
FLP=	-.227931-02	VLP=	1329.20	TSP=	-5148.88	DP=	-.151954-03		
CVP=	.237909-02	VGP=	87.6643	TGP=	-.491097	PP=	-28.5993		
X=	.100500	MG=	.184449	PO=	1359.14	TO=	456.203		
A/AO=	.956629	WV/WNC =	.178992-03						
CV=	.178950-03	VG=	192.701	TG=	453.389	P=	1327.18		
FL=	.466313-03	VL=	170.212	TS=	490.181	D=	.488509-04	DELT=	-37.092
FLP=	-.371977-04	VLP=	270.149	TSP=	-229.942	DP=	-.129894-05		
FL=	.476711-03	VL=	120.447	TS=	536.923	D=	.984226-04	DELT=	-83.834
FLP=	-.134677-03	VLP=	583.396	TSP=	-468.095	DP=	-.926857-05		
CVP=	.171813-03	VGP=	87.1638	TGP=	-2.17296	PP=	-28.8080		
X=	.150100	MG=	.188627	PO=	1359.14	TO=	456.228		

STATION =	2	RUN INFORMATION		SAMPLE CALCULATION : TWO INJECTION					
A/A0=	.936343	WV/WNC =	.184743-03						
CV=	.184709-03	VG=	197.042	TG=	452.973	P=	1325.73		
FL=	.464902-03	VL=	180.760	TS=	481.050	D=	.488016-04	DELT=	-28.077
FLP=	-.220472-04	VLP=	170.755	TSP=	-148.711	DP=	-.771445-06		
FL=	.472370-03	VL=	141.641	TS=	520.547	D=	.981230-04	DELT=	-67.574
FLP=	-.584431-04	VLP=	330.517	TSP=	-240.957	DP=	-.404670-05		
CVP=	.804606-04	VGP=	87.4941	TGP=	-2.49192	PP=	-29.6220		
X=	.201300	MG=	.192983	P0=	1359.13	T0=	456.246		
A/A0=	.916144	WV/WNC =	.187963-03						
CV=	.187928-03	VG=	201.562	TG=	452.840	P=	1324.19		
FL=	.463969-03	VL=	188.265	TS=	474.635	D=	.487689-04	DELT=	-21.796
FLP=	-.151781-04	VLP=	128.087	TSP=	-105.883	DP=	-.531801-06		
FL=	.470083-03	VL=	155.701	TS=	510.570	D=	.979644-04	DELT=	-57.730
FLP=	-.345209-04	VLP=	230.849	TSP=	-159.695	DP=	-.239803-05		
CVP=	.496403-04	VGP=	88.6818	TGP=	-2.69889	PP=	-30.5220		
X=	.252500	MG=	.197379	P0=	1359.13	T0=	456.260		
A/A0=	.896670	WV/WNC =	.190096-03						
CV=	.190050-03	VG=	206.122	TG=	452.697	P=	1322.60		
FL=	.463295-03	VL=	194.251	TS=	469.925	D=	.487453-04	DELT=	-17.228
FLP=	-.114927-04	VLP=	108.088	TSP=	-79.9794	DP=	-.403066-06		
FL=	.468624-03	VL=	166.072	TS=	503.533	D=	.978629-04	DELT=	-58.636
FLP=	-.236416-04	VLP=	179.221	TSP=	-119.060	DP=	-.164709-05		
CVP=	.351410-04	VGP=	89.4507	TGP=	-2.86146	PP=	-31.4426		
X=	.300500	MG=	.201538	P0=	1359.13	T0=	456.270		
A/A0=	.879049	WV/WNC =	.191580-03						
CV=	.191544-03	VG=	210.433	TG=	452.556	P=	1321.07		
FL=	.462798-03	VL=	199.186	TS=	466.504	D=	.487278-04	DELT=	-13.947

STATION = 2	RUN INFORMATION	SAMPLE CALCULATION : TWO INJECTION					
FLP= -.935774-05	VLP= 98.5421	TSP= -63.5097	DP= -.328425-06				
FL= .467637-03	VL= 173.931	TS= 498.412	D= .977941-04	DELT=-45.856			
FLP= -.179375-04	VLP= 150.423	TSP= -95.6063	DP= -.124969-05				
CVP= .272748-04	VGP= 90.1414	TGP= -2.99409	PP= -32.3136				
X= .351700	MG= .206010	PO= 1359.12	TO= 456.278				
A/AO= .860909	MV/MMC = .192830-03						
CV= .192792-03	VG= 215.066	TG= 452.400	P= 1319.39				
FL= .462360-03	VL= 204.081	TS= 463.594	D= .487125-04	DELT=-11.194			
FLP= -.782751-05	VLP= 93.2237	TSP= -50.8175	DP= -.274892-06				
FL= .466825-03	VL= 181.093	TS= 493.954	D= .977375-04	DELT=-41.554			
FLP= -.140973-04	VLP= 130.737	TSP= -79.2413	DP= -.981042-06				
CVP= .218784-04	VGP= 90.8398	TGP= -3.12331	PP= -33.2455				
X= .402900	MG= .210519	PO= 1359.12	TO= 456.286				
A/AO= .843421	MV/MMC = .193831-03						
CV= .193794-03	VG= 219.734	TG= 452.237	P= 1317.67				
FL= .461959-03	VL= 208.777	TS= 461.245	D= .486994-04	DELT= -9.008			
FLP= -.675278-05	VLP= 96.5494	TSP= -41.3695	DP= -.237276-06				
FL= .466195-03	VL= 187.433	TS= 490.261	D= .976936-04	DELT=-38.024			
FLP= -.106320-04	VLP= 117.759	TSP= -65.5013	DP= -.742665-06				
CVP= .173781-04	VGP= 91.4951	TGP= -3.24425	PP= -34.1785				
X= .454100	MG= .215062	PO= 1359.12	TO= 456.292				
A/AO= .826562	MV/MMC = .194654-03						
CV= .194618-03	VG= 224.434	TG= 452.068	P= 1315.89				
FL= .461664-03	VL= 213.377	TS= 459.320	D= .486880-04	DELT= -7.252			
FLP= -.596296-05	VLP= 89.2937	TSP= -34.1336	DP= -.209622-06				
FL= .465697-03	VL= 193.220	TS= 487.134	D= .976587-04	DELT=-35.068			
FLP= -.893018-05	VLP= 108.818	TSP= -56.9967	DP= -.624233-06				

STATION =	2	RUN INFORMATION							
X=	1.01090	MG=	.266155	PO=	1359.09	TO=	456.323		
A/A0=	.677729	WV/WNC =	.199661-03						
CV=	.199621-03	VG=	277.085	TG=	449.884	P=	1293.61		
FL=	.459422-03	VL=	263.398	TS=	450.196	D=	.486091-04	DELT=	-.312
FLP=	-.297097-05	VLP=	91.5425	TSP=	-7.81548	DP=	-.104781-06		
FL=	.462932-03	VL=	244.861	TS=	467.918	D=	.974651-04	DELT=	-18.034
FLP=	-.291789-05	VLP=	87.6430	TSP=	-21.5639	DP=	-.204776-06		
CVP=	.598651-05	VGP=	96.1360	TGP=	-4.44170	PP=	-44.6817		
X=	1.26690	MG=	.289881	PO=	1359.08	TO=	456.329		
A/A0=	.627146	WV/WNC =	.200997-03						
CV=	.200956-03	VG=	301.407	TG=	448.709	P=	1281.85		
FL=	.458726-03	VL=	286.804	TS=	448.520	D=	.485845-04	DELT=	.189
FLP=	-.250109-05	VLP=	90.4888	TSP=	-5.59431	DP=	-.882985-07		
FL=	.462293-03	VL=	267.186	TS=	463.170	D=	.974202-04	DELT=	-14.461
FLP=	-.214141-05	VLP=	86.4650	TSP=	-15.9638	DP=	-.150421-06		
CVP=	.464063-05	VGP=	89.6042	TGP=	-4.51384	PP=	-45.0061		
X=	1.52290	MG=	.312016	PO=	1359.07	TO=	456.333		
A/A0=	.597255	WV/WNC =	.202072-03						
CV=	.202031-03	VG=	324.001	TG=	447.528	P=	1270.12		
FL=	.459132-03	VL=	309.157	TS=	447.234	D=	.485635-04	DELT=	.293
FLP=	-.215957-05	VLP=	85.3854	TSP=	-4.61086	DP=	-.763071-07		
FL=	.461811-03	VL=	288.777	TS=	459.580	D=	.973864-04	DELT=	-12.053
FLP=	-.165888-05	VLP=	82.6873	TSP=	-12.3639	DP=	-.116608-06		
CVP=	.381690-05	VGP=	88.1273	TGP=	-4.77887	PP=	-47.2696		
X=	1.75330	MG=	.333370	PO=	1359.05	TO=	456.337		
A/A0=	.554131	WV/WNC =	.202691-03						
CV=	.202850-03	VG=	345.728	TG=	446.309	P=	1258.11		

STATION = 2 RUN INFORMATION SAMPLE CALCULATION : TWO INJECTION

FLP=	-.564096-06	VLP=	18.5205	TSP=	-2.21757	DP=	-.200271-07		
FL=	.459698-03	VL=	481.891	TS=	441.604	D=	.972376-04	DELT=	-6.731
FLP=	-.328703-06	VLP=	28.7245	TSP=	-3.30110	DP=	-.231763-07		
CVP=	.892428-06	VGP=	23.0196	TGP=	-1.95110	PP=	-17.9706		
X=	4.51810	MG=	.495450	PO=	1359.07	TO=	456.369		
A/AO=	.402919	MV/MNC =	.207661-03						
CV=	.207618-03	VG=	506.930	TG=	434.793	P=	1148.65		
FL=	.454735-03	VL=	503.734	TS=	435.168	D=	.484432-04	DELT=	-.375
FLP=	-.503189-06	VLP=	9.14606	TSP=	-1.59885	DP=	-.178683-07		
FL=	.459619-03	VL=	488.293	TS=	440.817	D=	.972320-04	DELT=	-6.024
FLP=	-.289989-06	VLP=	20.3574	TSP=	-2.80500	DP=	-.204490-07		
CVP=	.792849-06	VGP=	-6.86382	TGP=	.587965	PP=	5.35070		
X=	4.77410	MG=	.494924	PO=	1359.07	TO=	456.370		
A/AO=	.403233	MV/MNC =	.207852-03						
CV=	.207809-03	VG=	506.424	TG=	434.837	P=	1149.04		
FL=	.454613-03	VL=	505.125	TS=	434.832	D=	.484389-04	DELT=	.004
FLP=	-.455728-06	VLP=	3.51890	TSP=	-1.10552	DP=	-.161859-07		
FL=	.459549-03	VL=	492.556	TS=	440.159	D=	.972271-04	DELT=	-5.323
FLP=	-.257961-06	VLP=	13.9148	TSP=	-2.37062	DP=	-.181923-07		
CVP=	.713392-06	VGP=	.862684-02	TGP=	.199743-02	PP=	-.129745-01		
X=	5.00450	MG=	.494925	PO=	1359.06	TO=	456.370		
A/AO=	.403233	MV/MNC =	.208011-03						
CV=	.207968-03	VG=	506.426	TG=	434.837	P=	1149.04		
FL=	.454511-03	VL=	505.724	TS=	434.609	D=	.484353-04	DELT=	.228
FLP=	-.432021-06	VLP=	1.85835	TSP=	-.844245	DP=	-.153462-07		
FL=	.459492-03	VL=	495.345	TS=	439.647	D=	.972231-04	DELT=	-4.810
FLP=	-.236772-06	VLP=	10.4983	TSP=	-2.08465	DP=	-.166994-07		

UNCLASSIFIED

Security Classification

DOCUMENT CONTROL DATA - R & D

(Security classification of title, body of abstract and indexing annotation must be entered when the overall report is classified)

1. ORIGINATING ACTIVITY *(Corporate author)*
Arnold Engineering Development Center
Arnold Air Force Station, Tennessee 37389

2a. REPORT SECURITY CLASSIFICATION
UNCLASSIFIED

2b. GROUP
N/A

3. REPORT TITLE
ANALYTICAL STUDY OF ICING SIMULATION FOR TURBINE ENGINES IN ALTITUDE TEST CELLS

4. DESCRIPTIVE NOTES *(Type of report and inclusive dates)*
Final Report - June 1971 to June 1972

5. AUTHOR(S) *(First name, middle initial, last name)*
C. E. Willbanks and R. J. Schulz, ARO, Inc.

6. REPORT DATE	7a. TOTAL NO. OF PAGES	7b. NO. OF REFS
November 1973	97	28

8a. CONTRACT OR GRANT NO.	9a. ORIGINATOR'S REPORT NUMBER(S)
b. PROJECT NO.	AEDC-TR-73-144
c. Program Element 65802F	9b. OTHER REPORT NO(S) *(Any other numbers that may be assigned this report)*
d.	ARO-ETF-TR-73-59

10. DISTRIBUTION STATEMENT
Approved for public release; distribution unlimited.

11. SUPPLEMENTARY NOTES	12. SPONSORING MILITARY ACTIVITY
Available in DDC	Arnold Engineering Development Center, Arnold Air Force Station, Tennessee 37389

13. ABSTRACT

An analytical study of simulated icing for turbine engines in altitude test cells was made. A mathematical model of a typical direct-connect type of icing test cell was developed, and the governing equations were programmed for computer solution on FORTRAN computer language. A parametric study was performed to determine the effects of t test cell inlet and water spray conditions on the thermodynamic and kinetic state of the flow in the test section or at the engine compres sor face. The importance of correctly simulating droplet size distribution, mean effective droplet diameter, liquid water content, and humidity was investigated. The results of the investigation lend further support to the fact that ground test facilities provide the best capability for conducting turbine engine icing tests. The ability to define and control the simulated environment gives an altitude test ce distinct advantages not enjoyed by flight testing in natural icing environments or flight testing in artificial environments created by tanker aircraft.

DD FORM 1 NOV 65 1473

UNCLASSIFIED

Security Classification

14. KEY WORDS	LINK A		LINK B		LINK C	
	ROLE	WT	ROLE	WT	ROLE	WT
ice formation						
aircraft						
engines						
turbines						
simulation						
environment simulators						
mathematical models						
drops (liquid)						

1. Icing

2 Turbine engines -- Icing

AFSC
Arnold AFS Tenn.